

For Reference

NOT TO BE TAKEN FROM THIS ROOM

Ex LIBRIS
UNIVERSITATIS
ALBERTAENSIS





Digitized by the Internet Archive
in 2022 with funding from
University of Alberta Libraries

<https://archive.org/details/Kalra1973>

THE UNIVERSITY OF ALBERTA

RELEASE FORM

NAME OF AUTHOR Harish Kalra

TITLE OF THESIS ISOTOPIC EXCHANGE AND DIFFUSIVITY OF
..... HYDROGEN IN THE HYDROGEN-AMINOMETHANE
..... SYSTEM
.....

DEGREE FOR WHICH THESIS WAS PRESENTED Ph.D.

YEAR THIS DEGREE GRANTED 1973

Permission is hereby granted to THE UNIVERSITY OF
ALBERTA LIBRARY to reproduce single copies of this
thesis and to lend or sell such copies for private,
scholarly or scientific research purposes only.

The author reserves other publication rights, and
neither the thesis nor extensive extracts from it may
be printed or otherwise reproduced without the author's
written permission.

THE UNIVERSITY OF ALBERTA

PLEASE PRINT

NAME OF AUTHOR
TITLE OF THESIS
DEGREE FOR WHICH THESIS WAS PRESENTED
YEAR THIS DEGREE GRANTED
UNIVERSITY OF ALBERTA

PERMISSION IS HEREBY GRANTED TO THE UNIVERSITY OF
ALBERTA LIBRARY TO REPRODUCE COPIES OF THIS
THESIS AND TO LEND OR SELL SUCH COPIES FOR PRIVATE,
ACADEMIC OR SCIENTIFIC RESEARCH PURPOSES ONLY.

The author reserves other publication rights, and
notwithstanding the thesis not extensive extracts from it may
be printed or otherwise reproduced without the author's
written permission.



DATED
.....

THE UNIVERSITY OF ALBERTA

ISOTOPIC EXCHANGE AND DIFFUSIVITY OF HYDROGEN
IN THE HYDROGEN-AMINOMETHANE SYSTEM

by



HARISH KALRA

A THESIS

SUBMITTED TO THE FACULTY OF GRADUATE STUDIES AND RESEARCH
IN PARTIAL FULFILMENT OF THE REQUIREMENTS FOR THE DEGREE
OF DOCTOR OF PHILOSOPHY IN CHEMICAL ENGINEERING

DEPARTMENT OF CHEMICAL AND PETROLEUM ENGINEERING

EDMONTON, ALBERTA

SPRING, 1973

UNIVERSITY OF ALBERTA
FACULTY OF GRADUATE STUDIES AND RESEARCH

The undersigned certify that they have read, and recommend to the Faculty of Graduate Studies and Research for acceptance, a thesis entitled "ISOTOPIC EXCHANGE AND DIFFUSIVITY OF HYDROGEN IN THE HYDROGEN-AMINOMETHANE SYSTEM" submitted by Harish Kalra in partial fulfilment of the requirements for the degree of Doctor of Philosophy.

ABSTRACT

Mass transfer studies with a single sphere absorber were used to determine the diffusivity of hydrogen in liquid aminomethane over a temperature range of -20°C to -30°C . The diffusion coefficients were found to lie in the range of 90×10^{-6} to $110 \times 10^{-6} \text{ cm}^2/\text{sec}$. A modified Ferrell and Himmelblau correlation has been derived from the diffusion data for hydrogen in ammonia and in aminomethane. It is recommended for use in estimating the diffusion coefficients for hydrogen, hydrogen deuteride and deuterium in aliphatic amines where experimental data is not available. The accuracy of the diffusion data obtained is estimated to be within $\pm 5\%$.

Pseudo-first order reaction rate constants for the liquid phase hydrogen deuteride aminomethane exchange were determined over the temperature range of -10°C to -30°C . This was achieved by measuring the rates of absorption of hydrogen deuteride into a thin film of liquid aminomethane flowing over a sphere absorber operating in the fast reaction regime. Potassium methyl amide in solution with aminomethane was used to catalyze the exchange process. Rate constants were found to be in the range of 230 to 570 sec^{-1} at catalyst concentrations ranging up to 15.8 (gms K/kg Amine). The rate constant appears to vary linearly with catalyst concentration up to a value of 5.0 (gms K/kg Amine). The activation energy of the reaction was estimated to be 3.1 (kcal/gm mole). An expression was derived which represents the data in the range of investigation to $\pm 4\%$ and is recommended for predicting the rate constants at conditions of temperature and catalyst concentration where data are not available.

It is estimated that the accuracy of the rate constants obtained is within $\pm 10\%$.

ACKNOWLEDGEMENTS

The author wishes to express his appreciation of the criticism and guidance given by Dr. F.D. Otto who supervised this investigation.

The author gratefully acknowledges the assistance of Mr. W.M. Thurston, Chalk River Nuclear Laboratories of the Atomic Energy of Canada Ltd., for providing the standards used to calibrate the mass spectrometer.

The data and technical assistance provided by The Chemical Engineering Branch of the Fuels and Materials Division of The Atomic Energy of Canada Ltd. is acknowledged. Thanks are due:

To Mr. Peter Smits for his valuable assistance in building and running the equipment.

To Mr. G.T. Walsh and his staff for their aid in the construction and maintenance of the equipment and for the general support services provided by the workshop.

To Mr. D. Sutherland and his staff for providing the instrument shop facilities.

To Mr. J.P. Moser for assistance with laboratory analysis and general analytical support.

To Mr. Ihor Starchuk and his staff for helping to expedite the purchase of equipment.

To Mrs. G. Williams and Mrs. L. Letwiniuk for providing essential secretarial services and for typing this manuscript.

The financial assistance of the University of Alberta is gratefully acknowledged.

TABLE OF CONTENTS

	PAGE
TABLE OF CONTENTS	
LIST OF TABLES	
LIST OF FIGURES	
PART ONE	
<u>CHAPTER</u>	
1. INTRODUCTION	1
2. LITERATURE SURVEY	3
2.1 Past Experience with Single Sphere Absorber	3
2.2 Theoretical Analysis	6
2.2.1 Hydrodynamics of the Spherical Film	6
2.2.2 Physical Absorption of a Single Gas in a Spherical Liquid Film	9
2.3 Empirical Methods for Prediction of Diffusion Coefficients	16
3. EXPERIMENTAL	20
3.1 Apparatus	20
3.2 Operation and Procedure	24
4. RESULTS	28
5. DISCUSSION	34
5.1 Experimental Data	34
5.2 Experimental vs. Estimated Values	42
5.3 Hydrodynamics	50
6. CONCLUSIONS	53
NOMENCLATURE	54
REFERENCES	58
APPENDICES	
A1, Experimental Data	61

B1.	Operating Procedure for the Single Sphere Absorber	64
C1.	Error Analysis	67
PART TWO		
1.	INTRODUCTION	78
2.	LITERATURE SURVEY	82
2.1	Hydrogen-Ammonia System	82
2.1.1	Effect of Catalyst Concentration	85
2.2	Hydrogen-Aminomethane System	88
2.2.1	Effect of Catalyst Concentration	91
2.3	Catalyst Solubility	92
2.4	Reaction Mechanism	92
3.	ANALYSIS OF MASS TRANSFER AND CHEMICAL REACTION OVER A SPHERE	94
4.	EXPERIMENTAL	102
4.1	Apparatus	102
4.1.1	General	102
4.1.2	Hydrogen-Aminomethane Exchange Apparatus	104
4.1.3	Liquid Feed System	110
4.1.4	Catalyst Wash System	112
4.1.5	Catalyst Destruction System	112
4.1.6	Catalyst Make-Up Section	113
4.1.7	Gas Sampling System	115
4.1.8	Analysis	117
4.1.9	Hydrogen Make-up and Purification	118
4.2	Operating Procedures	119
4.2.1	The Exchange Experiment	119
4.2.2	PMA Solution Make-up	121
4.2.3	Analysis	123
4.2.4	Method of Interpretation of Data	128
5.	RESULTS	132
6.	DISCUSSION	139
6.1	Gas Phase Resistance	139
6.2	Effect of a Change in y_e on k_1	142
6.3	Modelling the Data of k_1 vs t and k_1 vs c	144

6.3.1	The Bayesian Approach to Model Discrimination	144
6.3.2	The Models	148
6.4	Comparison with Existing Data	154
6.5	Accuracy of the Data	161
7.	CONCLUSIONS	163
	NOMENCLATURE	164
	REFERENCES	171
	APPENDICES	
A2.	Detailed Operating Procedures	173
A2.1	The Exchange Experiment	173
A2.2	PMA Solution Make-up	180
B2.	Sample Calculation	184
C2.	Error Analysis	204
D2.	Detailed Experimental Data	210

LIST OF TABLES

TABLE		PAGE
PART ONE		
1.	Coefficients for Series Solution for G_s (Davidson and Cullen)	14
2.	Experimental Results for the Diffusivity of Hydrogen in Liquid Aminomethane Using the 3/4 Inch Sphere	29
3.	Experimental Results for the Diffusivity of Hydrogen in Liquid Aminomethane Using the 1 Inch Sphere	29
4.	Estimation of the Activity on the Support Rod and its Effect on the Diffusion Coefficients Obtained from the 1 Inch Sphere	38
5.	Estimation of the Activity on the Support Rod and its Effect on the Diffusion Coefficients Obtained from the 3/4 Inch Sphere	39
6.	Average Apparent Association Parameters for the Wilke- Chang Equation	44
7.	Comparison of $\frac{D_{\mu_1}}{T}^{\alpha_1}$ and $\frac{D_{\mu_1}}{T}$ for the Hydrogen- Aminomethane System	46
8.	Estimated vs. Experimental Values of Diffusivity of Hydrogen in Liquid Aminomethane and Ammonia at -30°C.	49
AI-1	Physical Absorption Data with the 1 Inch Sphere	62
AI-2	Physical Absorption Data with the 3/4 Inch Sphere	63
PART TWO		
1.	Comparison of the Reaction Rate Constants for the Hydrogen Ammonia System	87
2.	Kinetic Rate Constant Data for the Hydrogen-Amino- methane System	138
3.	Effect of a Change in y_e on the Rate Constant k_1	145
4.	Estimates of Model Parameters for the Rate Constant vs. Temperature Data	149
5.	Estimates of Model Parameters for the Rate Constant vs. Catalyst Concentration Data	152
6.	Comparison of the Calculated vs. Observed Data of Rate Constant vs. Temperature Using the Joint Model	155

7.	Comparison of the Calculated vs. Observed Data of Rate Constant vs. Catalyst Concentration Using the Joint Model	156
8.	Comparison of the Rate Constant k_1 Calculated by the Joint Model with k_1 Obtained by Extrapolating Rochard's Data	160
B2-1	Raw Data from a Typical Experiment	185
B2-2	Mass Spectrometer Analysis for the Gas Standards	186
B2-3	Converted form of the Gas Standards' Analysis	187
B2-4	Data of Absolute D/H Concentrations vs. Time	188
B2-5	Data of Absolute D/H Concentrations vs. Time Used for Rate Constant Estimation	189
B2-6	Data of Cumulative Depletion vs. Time	193
D2-1	Detailed Experimental Data	211

LIST OF FIGURES

FIGURE		PAGE
	PART ONE	
1.	Cross Section of Sphere and Liquid Film	8
2.	Schematic Diagram of Single Sphere Absorber	21
3.	Schematic Diagram of Absorption Chamber	22
4.	Rate of Absorption of Hydrogen in Aminomethane at -29°C on a 1 Inch Sphere	30
5.	Effect of Take-Off Length on Hydrogen Absorption Rate	31
6.	Effect of Temperature on the Diffusivity of Hydrogen in Ammonia and Aminomethane	33
7.	Effect of Liquid Flow Rate on the Transformation Parameter α	41
8.	Estimation of Best Parameters for Equation (1-44)	48
	PART TWO	
1.	Co-ordinate Representation for Flow over a Sphere Absorber	95
2.	Gas-Liquid Exchange Apparatus	106
3.	The Catalyst Wash System	109
4.	The Liquid Feed System	111
5.	The Catalyst Make-up and Liquid Sampling Section	114
6.	The Gas Sampling Apparatus	116
7.	A Typical Mass-Spectrometer Calibration Curve	125
8.	A Calibration Curve for the Atomic Absorption Spectrophotometer	127
9.	The Cumulative Depletion of Hydrogen-Deuteride in the Gas Phase with Time	133
10.	The Variation of the Kinetic Rate Constant with Temperature (Hydrogen-Aminomethane System)	135
11.	The Variation of the Kinetic Rate Constant with Catalyst Concentration in Solution (Hydrogen-Aminomethane System)	137

12.	Estimation of the Variation of the Rate Constant with Catalyst Concentration and Temperature	157
B2-1	Plot of y vs. t to Determine the Gas Phase Equilibrium Value	192

PART I

DIFFUSIVITY OF HYDROGEN
IN AMINOMETHANE

CHAPTER 1

INTRODUCTION

The isotopic exchange of deuterium between gaseous hydrogen and liquid aliphatic amines has considerable potential as a basis for a commercial process to produce heavy water. The economics of this route indicate that there is promise to produce heavy water more cheaply than processes based on the exchange between hydrogen-ammonia or hydrogen sulphide-water. Amongst the aliphatic amines, aminomethane has been reported to be the most attractive [1].

In order to design industrial contactors for systems such as hydrogen-aminomethane which undergo a simultaneous absorption and chemical reaction, it is desirable that sufficient information for estimating mass transfer coefficients be available. The diffusion coefficient for physical absorption and the kinetic rate constant are two parameters which are useful for estimating transfer coefficients when chemical reaction is involved.

Physical gas absorption into a liquid flowing over a sphere has been successfully used by a number of workers [2,3,4,5,6] to obtain estimates of the diffusion coefficients in gas-liquid systems. The single sphere contactor minimizes the end effects common to other gas liquid contactors. It is also reported [3,7] that relatively high liquid flow rates, with absence of surface rippling, may be employed with this absorber. Compared to the laminar jet, the single sphere absorber provides longer contact times (0.1 sec to 1.0 sec) and a higher surface area per unit volume of flowing liquid which makes

the sphere absorber more suitable for studies involving sparingly soluble gases.

Preliminary measurements of the diffusion coefficient of hydrogen in aminomethane were made by Moore [8] but the results obtained indicated inconsistencies which were attributed to experimental difficulties. Subsequent refinements of the experimental apparatus and additional operating experience have allowed reliable results to be obtained. These results are reported as part of this investigation.

CHAPTER 2

LITERATURE SURVEY

A fairly comprehensive literature review of the various experimental techniques employed in the measurement of diffusion coefficients has been undertaken by Moore [8]. A repetition of that material is deemed unnecessary for this investigation. A review of the operating experience pertinent to the sphere absorber and details of the mathematical techniques used to analyze the data obtained will be presented.

2.1 Past Experience with the Single Sphere Absorber

A single sphere absorber consists of a sphere over which a liquid flows in a laminar film. The liquid is introduced through an orifice onto the top pole of the sphere and is collected in a constant liquid level take-off tube situated directly below the sphere. The sphere is enclosed in a gas tight chamber which is in turn located in a constant temperature environment. The molecular diffusivity can be calculated from the measured rate of absorption of a gas into the liquid film on the sphere.

Past experience with the design and operation of an absorption system using the single sphere absorber has indicated the following important observations:

(i) A large volume of the gas absorption chamber results in excessive errors in the measured gas absorption rate caused by minor temperature fluctuations of the gas phase [5].

(ii) A more stable surface film of liquid over the sphere may

be obtained by using a laminar jet as the liquid feeding device [7,9] in preference to having the support rod extend through the liquid feed nozzle [3].

(iii) The surface film is very sensitive to vibrations of the apparatus. Use of vibration arrestors is recommended.

(iv) The sphere size should be chosen in a manner to eliminate wall effects of the absorption chamber and at the same time prevent the effects indicated in (i).

(v) Depending on the system being studied, there is:

(a) an upper and a lower limit to the jet length that should be used; and

(b) a range of permissible distances between the sphere and the take-off level for which the stagnant layer reported by previous workers [2,3,4,7], may be maintained on the support rod. Shorter distances cause the stagnant layer to move on to the sphere absorber thus reducing the effective interfacial area and resulting in a marked decrease in the measured absorption rates.

(vi) The use of the single sphere absorber has associated with it some end effects which may be subdivided as follows:

(a) Entrance Effects

When a laminar jet is used as the liquid feeding device, the fresh liquid issuing from it will absorb some solute gas. The amount of gas absorbed on the jet is reported to be significant [9]. This amount may, however, be calculated using the equation for physical absorption by an ideal jet [9,10,11]:

$$G_j = 4 \sqrt{h_j LD} (C_i - C'_o) \quad (1-1)$$

Assuming complete mixing of the solute gas and the liquid at the sphere-jet junction [9], the bulk concentration of the liquid flowing on to the sphere may be evaluated as

$$C_o = \frac{G_j}{L} \quad (1-2)$$

Goettler [9] investigated the cases of complete mixing and no mixing at the sphere-jet junction while studying carbon dioxide absorption in water. His results indicated that complete mixing at the sphere-jet junction was a more likely representation of the fluid conditions at the top pole of the sphere.

(b) Exit Effects

If the distance between the bottom of the sphere and the take-off level is properly adjusted the absorption of the solute gas on the exposed support rod is reported to be negligible due to the presence of a stagnant layer [2,3,4,9]. This stagnant layer is attributed to the presence of trace impurities of surface active agents in the outgoing liquid [4,9]. As a consequence of this layer, it is suggested that the velocity profile of the liquid over the support rod might be fully parabolic. This would reduce the gas absorption on the rod sufficiently to be neglected [4,9].

Experience with the sphere absorber as reported above is limited to studies involving water as the absorbing liquid wherein the experiments were conducted at temperatures generally within 15 to 30°C. Moore's investigation [8] has indicated that use of the single sphere absorber for low temperature studies involving the hydrogen-aminomethane system requires that emphasis also be placed on the following aspects of its operation:

(i) Minor temperature fluctuations of the absorption system or the room where the experiment is conducted can cause large errors in the measurement of the gas absorption rate. This requires that:

- (a) The experiments be conducted in a controlled temperature laboratory.
- (b) The incoming liquid feed be pre-cooled to a temperature which is close to the constant temperature environment surrounding the absorption system.
- (c) The liquid leaving the absorber must be maintained at a temperature equal to, or lower than, the temperature of the absorption system to prevent inverse pressure gradients from impeding flow.

(ii) The take-off level control device (lute vessel) used by Davidson et al. [3] may not be used for this system. A fine metering valve on the outgoing liquid line is a suitable substitution.

(iii) The choice of the size of the sphere absorber should take into consideration the saturation levels of the outgoing liquid. Very high saturations can cause the errors due to temperature fluctuations and measured gas rates to be magnified considerably.

2.2 Theoretical Analysis

2.2.1 Hydrodynamics of the Spherical Film. The hydrodynamic behaviour of the spherical film of liquid flowing over the sphere absorber may be described by using the solution of Nusselt [12] for laminar flow down an inclined plane. This approach was first attempted by Kramers et al. [2] and was subsequently verified and used by other

investigators also [3,9,13,14].

It may be assumed that the film thickness of the liquid flowing at any latitude on the sphere is the same as it would be for the same flow rate per unit length on an inclined plane making the same angle with the vertical. Thus, for a liquid flowing over the surface of a sphere (Figure 1) the liquid film thickness is given by

$$\Delta = \left(\frac{3 \nu L}{2 \pi R g} \right)^{1/3} \sin^{-2/3} \theta \quad (1-3)$$

and the velocity distribution is represented as

$$V_{\psi} = V_0 \left(1 - \left(\frac{x}{\Delta} \right)^2 \right) \quad (1-4)$$

where V_0 is the velocity at the surface of the film ($x = 0$) and is given as

$$V_0 = \frac{g \Delta^2 \sin \theta}{2 \nu} \quad (1-5)$$

Combining equations (1-3) and (1-5) one gets

$$V_0 = \left(\frac{9g}{32 \nu \pi^2} \right)^{1/3} L^{2/3} R^{-2/3} \sin^{-1/3} \theta \quad (1-6)$$

For an element of liquid flowing over the sphere θ varies from 0 to π ; the diffusion or contact time is therefore given as

$$t = \int_0^{\pi} \frac{R d\theta}{V_0} = \left(\frac{9g}{32 \pi^2 \nu} \right)^{1/3} L^{-2/3} R^{5/3} \int_0^{\pi} \sin^{1/3} \theta d\theta \quad (1-7)$$

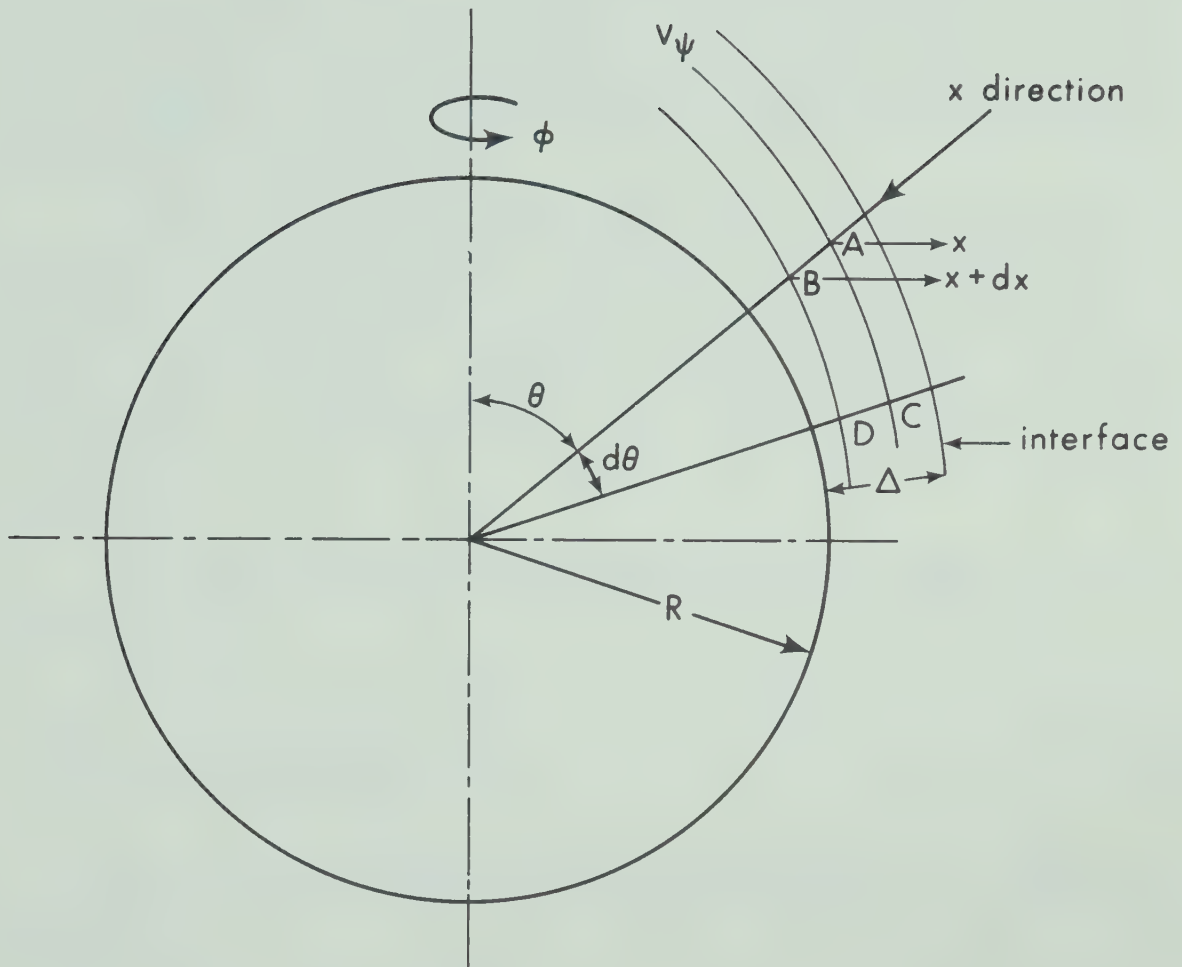


FIGURE 1

Cross Section of Sphere and Liquid Film

where

$$\int_0^{\pi} \sin^{1/3} \theta \, d\theta = \frac{\Gamma(2/3) \Gamma(1/2)}{\Gamma(7/6)} = 2.58 \quad (1-8)$$

2.2.2 Physical Absorption of a Single Gas in a Spherical

Liquid Film. The equation representing the physical absorption process of a gas in a spherical film may be derived by a simple steady state mass balance around an elemental section ABCD of the liquid film (Figure 1).

In making this balance it is assumed that, (i) transport by molecular diffusion in the direction of bulk flow, i.e., across the radial lines AB and CD is negligible, and (ii) transport of mass by convection, i.e., bulk flow across the streamlines AC and BD is negligible.

The net transport of material across the radial lines AB and CD by convection is:

$$2\pi R \sin \theta \, V_{\psi} \left[\frac{\partial C}{\partial \theta} \right]_{\psi} dx \, d\theta \quad (1-9)$$

The net material transferred by diffusion across the streamlines AC and BD is:

$$2\pi D \sin \theta \left\{ R^2 \left[\frac{\partial^2 C}{\partial x^2} \right]_{\theta} - 2R \left[\frac{\partial C}{\partial x} \right]_{\theta} \right\} dx \, d\theta \quad (1-10)$$

Under steady state conditions equations (1-9) and (1-10) may be equated to give:

$$\left[\frac{\partial^2 C}{\partial x^2} \right]_{\theta} - \frac{2}{R} \left[\frac{\partial C}{\partial x} \right]_{\theta} = \frac{V_{\psi}}{RD} \left[\frac{\partial C}{\partial \theta} \right]_{\psi} \quad (1-11)$$

Since the liquid film around the sphere is usually very thin, it may be assumed that:

$$\left[\frac{\partial^2 C}{\partial x^2} \right]_{\theta} \gg \frac{2}{R} \left[\frac{\partial C}{\partial x} \right]_{\theta} \quad (1-12)$$

Equation (1-11) then becomes

$$\left[\frac{\partial^2 C}{\partial x^2} \right]_{\theta} = \frac{V_{\psi}}{RD} \left[\frac{\partial C}{\partial \theta} \right]_{\psi} \quad (1-13)$$

The above equation has been solved by a number of authors [2,3,15].

The analysis of Davidson and Cullen [3] has been used for this investigation. The above authors considered the effect of the stretching of the liquid film and introduced a dimensionless length $y = \frac{x}{\Delta}$ into equation (1-13) to obtain:

$$\left[\frac{\partial^2 C}{\partial y^2} \right]_{\theta} = \frac{V_{\psi} \Delta^2}{RD} \left[\frac{\partial C}{\partial \theta} \right]_{\psi} \quad (1-14)$$

Substituting for V_{ψ} from equation (1-4) one obtains:

$$\left[\frac{\partial^2 C}{\partial y^2} \right]_{\theta} = \frac{V_o (1 - y^2) \Delta^2}{RD} \left[\frac{\partial C}{\partial \theta} \right]_{\psi} \quad (1-15)$$

Define a stream function $\psi(y)$ as

$$\psi(y) = \int_0^x V_\psi 2\pi(R+\Delta-x') \sin \theta \, dx' \quad (1-16)$$

By substituting for V_ψ from equation (1-4) and neglecting Δ and x' in comparison to R equation (1-16) may be represented as

$$\psi = \frac{3}{2} L (y - y^3/3) \quad (1-17)$$

Since ψ is a function of y only one may say that

$$\left(\frac{\partial C}{\partial \theta} \right)_\psi = \left(\frac{\partial C}{\partial \theta} \right)_y \quad (1-18)$$

and defining

$$\left(\frac{\partial \phi}{\partial \theta} \right)_y = \frac{R}{V_0 \Delta^2} \quad (1-19)$$

one obtains

$$D \left[\frac{\partial^2 C}{\partial y^2} \right]_\phi = (1-y^2) \left[\frac{\partial C}{\partial \phi} \right]_y \quad (1-20)$$

which is the final form of the differential equation derived by Davidson and Cullen [3].

The above authors considered two sets of boundary conditions to cover cases where the depth of penetration of the solute in the liquid film may be low or high.

(a) Low Depth of Penetration Model

For this case $y^2 \ll 1$ and equation (1-20) becomes

$$D \left[\frac{\partial^2 C}{\partial y^2} \right]_\phi = \left[\frac{\partial C}{\partial \phi} \right]_y \quad (1-21)$$

with boundary conditions

$$\left. \begin{array}{lll} (1) & \phi = 0; & y \geq 0; \quad C = C_o \\ (2) & \phi > 0; & y = 0; \quad C = C_i \\ (3) & \phi \geq 0; & y = \infty; \quad C = C_o \end{array} \right\} \quad (1-22)$$

The solution of equation (1-21) with the B.C. set (1-22) is

$$(C - C_o) = (C_i - C_o) \operatorname{erfc} \left[\frac{y}{2\sqrt{D\phi}} \right] \quad (1-23)$$

The total rate of gas absorption may thus be obtained from

$$G_s = \frac{3}{2} LD \int_0^{\phi_2} - \left(\frac{\partial C}{\partial y} \right)_{y=0} d\phi \quad (1-24)$$

$$\text{For a sphere } \phi_2 = \frac{2}{3} \times 1.68\pi \left[\frac{2\pi g}{3\nu} \right]^{1/3} \frac{R^{7/3}}{L^{4/3}} \quad (1-25)$$

Thus

$$G_s = (12 \times 1.68)^{1/2} \left[\frac{2\pi g}{3\nu} \right]^{1/6} \frac{R^{7/6}}{L^{1/3}} \frac{1}{D^{1/2}} (C_i - C_o) \quad (1-26)$$

(b) High Depth of Penetration Model

In this case y^2 may not be neglected in comparison

to 1 and the B.C. are:

$$\left. \begin{array}{lll} (1) & \phi = 0; & y \geq 0; \quad C = C_o \\ (2) & \phi > 0; & y = 0; \quad C = C_i \\ (3) & \phi \geq 0; & y = 1; \quad \frac{\partial C}{\partial y} = 0 \end{array} \right\} \quad (1-27)$$

B.C. (3) merely states that no solute crosses the solid sphere boundary.

Davidson and Cullen [3] adapted the solution of Pigford [16] and Vyazovov [17] for gas absorption in a liquid film flowing down a

wetted wall column. The solutions for the single sphere and the wetted wall column are equivalent so long as the value of ϕ_2 is the same for the two equations.

The total gas absorption rate may be expressed as a series given by:

$$G_s = L(C_i - C_o) \left[1 - \sum_{i=1}^n \beta_i \exp(-\gamma_i \alpha) \right] \quad (1-28)$$

$$\text{or } G_s = L(C_i - C_o) f(\alpha) \quad (1-28a)$$

$$\text{where } \alpha = 3D\phi_2 \quad (1-29)$$

The coefficients β_i and γ_i are reported in Table 1.

Davidson and Cullen [3] recommend use of equation (1-28) with coefficients as in Table 1 for cases where the outlet liquid saturation exceeds 40%.

Olbrich and Wild [15] extended the solution of Davidson and Cullen so that it may be used for both low and high depth of penetration cases. Their solution corresponds to equation (1-28) with ten terms being used in the series whereas Davidson and Cullen used only four. For high depths of penetration the calculated gas absorption rate using the coefficients of Davidson and Cullen or Olbrich and Wild is almost identical.

Equations (1-26) and (1-28) consider the surface area of the liquid in contact with the gas to be equivalent to the surface area of a dry sphere. Goettler [9] and Ratcliff and Reid [4] pointed out that the actual surface area of the liquid is larger than the area of a dry sphere owing to the thickness of the liquid film

TABLE 1

Coefficients for Series Solution for G_s
(Davidson and Cullen [3])

n	β_n	γ_n
1	0.7857	3.414
2	0.1001	26.21
3	0.03599	70.43
4	0.01811	136.5

flowing over it. Goettler used an average correction which was based on the average liquid depth over the complete sphere. The correction is of the form

$$\frac{A_A}{A_S} = 1 + 2.58 \frac{\Delta^+}{R} \quad (1-30)$$

where

A_A = corrected interfacial area

A_S = surface area of the dry sphere

Δ^+ = depth of the liquid film at the sphere equator given as

$$\Delta^+ = \left[\frac{3vL}{2\pi Rg} \right]^{1/3} \quad (1-31)$$

Equation (1-26) was used to estimate a starting value of diffusivity and this first estimate was used in equation (1-28) to generate an iterative scheme which was considered to have converged to a final value when two successive estimates of diffusivity did not vary by more than 0.5%.

Calculated diffusivities are very dependent on solubility data, and accurate values can only be obtained if very accurate solubility data are available. This is evident from equations (1-26) and (1-28) where C_i may be taken to be a saturation concentration of the gas in the liquid at the gas-liquid interface. The solubility of hydrogen in aminomethane at pressures up to 20 atm. and over the temperature range -62°C to 23°C has been determined by Moore [8]. The Henry's Law constant is given by

$$\ln H_2 = 4.1403 + 1.6612\beta - 0.1160\beta^2 \quad (1-32)$$

where

$$\beta = \frac{1000}{T(^{\circ}\text{K})} \quad (1-32a)$$

$$\text{and } P_2 = x_2 H_2 \quad (1-32b)$$

The viscosity of aminomethane has been determined as a function of temperature by several authors [18,19,20]. This data has been assimilated and a mean curve of viscosity vs. temperature has been reported by AECL [21].

2.3 Empirical Methods for Prediction of Diffusion Coefficients

Moore [8] has reviewed a number of correlations employed for the purpose of predicting diffusion coefficients of sparingly soluble gases in non-aqueous solvents. Only those correlations that have been used for comparison with data obtained during this investigation will be given here.

(a) Wilke-Chang Correlation [22]

The empirical form of this correlation is

$$\frac{D_{\mu 1}}{T} = 7.4 \times 10^{-8} \frac{(aM_1)^{1/2}}{V_2^{0.6}} \quad (1-33)$$

where 'a' is an "association parameter" which defines the effective molecular weight of the solvent. The "association parameter" must be determined from experimental diffusivity data for the solvent in question. Wilke and Chang [22] report a value of 2.6 for water and 1.0 for non-associated solvents.

(b) Lusis and Ratcliff Correlation [23]

The Lusis and Ratcliff correlation is of the form:

$$\frac{D_{\mu 1}}{T} = 8.52 \times 10^{-8} (V_1)^{1/3} \left[1.40 \left(\frac{V_1}{V_2} \right)^{1/3} + \left(\frac{V_1}{V_2} \right) \right] \quad (1-34)$$

This equation is reported to be applicable for the entire range of solvent and solute molar volumes but its applicability at temperatures substantially below 0°C is questionable owing to the lack of available data at low temperatures.

(c) Ferrell and Himmelblau Correlation [24]

This correlation was developed for the solution of sparingly soluble gases in water and as such one cannot expect it to predict accurate data for a non-aqueous solvent. In spite of this, it may be used to provide reasonable estimates of the diffusivity of hydrogen in ammonia. The correlation is of the form:

$$\frac{D_{\mu 1}^{\alpha_1}}{T} = 4.8 \times 10^{-7} \left[\frac{1 + \Lambda^{*2}}{V_2} \right]^{0.6} \quad (1-35)$$

where α_1 was reported by the authors to have an equality with $\frac{E_D}{E_{\mu}}$ if α_1 is computed from the relation

$$\alpha_1 = \frac{\sigma}{\left(\frac{V_2}{N} \right)^{1/3}} \quad (1-36)$$

σ in equation (1-36) is the collision diameter of the solute molecules.

Λ^* is the quantum parameter of Hildebrand et al. [25] which accounts for the presence of quantum effects when gases such as helium or hydrogen diffuse through liquids with high internal pressures.

Ferrell and Himmelblau [24] suggested the use of the theory of absolute reaction rates to provide a molecular model which could serve as a basis for correlation of diffusivities.

The expression of Eyring [26] for the molecular diffusion coefficient is written as:

$$D = A_1 T \exp \left(- \frac{E_D}{R^* T} \right) \quad (1-37)$$

$$\therefore \frac{d}{dT} \left[\ln \left(\frac{D}{T} \right) \right] = \frac{E_D}{R^* T^2} \quad (1-38)$$

A similar treatment of the corresponding expression for viscosity yields

$$\frac{d}{dT} [\ln(\mu)] = \frac{-E_\mu}{R^* T^2} \quad (1-39)$$

$$\therefore \frac{\frac{d}{dT} \left[\ln \left(\frac{D}{T} \right) \right]}{\frac{d}{dT} [\ln(\mu)]} = \frac{-E_D}{E_\mu}$$

$$\text{or } \frac{d}{dT} \left[\ln \left(\frac{D}{T} \right) \right] = \frac{-E_D}{E_\mu} \frac{d}{dT} [\ln(\mu)] \quad (1-40)$$

Integrating equation (1-40) with respect to T one obtains:

$$\ln \left(\frac{D}{T} \right) = \frac{-E_D}{E_\mu} \ln(\mu) + \ln(A_2) \quad (1-41)$$

where $\ln(A_2)$ is a constant of integration. A_2 is reported to be independent of temperature but it is a function of the properties of the solute and the solvent.

Accepting the equality of α_1 with $\frac{E_D}{E_\mu}$ equation (1-41) may be replaced by:

$$D = \frac{A_o T}{\mu \alpha_1} \quad (1-42)$$

Once again A_o is a function of the properties of the solute-solvent pair and μ is the viscosity of the solution. For sparingly soluble gases μ may be taken to be the viscosity of the solvent also.

The quantum parameter Λ^* of Hildebrand et al. [25] may be defined as:

$$\Lambda^* = \frac{h}{\sigma(m\epsilon)^{1/2}} \quad (1-43)$$

Ferrell and Himmelblau postulated that for sparingly soluble gases in water A_o would be represented by

$$A_o = \bar{a} \left[\frac{1 + \Lambda^{*2}}{V_2} \right]^b \quad (1-44)$$

Values of ' \bar{a} ' and ' b ' were determined by linear regression and the resulting expression for A_o when substituted in equation (1-42) yielded the final form of the correlation represented as equation (1-35). The authors have reported a much better agreement of equation (1-35) to their data than the correlation of Wilke-Chang [22].

CHAPTER 3

EXPERIMENTAL3.1 Apparatus

Moore [8] designed and built the basic equipment for the measurement of molecular diffusion coefficients of hydrogen in aminomethane. As mentioned earlier, preliminary measurements made by him indicated experimental difficulties. The apparatus was thus modified to improve its performance and more reliable data was obtained with it for this investigation. Detailed description of the equipment used may be obtained from Moore's thesis [8] and only a short review of the set-up is included here. Details of supporting equipment used such as:

- (a) The refrigeration system
- (b) The hydrogen purification system
- (c) The aminomethane purification unit
- (d) The vacuum system

are given in Moore's thesis.

A schematic diagram of the single sphere absorber is given in Figure 2.

The design of the single sphere absorption chamber was similar in concept to the absorber of Goettler [7,9] in that a laminar jet was used for introducing aminomethane onto the sphere. A number of modifications on the equipment used by the above authors were necessary due to the properties of aminomethane. A diagram of the absorption chamber is given in Figure 3.

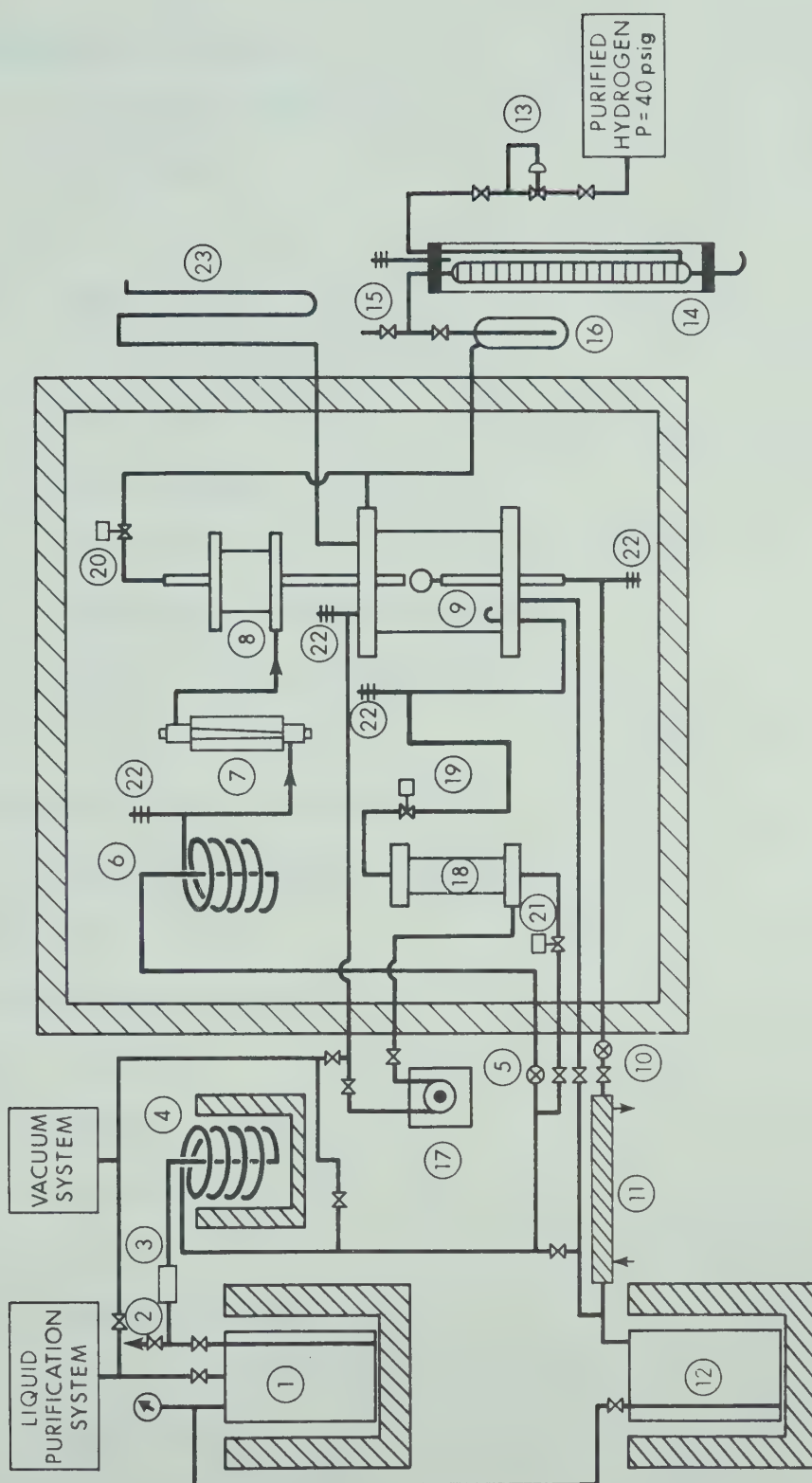


FIGURE 2
Schematic Diagram of Single Sphere Absorber

Symbols for Figure 2

1. Liquid Amine Feed Tank
2. Relief Valve
3. Glass Wool Filter
4. Liquid Feed Chiller
5. Liquid Feed Rate Control Valve
6. Liquid Feed Chiller
7. Liquid Rotameter
8. Liquid Distributor
9. Single Sphere Absorption Chamber
10. Take-Off Level Control Valve
11. Liquid Outlet Chiller
12. Spent Liquid Amine Dump Tank
13. Hydrogen Low Pressure Regulator
14. Soap Film Meter
15. Hydrogen Vent Valve
16. Soap Trap
17. Hydrogen Circulator
18. Hydrogen Saturator
19. Solenoid Valve S_1
20. Solenoid Valve S_2
21. Solenoid Valve (Hydrogen Saturator)
22. Thermocouples
23. Mercury Manometer

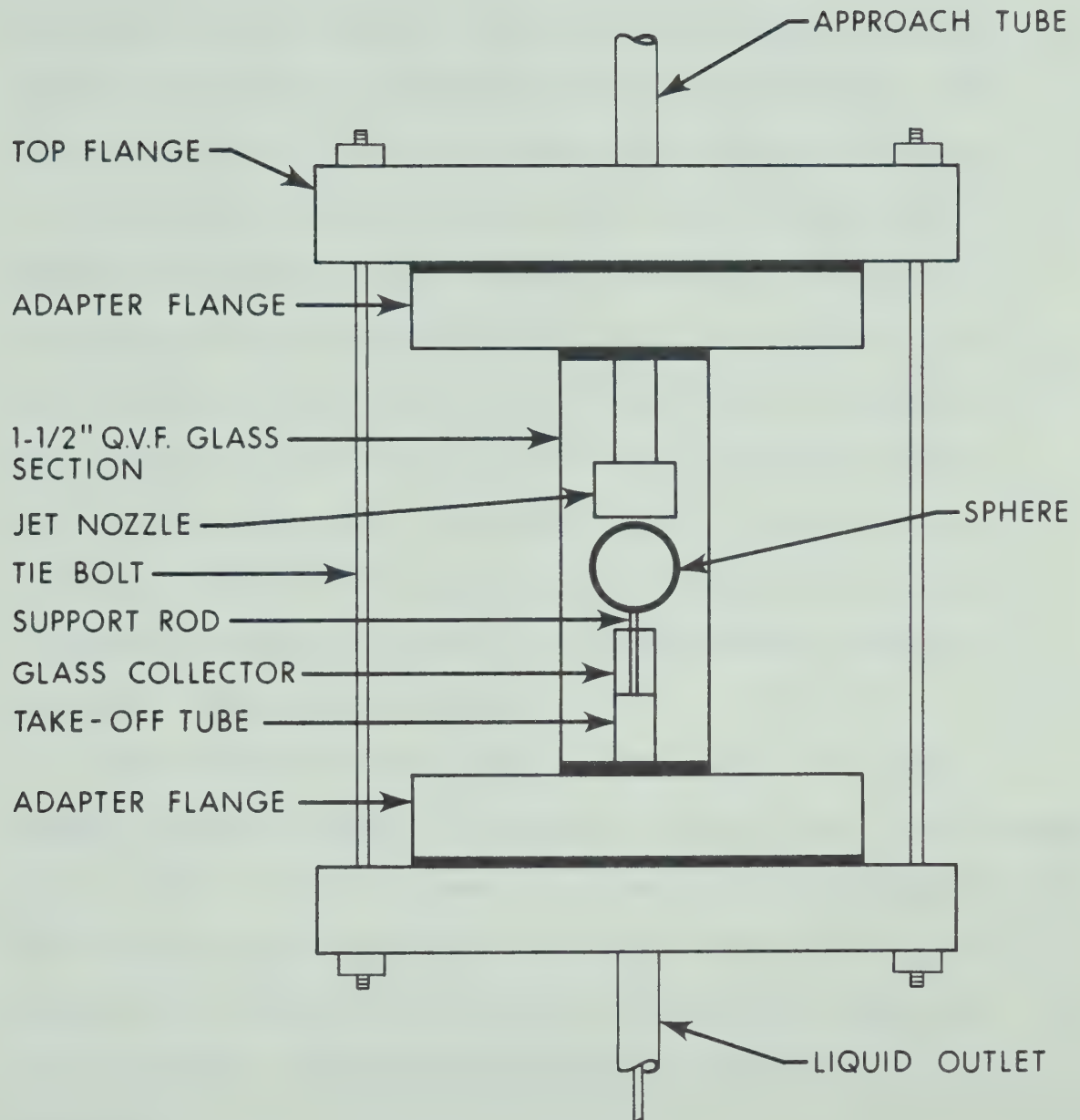


FIGURE 3

Schematic Diagram of Absorption Chamber

The laminar jet was designed in a similar manner to those of Goettler [9], Scriven [27,28] and Hatch [29]. The nozzle design was modified to incorporate the use of ruby watch jewels for the cylindrical throat sections. Their use was considered desirable because they could be accurately bored and press fitted into the nozzle caps. The nozzle diameter used for this work was 0.046 cm.

The spheres used in this study were 1 inch and 3/4 inch diameter ball bearings which had been softened by heat treating. They were suitably drilled so that they may be mounted on a 1/8 inch diameter shaft or support rod and had a 1/16 inch diameter mark machined on the top pole to facilitate aligning the laminar jet. Precise alignment of the laminar jet over the top pole of the sphere was achieved by an eccentric mechanism mounted in the top flange of the absorption chamber. Acetone was passed through the jet during the alignment procedure.

Liquid flowing over the sphere and the support rod passed through a glass collector cap mounted on a take off tube. This assembly passed through the absorber base flange before being connected to the liquid return line. The distance between the bottom of the sphere and the level of the outgoing liquid in the glass collector cap (take-off height) could be varied by moving the steel support rod up or down.

Details of the top flange housing, the eccentric mechanism and the bottom base flange may be obtained from Moore's thesis [8].

The support rod was roughened to enhance wetting and was centered in the liquid take-off tube by two teflon guides. The rod

passed through the base of the take-off tube and was attached to the frame supporting the entire absorption apparatus by a threaded adjustment nut which was used to adjust the sphere height relative to the floor of the absorber.

A 1/2 inch Swagelok connector was used to seal the glass connector cap to the top of the 1/2 inch stainless steel take-off tube. The take-off tube in turn was sealed to the base flange by an O-ring seal.

All the equipment, as shown in Figure 2, was fabricated out of 316 stainless steel except for those parts where visual observation was necessary. The latter parts were made of QVF glass sections and Pyrex glass. Neoprene was used exclusively for all gasketing material and O-rings. Zytel (Nylon) ferrules were used for glass to stainless steel Swagelok fittings.

The absorption chamber and the hydrogen saturator were enclosed in a refrigerated air bath to enable operation in the temperature range of -30°C to -20°C .

3.2 Operation and Procedure

Fresh aminomethane was purified by contacting with lithium metal to remove water followed by a simple flash vacuum distillation. Aminomethane has a normal boiling point of -6.33°C and thus it could be fed to the absorber under its own vapour pressure by maintaining the feed tanks close to room temperature. The liquid feed was precooled before entering the refrigerated air bath to minimize thermal gradients, and after leaving the absorber it was collected in a dump tank immersed in liquid nitrogen. The amine was subse-

quently degassed and reused. In order to obtain an unimpeded flow through the exit liquid line to the dump tank, it was necessary to chill the liquid line through the use of a concentric tube cooler. When this was not done, a back pressure was set up in the liquid line and the flow of aminomethane was impeded. The liquid feed and liquid outlet control valves were both "Whitey 21RS4-316" micrometering valves and their use allowed excellent flow control.

Hydrogen was introduced through a "Matheson Model 70A" low pressure regulator. The absorption chamber was pressurized to a preselected system pressure which was recorded with a mercury manometer and the gas phase was saturated with aminomethane prior to a run. The hydrogen absorption rate was measured with a soap film meter constructed from a 50 c.c. burette with 0.10 c.c. graduations.

The operating variables that required consideration were liquid flow rate, absorber temperature, absorber pressure, sphere size, distance between the sphere and the feed jet (i.e. jet length), and the distance between the base of the sphere and the liquid level in the take-off tube (i.e. take-off height).

The liquid flow rate should be such that laminar flow is maintained on the sphere surface. Although the flow of liquids in a thin film over a solid surface has received a large amount of attention [30,31], the criterion for conditions that will eliminate convective mixing is not well defined. Previous work with gas-water systems [3,4,9] based on a Reynolds number criterion evaluated

at the sphere equator suggests that a film of aminomethane should be laminar at flow rates upto 1.0 cc/sec at temperatures from -15°C to -30°C . However, experimental data which agreed with the absorption model could only be obtained at liquid flow rates upto approximately 0.45 cc/sec or at Reynolds numbers less than about 50. The occurrence of surface activity was much more apparent on the support rod than on the sphere and it was generally observed that when ripples were present on the rod, they were also present on the sphere.

The Reynolds number criterion, however, does not incorporate the effects of surface tension of the liquid which appear to affect the rippling phenomena. The surface tension of aminomethane is about one third that of water and this significant difference could well be responsible for reducing the upper limit of the Reynolds number for stable flow over the sphere absorber. The effect of surface tension needs to be studied in more detail than has been done at present before conclusive evidence in this direction is available.

The laminar jet was operated within its upper and lower limits of stability. These limits have been defined and observed by Goettler [9] and reconfirmed by Moore [8]. A jet length of 2.0 mm and a take-off height of 1.25 cm was used throughout this investigation.

The startup and operating procedure for the single sphere absorber is essentially the same as that reported by Moore [8] with some modifications. Details of this procedure are included in Appendix B1.

The manner in which the data obtained from a run was used to determine the diffusivity of hydrogen in aminomethane using equations

(1-28) and (1-29) has been described in detail by Moore [8]. From the measured values of the different variables indicated earlier like liquid flow rate, temperature and hydrogen absorption rate, the molecular diffusion coefficient D was taken to be the value which minimized the function

$$E = \sum_{k=1}^N \left| [(G_s)_k - (L(C_i - C_o) f(\alpha))_k] \right| \quad (1-45)$$

where N = number of determinations.

The experimental data is reported in Appendix A1.

CHAPTER 4

RESULTS

Experimental measurements of the rate of physical absorption of hydrogen in aminomethane were taken on the 3/4 inch and the 1 inch spheres. These are reported in Tables 2 and 3 along with the calculated values of the diffusion coefficient.

Figure 4 is a plot of the hydrogen absorption rate corrected to 1 atmosphere hydrogen partial pressure versus the liquid flow rate over the sphere at -29°C . Average values of the gas flow meter temperature and system temperature were used to generate the plots shown. The gas flow meter temperature is required to estimate the appropriate gas density for use in expressing mass flow rates. The maximum deviation of both these temperatures about the mean over a period of approximately four hours, did not exceed $\pm 0.2^{\circ}\text{C}$. The solid curves shown represent the simulated variation of the hydrogen absorption rate versus the liquid flow rate, using the high depth of penetration model, for two assumed values of the diffusion coefficient. This was done using a computer program written by Moore [8]. The plot depicts the degree of agreement of the absorption rates with those predicted by the model.

Figure 5 shows the variation of the absorption rate with the length of the exposed support rod. This plot indicates that a length of 1.25 cms. corresponds to the case where the stagnant layer lies at the junction of the sphere and the support rod and shorter lengths would cause it to move on to the sphere.

The logarithm of the diffusion coefficient as determined with

TABLE 2

Experimental Results for the Diffusivity of Hydrogen
in Liquid Aminomethane Using the 3/4 inch Sphere

T(°C)	L (cc/sec)	G(1 atm)×10 ⁵ (gms/sec)	% Saturation	D × 10 ⁶ (cm ² /sec)
-25.9	0.349	0.157	75.6	106.3
-25.2	0.350	0.161	76.8	110.9
-25.8	0.303	0.146	80.7	105.4
-26.6	0.351	0.156	74.9	105.0
-27.8	0.336	0.149	75.6	102.1

TABLE 3

Experimental Results for the Diffusivity of Hydrogen
in Liquid Aminomethane Using the 1 inch Sphere

T(°C)	L (cc/sec)	G(1 atm)×10 ⁵ (gms/sec)	% Saturation	D × 10 ⁶ (cm ² /sec)
-30.0	0.400	0.192	83.9	91.4
-29.9	0.378	0.188	86.5	94.1
-29.0	0.403	0.196	84.3	93.4
-28.9	0.372	0.188	87.3	94.8
-26.7	0.402	0.207	86.9	102.2
-26.7	0.405	0.203	84.9	95.1
-24.0	0.418	0.218	85.8	101.8
-23.9	0.418	0.219	86.1	102.7
-23.9	0.410	0.217	87.0	104.0
-20.0	0.426	0.235	87.0	107.7
-20.0	0.421	0.235	87.9	110.0

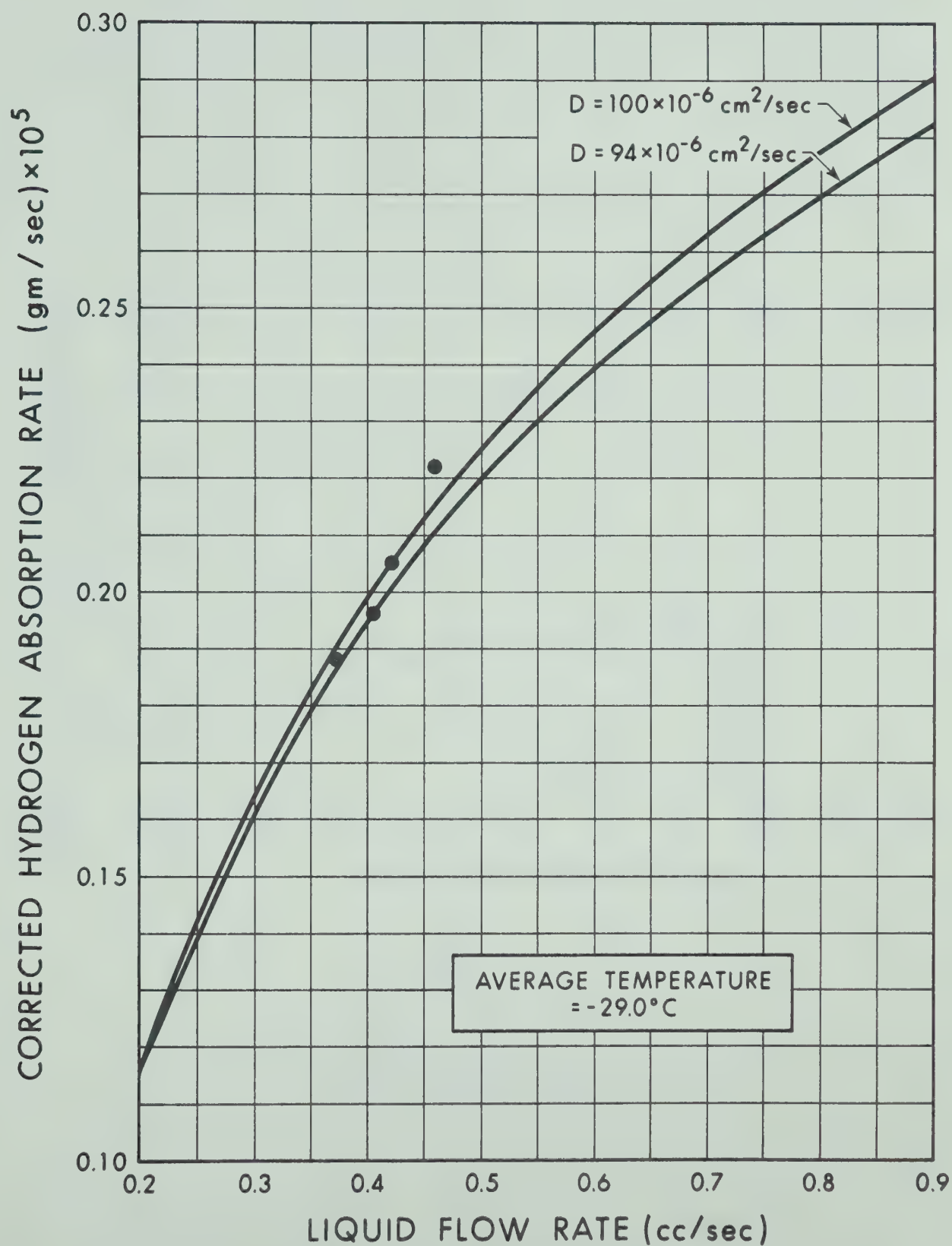


FIGURE 4

Rate of Absorption of Hydrogen in Aminomethane at -29°C on a 1 inch Sphere

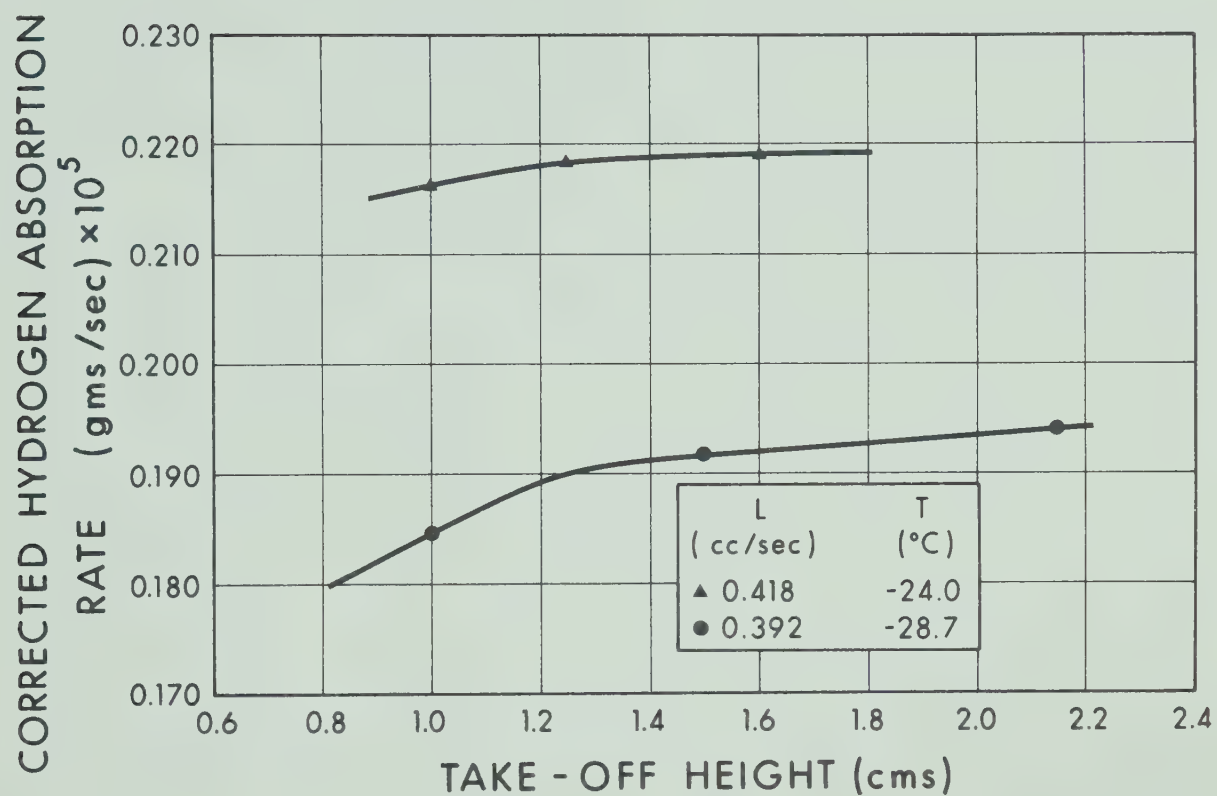


FIGURE 5

Effect of Take-off Length on
Hydrogen Absorption Rate

the 1 inch sphere is plotted versus the reciprocal absolute temperature in Figure 6. Experimental data for hydrogen ammonia [32] is also shown for comparison.

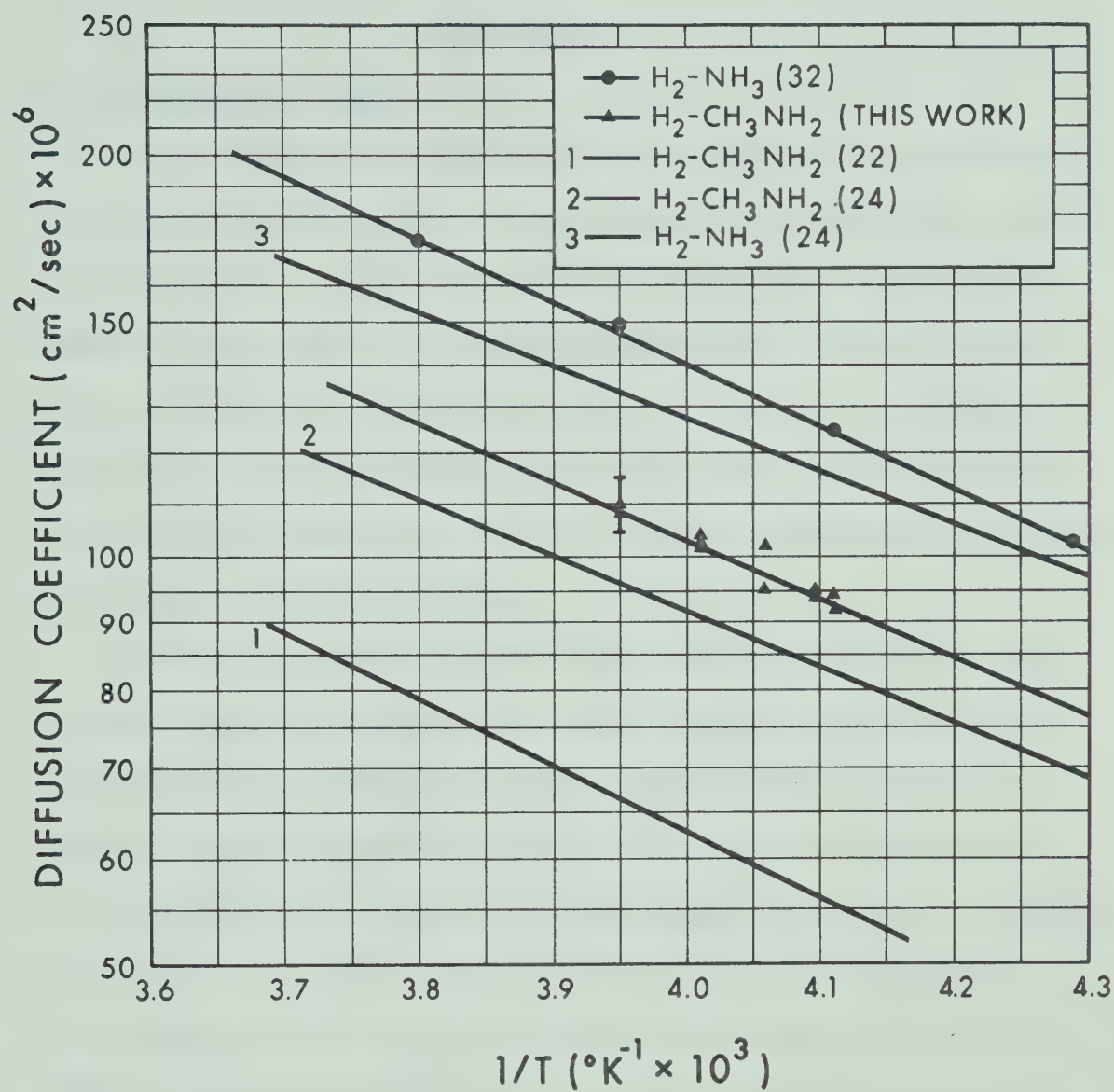


FIGURE 6

Comparison of Predicted and Experimental Diffusivities for
Hydrogen in Ammonia and Aminomethane

CHAPTER 5

DISCUSSION5.1 Experimental Data

It is apparent from Figure 4 that for liquid flow rates where the absorption data agree with the theoretical model (<0.45 cc/sec), a small change in the measured absorption rate will cause a large change in the calculated diffusion coefficient. This also means that, at flow rates of about 0.4 cc/sec a 2% error in the measurement of the hydrogen absorption rate will cause a 6% error in the value of D , and emphasizes the importance of having very good control of the experimental conditions.

Use of the $3/4$ inch diameter sphere was prompted by the fact that the resulting lower saturations of the outgoing liquid might provide better agreement with the absorption model by reducing possibilities of high errors occurring at very high saturations. As may be seen from Tables 2 and 3 the values of diffusivity obtained were always higher than those obtained using the 1 inch sphere. The reason for this is uncertain but may have been due to an end effect on the take-off rod.

Deviations of the measured absorption rates from the theoretical model for liquid flow rates in excess of 0.45 cc/sec are probably due to convective mixing in the liquid film around the sphere. Although, at these flow rates, considerable activity was observed on the take-off level, the liquid film around the sphere appeared smooth. The condition of the take-off level as observed visually, was therefore taken to be a more reliable criteria for detecting

convective mixing than a similar observation of the liquid film around the sphere.

The reported values of the take-off length used in previous investigations [3,4,7,9,33] with gas-water systems cover a fairly wide range. Lynn et al. [33] indicate that the allowable take-off length varies inversely as the liquid flow rate and report values ranging from 0.1 cm for high to 2.0 cms for low flow rates. Davidson and Cullen [3] took all their data at 1.5 cms though their data indicates that 1.0 cms would also have been adequate. Goettler [7,9] and Ratcliff and Reid [4] used values of 2.0 and 4.0 cms respectively. Their data indicates no discernable dependence of the take-off length on liquid flow rate. It is apparent that each investigator repeated the original experiment of Lynn et al. to determine the take-off height best suited to their system. It is probable therefore that apart from the hydrodynamics, system properties and general surface characteristics may also play a role in deciding the best take-off height for any one investigation. The value best suited for this investigation was 1.25 cms.

When the stagnant layer is on the support rod the velocity profile on the rod may be assumed to be fully parabolic. This implies that the rate of gas absorption on the rod is reduced considerably. A plot of the gas absorption rate versus take-off height will thus show a decrease in slope when the stagnant layer reaches the junction between the bottom of the sphere and the support rod. If in addition, the surface area of the rod exposed for gas absorption is very much smaller than that of the sphere,

the slope of the plot will tend towards a limiting value of zero. In such an event using a value of take-off height somewhat larger than that for which the stagnant layer is at the bottom of the sphere would cause a negligible error in the measured gas absorption rate. The data of Goettler [7,9], Davidson and Cullen [3] and Ratcliff and Reid [4] apparently fall in this category. If, however, the surface area on the exposed rod is such that the gas absorbed on it could form a considerable part of the total, then the take-off level should be maintained such that the stagnant layer is at the bottom of the sphere. This condition would minimize errors in the measured gas absorption rate and thus in the calculated value of the diffusivity.

Ratcliff and Reid [4] have reported an equation for the rate of gas absorption in a liquid flowing over a sphere assuming the velocity profile in the liquid film to be fully parabolic. The equation is of the form:

$$G_s = \frac{3}{2.68} (3 \times 1.68)^{2/3} \left[\frac{\pi^4 g}{6v} \right]^{2/9} R^{14/9} D^{2/3} L^{1/9} (C_i - C_o) \quad (1-46)$$

They assumed the low depth of penetration model of Davidson and Cullen [3]. The ratio η of the absorption rates given by equations (1-46) and (1-26) thus represents the reduction of mass transfer due to the stagnant layer. Since the equation for gas absorption over a sphere was derived [3] using the approach of Pigford [16] and Vyazovov [17] for gas absorption over a cylinder, the above ratio is identical for a cylinder of an equivalent radius. It may also be assumed that the ratio is the same for both the low

and the high depth of penetration models. Table 4 gives the calculated values of the diffusivity assuming the exposed rod to be (i) completely inactive ($\eta=0$), (ii) completely active ($\eta=1.0$) and (iii) partially active ($\eta=\eta$). It is seen that under condition (iii) about 1% of the total measured absorption occurs on the support rod and this yields diffusivity values about 3.5% lower than those under condition (i).

It was suggested earlier that the diffusivity values obtained using the 3/4 inch sphere were always high possibly because of an end effect on the support rod. Table 5 gives the calculated values of the diffusivity in a manner similar to that in Table 4 for the 1 inch sphere. It is apparent that the end effect can be much more significant for the 3/4 inch sphere than for the 1 inch sphere. The diffusivities obtained under condition (iii) are within 3% of the corresponding values obtained using the 1 inch sphere. In the range of liquid flow rates investigated the average values of η obtained with the 1 inch and 3/4 inch spheres were 0.3024 and 0.3157 respectively. The 1 inch sphere data reported in Figure 6 corresponds to the case where the support rod is considered inactive (i.e. $\eta=0$). The reliability of the data being within $\pm 5\%$ it was considered unnecessary to incorporate condition (iii).

Moore [8] has indicated that the model of Davidson and Cullen [3] or Olbrich and Wild [15] is sensitive when the liquid saturation levels get high resulting in an increasing possibility of errors in the diffusion coefficient. A detailed derivation of the equations involved in developing the error analysis of the data obtained during this investigation is given in Appendix C1. The final form

Estimation of the Activity on the Support Rod and its
Effect on the Diffusion Coefficients
Obtained from the 1 inch Sphere

* % Abs. = Percent Absorption, on the rod, of the total gas absorbed.

Estimation of the Activity on the Support Rod and its Effect on the Diffusion Coefficients

Obtained from the 3/4 Inch Sphere

* % Abs. = Percent Absorption, on the rod, of the total gas absorbed.

of the error equation is

$$\left(\frac{\alpha_D}{D}\right)^2 = (Z - 4/3)^2 \left(\frac{\alpha_L}{L}\right)^2 + Z^2 \left(\frac{\alpha_{C_i - C_o}}{C_i - C_o}\right)^2 + Z^2 \left(\frac{\alpha_{G_s}}{G_s}\right)^2 + \frac{1}{9} \left(\frac{\alpha_v}{v}\right)^2 \quad (1-47)$$

where α_D , α_L , $\alpha_{C_i - C_o}$, α_{G_s} and α_v are the standard errors of the diffusivity, liquid flowrate, concentration driving force, gas absorption rate and viscosity respectively. Z is defined as

$$Z = \frac{f(\alpha)}{\alpha\beta(\alpha)} \quad (1-47a)$$

$f(\alpha)$ and α are as defined by equations (1-28a) and (1-29) and $\beta(\alpha)$ is given as

$$\beta(\alpha) = \frac{d f(\alpha)}{d\alpha} \quad (1-47b)$$

It may be noticed that as the saturation level approaches 100%, $f(\alpha) \rightarrow 1$, $\beta(\alpha) \rightarrow 0$ and $Z \rightarrow \infty$ which implies that $\left(\frac{\alpha_D}{D}\right) \rightarrow \infty$ at high saturations. Examining these equations it is also apparent that $\left(\frac{\alpha_D}{D}\right) \rightarrow \infty$ as $\alpha \rightarrow \infty$ and consequently as $L \rightarrow 0$. This implies that the saturation level of 100% is a limiting value at a limiting liquid flowrate of zero. Figure 7 is a plot of α vs. L over a liquid flow range of 0 to 0.65 cc/sec. The saturation levels have also been indicated relative to the liquid flow rate. It is apparent that $\frac{d\alpha}{dL}$ is very large at low values of L where the errors in diffusivity would indeed be large, but $\frac{d\alpha}{dL}$ decreases sharply with increasing liquid flow rate. In the range of flow rates corresponding to this

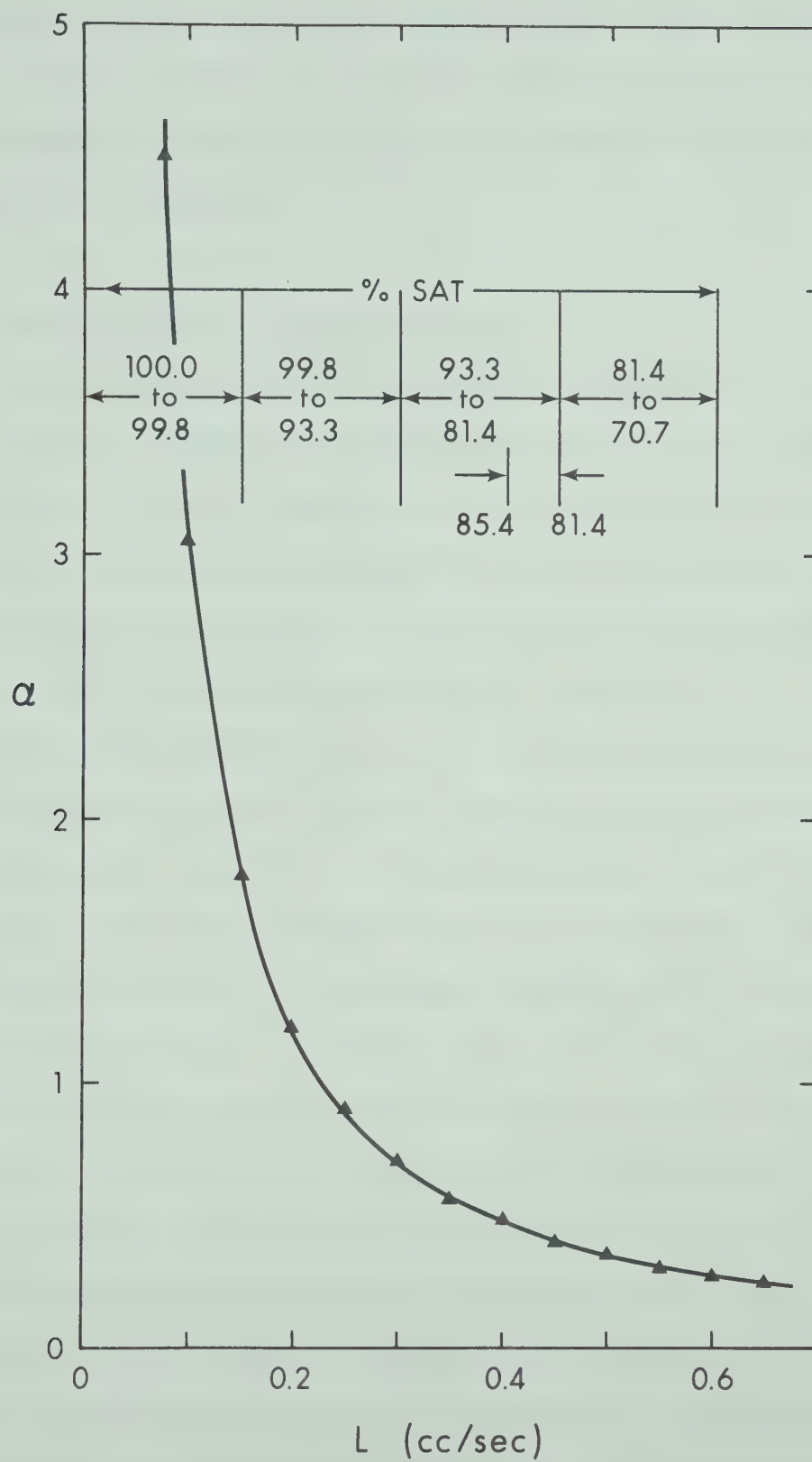


FIGURE 7

Effect of Liquid Flow Rate on the Transformation Parameter α

investigation (i.e. saturation levels of 80 to 85%) the value of $\frac{d\alpha}{dL}$ is not very different from that at flow rates of 0.65 cc/sec. The reproducibility of the model in this region is therefore thought to be adequate.

5.2 Experimental vs. Estimated Values

Several semi-empirical correlations are available which are suitable for estimating the diffusivities of sparingly soluble gases in liquids. Figure 6 compares the measured diffusivities with values predicted using the Wilke-Chang [22] and Ferrell and Himmelblau [24] correlations. A comparison is also made with the experimental data of Haul and Putzbach [32] for hydrogen in ammonia.

Moore [8] indicated that the correlation of Lysis and Ratcliff [23] was best suited for the data obtained with the hydrogen-aminomethane system. The diffusivity data obtained by Moore was, however, preliminary and further work during this investigation indicated that the correlation of Ferrell and Himmelblau [24] is better suited for both the hydrogen aminomethane and hydrogen-ammonia systems. Despite the fact that the equation of Ferrell and Himmelblau was developed for water, the estimated values of the diffusivity of hydrogen in aminomethane using this equation were found to be within 12% of the experimental values obtained during this investigation. In addition, the deviation of the estimated values from the experimental data was approximately constant over the entire range of temperature investigated. Although, the average deviation obtained using the Lysis and Ratcliff correlation was 11%, the errors at higher temperatures were larger than those at lower temperatures. In other words,

a plot of diffusivity vs. temperature as shown in Figure 6 is not parallel to the mean line through the experimental data. For the hydrogen-ammonia system the equation of Ferrell and Himmelblau predicts values of diffusivity that are low, on an average, by about 9%, the deviation being about 12% at -10°C and about 4.5% at -40°C . In comparison, the equation of Lusis and Ratcliff predicts values that are low by about 19% through the entire range of -10°C to -40°C . The experimental data of Haul and Puttbach [32] was used for comparison.

It is evident from Figure 6 that the correlation of Wilke-Chang [22] with an assumed association parameter of 1.0 is quite unsuitable for estimating the diffusivity of hydrogen in aminomethane. A similar situation is encountered for the hydrogen-ammonia system.

The Wilke-Chang correlation employs an association parameter which accounts for the effective molecular weight of the solvent. In the absence of more reliable data, a value of 1.0 was used for the curve presented in Figure 6. In general, predictions obtained from the Wilke-Chang equation are poor when the solute gas is hydrogen. The experimental data for the hydrogen-aminomethane, hydrogen-water [24] and hydrogen-ammonia [32] systems were used to evaluate average apparent association parameters that may be used in the Wilke-Chang equation for predicting data for these and other similar systems. The average apparent association parameters are given in Table 6. Molar volumes for this correlation and the correlation of Lusis and Ratcliff were estimated by the method of Le Bas [34].

TABLE 6

Average Apparent Association Parameters for
the Wilke-Chang Equation

System	Average Apparent Association Parameter $\pm 2 \sigma$	Reference of Experimental Data Used
$\text{H}_2\text{-H}_2\text{O}$	4.4 ± 1.2	Ferrell & Himmelblau [24]
$\text{H}_2\text{-CH}_3\text{NH}_2$	2.7 ± 0.2	This Work
$\text{H}_2\text{-NH}_3$	4.1 ± 0.4	Haul and Puttbach [32]
$\text{D}_2\text{-NH}_3$	3.7 ± 0.2	Haul and Puttbach [32]

It was pointed out earlier that Ferrell and Himmelblau [24] used the theory of absolute reaction rates to arrive at a generalised correlation that expressed the change of diffusivity with temperature. The generalised form of the equation was given as

$$D = A_0 \frac{T}{\mu_1^{\alpha_1}}$$

or $\frac{D\mu_1^{\alpha_1}}{T} = A_0$ (1-48)

where A_0 is a constant for a particular solute-solvent pair. This is in contrast to the Stokes-Einstein [35] or the Eyring [26] models which suggest that $\frac{D\mu_1}{T}$ is a constant for a particular size of the solute molecule and for a particular solvent. Ferrell and Himmelblau indicated that $\frac{D\mu_1}{T}$ tends to decrease with an increase in temperature for the hydrogen-water and helium-water systems. The same fact is borne out for the hydrogen-aminomethane system. Average values of $\frac{D\mu_1^{\alpha_1}}{T}$ and $\frac{D\mu_1}{T}$ are given for different temperatures in Table 7. A word of caution is, however, in order with regards to the use of Table 7. The experimental data have been obtained between the temperature range of -20°C to -30°C but Table 7 includes values at -10°C and -40°C which were obtained by extrapolating the mean line of the D vs. $1/T$ curve shown in Figure 6.

In order to take account of the presence of quantum effects in the diffusion of lighter gases dissolved in liquids, the quantum parameter

TABLE 7

Comparison of $\frac{D\mu_1^{\alpha_1}}{T}$ and $\frac{D\mu_1}{T}$
for the Hydrogen-Aminomethane System

$T (^{\circ}\text{K})$	$\frac{D\mu_1^{\alpha_1}}{T} \times 10^7$	$\frac{D\mu_1}{T} \times 10^7$
263	1.68	1.34
253	1.68	1.37
243	1.66	1.39
233	1.65	1.41

Λ^* of Hildebrand et al. [25] was used to give the following equation:

$$\frac{D\mu_1^{\alpha_1}}{T} = A_o = \bar{a} \left[\frac{1 + \Lambda^{*2}}{V_2} \right]^b \quad (1-44)$$

Although Ferrell and Himmelblau [24] used this equation for predicting diffusivities of sparingly soluble gases in water, in principle there is a set of constants \bar{a} and b for each solvent.

Average values of $\frac{D\mu_1^{\alpha_1}}{T}$ were determined from the data of Haul and Puttbach [32] for hydrogen-ammonia and deuterium-ammonia systems along with the values for hydrogen-aminomethane obtained from the best fit line of Figure 6. These are plotted vs. $\left[\frac{1 + \Lambda^{*2}}{V_2} \right]$ on Figure 8. The best values of \bar{a} and b determined from this plot are given as

$$\bar{a} = 4.66 \times 10^{-7}$$

$$\text{and } b = 0.53$$

The general equation (1-44) thus becomes

$$D = 4.66 \times 10^{-7} \frac{T}{\mu_1^{\alpha_1}} \left[\frac{1 + \Lambda^{*2}}{V_2} \right]^{0.53} \quad (1-49)$$

The molar volumes of the solute species used in this equation are as reported by Scott [36].

Equation (1-49) was used to predict the diffusivities of hydrogen, hydrogen deuteride and deuterium in aminomethane and ammonia. Representative values of the diffusion coefficient using this equation are compared with available experimental data in Table 8. The predicted data are

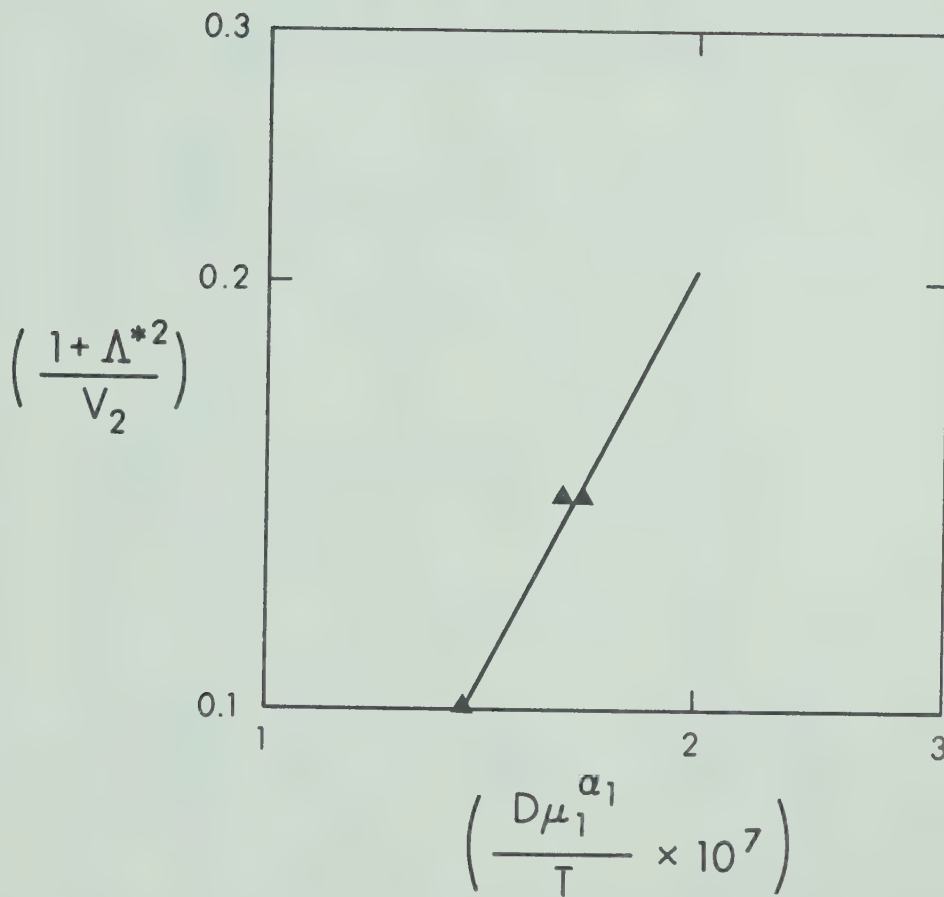


FIGURE 8

Estimation of Best Parameters for Equation (1-44)

System	$D \times 10^6$ (cm ² /sec) Experimental	$D \times 10^6$ (cm ² /sec) Eqn. (1-49)	V_2 (36) (cc/gm-mole)	α_1	Λ^*
H ₂ -CH ₃ NH ₂	92.3 (this work)	91.5	28.40	0.8215	1.729
HD-CH ₃ NH ₂	-	83.1	26.41	0.8388*	1.412
D ₂ -CH ₃ NH ₂	-	79.1	24.84	0.8533	1.223
H ₂ -NH ₃	124.7 (32)	128.5	28.40	0.8215	1.729
HD-NH ₃	-	117.5	26.41	0.8388*	1.412
D ₂ -NH ₃	111.5 (32)	112.5	24.84	0.8533	1.223

* σ value for HD taken as
mean of H₂ and D₂ values

TABLE 8

Estimated vs. Experimental Values of Diffusivity of
Hydrogen in Liquid Aminomethane and Ammonia at -30°C

within 5% of the experimental values. It is suggested that this equation be used to predict diffusivities of these systems in absence of experimental data.

5.3 Hydrodynamics

In order to be able to use the models of Davidson and Cullen [3] for evaluating the diffusivity of hydrogen in aminomethane, it is necessary that the flow over the sphere absorber be laminar. This is evident from the fact that both the low depth and the high depth of penetration models assume the film thickness around the ball to be represented by Nusselt's equation of flow over a flat plate [12].

Based on a Reynolds number criteria the data of Davidson and Cullen [3] and that of Goettler and Pigford [9] indicate that the condition of ripple free flow was maintained for values of Re in excess of 110. In comparison with this, the experimental data of a number of other authors [37-42] have indicated that wave inception begins on the liquid at extremely low flow rates well within the viscous flow region. Kapitza [43] has deduced that the Reynolds number at wave inception is given by

$$Re_1 = 2.4 \left[\frac{\delta^3}{g\nu^4} \right]^{1/11} \quad (1-50)$$

and has shown that in the pseudo laminar region for Reynolds numbers $Re > Re_1$ the velocity profile in a liquid film flowing over a vertical plate remains parabolic (as derived by Nusselt), but the mean film thickness is given by

$$\Delta = \left[\frac{2.4 \nu \Gamma_v}{g} \right]^{1/3} \quad (1-51)$$

The work of Tailby and Portalski [44-48] has contributed to a better understanding of the flow of liquid films. Portalski defines the following flow regimes with increasing liquid flow rate [47]:

- (i) Steady Laminar (no waves or ripples)
- (ii) Pseudo Laminar (wavy flow)
- (iii) Transition
- (iv) Pseudo Turbulent
- (v) Turbulent

(i) and (ii) constitute what has been known as the viscous or laminar flow regime, and (iv) and (v) constitute the turbulent regime. Portalski [47] suggests that Nusselt's equation applies only in the steady laminar region but not in the pseudo laminar regime where Kapitza's equation represents the experimental data better. Beyond the pseudo laminar region even Kapitza's equation deviates from experimental data considerably. He also indicates that the physical properties of the system, namely specific gravity, viscosity and surface tension affect the film thickness and suggests that in the pseudo laminar region as the surface tension becomes smaller the deviation between the values predicted by Nusselt's and Kapitza's equation becomes smaller. This implies that the use of Nusselt's equation in the pseudo laminar region for a system such as aminomethane could well be justified.

In order to establish the above regimes firmly, however, it is necessary that more work be done with systems where effects of viscosity, specific gravity and surface tension can be independently investigated through actual measurements of the liquid film thickness.

For the flow of liquid aminomethane over the sphere absorber it was

found that the maximum Reynolds number that could be attained without any rippling as seen through the naked eye corresponded to about 50.

CHAPTER 6

CONCLUSIONS

The single sphere absorber has been used to obtain reasonable values of the molecular diffusion coefficient for hydrogen in aminomethane. The accuracy of the reported diffusivities is dependent upon the careful control of experimental conditions, on the accuracy of solubility and viscosity data, and on the applicability of the hydrodynamic model. It is estimated to be within the $\pm 5\%$ range reported by others who have used the sphere absorber.

Agreement with the theoretical model of Davidson and Cullen [3] was obtained only for liquid flow rates where the depth of penetration of the solute gas into the liquid film was high. Deviations from the model are thought to be due to convective mixing. Surface tension may be an important factor in determining allowable flow rates, but additional work is required to establish criteria useful for predicting the onset of convective mixing in films over spherical surfaces.

The method suggested by Ferrell and Himmelblau [24] has been used to correlate experimental data for the diffusivities of hydrogen in aminomethane and ammonia. Equation (1-49) is recommended for use in estimating the diffusion coefficients for hydrogen, hydrogen deuteride and deuterium in aliphatic amines.

NOMENCLATURE

A	interfacial area (cm^2)
A_A	corrected interfacial area (cm^2)
A_s	surface area of a dry sphere (cm^2)
A_o	a constant for a given solute-solvent pair defined by equations (1-42) and (1-44) $\left(\frac{\text{gms cm}}{\text{sec}^2 \text{ } ^\circ\text{K}} \right)$
A_1	constant in Eyring's equation (1-37)
A_2	constant of integration in equation (1-41)
a	association parameter in equation (1-33)
\bar{a}	constant in equation (1-44)
b	exponent in equation (1-44)
C	concentration of solute ($\frac{\text{gms}}{\text{cm}^3}$)
C_i	concentration of solute at the interface ($\frac{\text{gms}}{\text{cm}^3}$)
C_o	concentration of solute in the bulk liquid ($\frac{\text{gms}}{\text{cm}^3}$)
C_o'	concentration of solute in the bulk liquid leaving the nozzle ($\frac{\text{gms}}{\text{cm}^3}$)
D	diffusion coefficient of the dissolved solute ($\frac{\text{cm}^2}{\text{sec}}$)
d	diameter of take-off tube (cm)
d_j	diameter of the jet (cm)
E	given as the function defined in equation (1-45)
E_D	energy of activation for diffusion ($\frac{\text{cal}}{\text{gm-mole}}$)
E_μ	energy of activation for viscosity ($\frac{\text{cal}}{\text{gm-mole}}$)
G	rate of absorption of the solute gas in the liquid ($\frac{\text{gms}}{\text{sec}}$)
$G(1 \text{ atm})$	rate of absorption of solute gas corrected to 1 atm solute partial pressure ($\frac{\text{gms}}{\text{sec}}$)

G_j	rate of absorption of solute gas in the liquid jet ($\frac{\text{gms}}{\text{sec}}$)
G_s	rate of absorption of solute gas in liquid over the sphere ($\frac{\text{gms}}{\text{sec}}$)
G_A	rate of absorption of solute gas in liquid over the sphere after area correction due to surface film ($\frac{\text{gms}}{\text{sec}}$)
G_T	rate of absorption of solute gas due to a temperature fluctuation ($\frac{\text{gms}}{\text{sec}}$)
G_{TL}	rate of absorption of solute gas due to a take-off level fluctuation ($\frac{\text{gms}}{\text{sec}}$)
g	acceleration due to gravity $\left(\frac{\text{cm}}{\text{sec}^2} \right)$
H_2	Henry's Law coefficient ($\frac{\text{atm}}{\text{mole fraction}}$)
h	Planck's constant (erg-sec)
h_j	height or length of jet (cm)
h_{TL}	take-off height (cm)
L	liquid flow rate ($\frac{\text{cm}^3}{\text{sec}}$)
M_1	molecular weight of solvent ($\frac{\text{gms}}{\text{gm-mole}}$)
m	molecular mass (gms)
N	Avogadro's number ($\frac{\text{atoms}}{\text{mole}}$)
n	number of moles
n	total number of terms in equation (1-28)
P_1	vapour pressure of the solvent (atm)
P_2	partial pressure of solute gas (atm)
P_T	total system pressure (atm)
Q_H	volumetric flow rate of solute gas ($\frac{\text{cm}^3}{\text{sec}}$)
R	radius of sphere (cm)

R^*	gas constant ($\frac{\text{cal}}{\text{gm-mole } ^\circ\text{K}}$)
Re	Reynolds number
Re_1	Reynolds number at wave inception
T	temperature ($^\circ\text{K}$)
T_A	absorber temperature ($^\circ\text{C}$)
T_H	hydrogen soap-meter temperature ($^\circ\text{C}$)
t	contact time (sec)
V	volume of absorption system (cm^3)
V_s	volume of absorption system excluding take-off volume (cm^3)
V_1	molar volume of solvent ($\frac{\text{cm}^3}{\text{gm-mole}}$)
V_2	molar volume of solute ($\frac{\text{cm}^3}{\text{gm-mole}}$)
V_ψ	velocity of liquid along a stream line ($\frac{\text{cm}}{\text{sec}}$)
V_o	velocity of liquid at the surface of the film ($\frac{\text{cm}}{\text{sec}}$)
x	distance measured perpendicular to the stream lines from the surface of the film inwards (cm)
x_2	mole fraction of the solute gas in the liquid
y	dimensionless distance = $\frac{x}{\Delta}$
Z	function defined in equation (1-47a)

Greek Symbols

Δ	thickness of the liquid film around the sphere (cm)
Δ^+	thickness of the liquid film at the equator of the sphere (cm)
ν	kinematic viscosity of aminomethane liquid ($\frac{\text{cm}^2}{\text{sec}}$)
θ	the angle between the vertical and a radial line (radians)
ψ	a stream function as defined by equation (1-16)

ϕ	a transformation variable defined by equation (1-19)
ϕ_2	the limit of ϕ for a sphere; defined by equation (1-25)
α	a transformation variable defined by equation (1-29)
α_1	a property of the solute defined by equation (1-36)
α_D	standard error in diffusivity
α_L	standard error in liquid flow rate
$\alpha_{C_i - C_o}$	standard error in driving force
α_{G_s}	standard error in gas absorption rate
α_v	standard error in kinematic viscosity
β	a transformation variable defined by equation (1-32a) ($^{\circ}\text{K}^{-1}$)
β_i	pre-exponential coefficients of equation (1-28)
γ_i	exponential coefficients of equation (1-28)
μ	viscosity (centipoise)
μ_1	viscosity of solvent (centipoise)
Λ^*	quantum parameter defined by equation (1-43)
σ	collision diameter of the solute molecules (\AA)
σ_1	surface tension of the solvent (dynes/cm)
ϵ	collision energy of a solute molecule $\left(\frac{\text{gms cm}^2}{\text{sec}^2} \right)$
η	ratio of absorption rates as defined by equations (1-46) and (1-26)
δ	kinematic surface tension of the solvent $= \frac{\sigma_1}{\rho} \left(\frac{\text{cm}^3}{\text{sec}^2} \right)$
ρ	density of the solvent $\left(\frac{\text{gms}}{\text{cm}^3} \right)$
Γ_v	liquid volumetric rate per unit length $\left(\frac{\text{cm}^2}{\text{sec}} \right)$

REFERENCES

1. Bar-Eli, K., and Klein, F.J., J. Chem. Soc. (London), 36, 3083 (1962).
2. Lynn, S., Straatemeir, J.R., and Kramers, H., Chem. Eng. Sci., 4, 63 (1955).
3. Davidson, J.F., and Cullen, E.J., Trans. Instn. Chem. Engrs., 35, 51 (1957).
4. Ratcliff, G.A., and Reid, K.J., *ibid.*, 39, 424 (1961).
5. Baird, M.H.I., and Davidson, J.F., Chem. Eng. Sci., 17, 473 (1962).
6. Stewart, G., Doctoral Dissertation, University of Edinburgh, 1962.
7. Goettler, L.A., and Pigford, R.L., Tripartite Chemical Engineering Conference, Symposium on Mass Transfer with Chemical Reaction, September 23, 5 (1968).
8. Moore, R.G., Doctoral Dissertation, University of Alberta, 1971.
9. Goettler, L.A., Doctoral Dissertation, University of Delaware, 1967.
10. Astarita, G., "Mass Transfer with Chemical Reaction", Elsevier Publishing Company, Amsterdam, 1967.
11. Himmelblau, D.M., Chem. Rev., 64, 527 (1964).
12. Nusselt, W., Ver. Deut. Ingr. Z., 60, 549 (1916).
13. Ratcliff, G.A., and Holdcroft, J.G., Chem. Eng. Sci., 15, 100 (1961).
14. Wild, J.D., and Potter, O.E., Tripartite Chemical Engineering Conference, Symposium on Mass Transfer with Chemical Reaction, September 23, 34 (1968).
15. Olbrich, W.E., and Wild, J.D., Chem. Eng. Sci., 24, 25 (1969).
16. Pigford, R.L., Doctoral Dissertation, University of Illinois, 1941.
17. Vyazovov, V.V., J. Tech. Phys. (U.S.S.R.), 10, 1519 (1940).
18. Dye, J.L., and Dalton, L.R., J. Phys. Chem., 71, 184 (1967).
19. Berns, D.S., et al., J. Am. Chem. Soc., 82, 310 (1960).

20. Makhija, R.C., and Stairs, R.A., University of Trent Progress Report, March, 1969.
21. Atomic Energy of Canada Ltd., Report No. CRNL-207-18, A11-1, February, 1970.
22. Wilke, C.R., and Chang, Pin, A.I.Ch.E. J., 1, 264 (1955).
23. Lusi, M.A., and Ratcliff, G.A., Can. J. Chem. Eng., 46, 385 (1968).
24. Ferrell, R.T., and Himmelblau, D.M., A.I.Ch.E. J., 13, 702 (1967).
25. Hildebrand, J.H., Nakanishi, Koichiro, and Voigt, E.M., J. Chem. Phys., 42, 1860 (1965).
26. Glasstone, S., Laidler, K., and Eyring, H., "Theory of Rate Processes", McGraw-Hill, New York, 1941.
27. Scriven, L.E., and Pigford, R.L., A.I.Ch.E. J., 5, 397 (1959).
28. Scriven, L.E., and Pigford, R.L., *ibid.*, 4, 382 (1958).
29. Hatch Jr., T.F., and Pigford, R.L., Ind. Eng. Chem. Fund., 1, 209 (1962).
30. Fulford, G.D., "Advances in Chemical Engineering", Edited by Drew, T.B., Hoopes, J.W., and Vermulen, T., Vol. 5, pp. 151-236, Academic Press, New York, 1964.
31. Levich, V.G., "Physicochemical Hydrodynamics", Prentice-Hall, Englewood Cliffs, N.J., 1962.
32. Haul, R., and Puttbach, E., Z. Naturforsch., 219, 1914 (1969).
33. Lynn, S., Straatemeir, J.R., and Kramers, H., Chem. Eng. Sci., 4, 58 (1955).
34. Reid, R.C., and Sherwood, T.K., "The Properties of Gases and Liquids", McGraw-Hill, New York, 1966.
35. Einstein, A., "Investigations on the Theory of Brownian Movement", Dover Publications, New York, N.Y., 1956.
36. Scott, R.B., "Cryogenic Engineering", D. Van Nostrand Company Inc., 1959.
37. Kirkbride, C.G., Ind. Eng. Chem., 26, 425 (1934).
38. Friedman, S.J., and Miller, C.O., Ind. Eng. Chem., 33, 885 (1941).

39. Grimley, S.S., Trans. Instn. Chem. Engrs., 23, 228 (1945).
40. Grimley, S.S., Doctoral Dissertation, London University, 1947.
41. Jackson, M.I., A.I.Ch.E. J., 1, 231 (1955).
42. Stirba, C., and Hurt, D.M., *ibid.*, pp. 178-184.
43. Kapitza, P.L., Zh. eksp. teoret. fiz. SSSR, 18, 3 (1948).
44. Tailby, S.R., and Portalski, S., Trans. Instn. Chem. Engrs., 39, 328 (1961).
45. Tailby, S.R., and Portalski, S., *ibid.*, 40, 114 (1962).
46. Tailby, S.R., and Portalski, S., Chem. Eng. Sci., 17, 283 (1962).
47. Portalski, S., Chem. Eng. Sci., 18, 787 (1963).
48. Portalski, S., Chem. Eng. Sci., 19, 575 (1964).

APPENDIX A1Experimental Data

The experimental data on the physical rate of absorption of hydrogen in aminomethane are summarized in Tables A1-1 and A1-2.

Only those runs where the experimental control of the variables was satisfactory have been included.

The significance of the variables listed in the tables is indicated in the nomenclature.

TABLE AI-1

Physical Absorption Data with the 1 inch Sphere

Date	T _A °C	P _T atm	L cc/sec	h _{TL} cm	h _j cm	d _j cm	G x 10 ⁵ gm/sec	G (1 atm) x 10 ⁵ gm/sec	Percent Saturation	D x 10 ⁶ cm ² /sec
5/03/71	-30.0	1.352	0.400	1.25	0.205	0.046	0.201	0.192	83.9	91.4
5/03/71	-29.9	1.352	0.378	1.25	0.205	0.046	0.196	0.188	86.5	94.1
5/06/71	-29.1	1.364	0.460	1.25	0.205	0.046	0.232	0.222	83.5	107.9
5/06/71	-29.1	1.364	0.421	1.25	0.205	0.046	0.214	0.205	84.2	98.5
5/06/71	-29.0	1.364	0.403	1.25	0.205	0.046	0.205	0.196	84.3	93.4
5/06/71	-28.9	1.364	0.372	1.25	0.205	0.046	0.196	0.188	87.3	94.8
5/06/71	-28.8	1.364	0.366	1.25	0.205	0.046	0.195	0.187	88.2	96.3
5/10/71	-28.8	1.369	0.397	1.00	0.205	0.046	0.192	0.185	80.3	78.9
5/10/71	-28.8	1.369	0.394	1.50	0.205	0.046	0.200	0.192	84.0	89.6
5/10/71	-28.7	1.369	0.386	2.15	0.205	0.046	0.202	0.194	86.8	97.1
5/20/71	-26.7	1.361	0.402	1.60	0.205	0.046	0.206	0.207	86.9	102.2
5/20/71	-26.7	1.361	0.405	1.25	0.205	0.046	0.203	0.203	84.9	95.1
6/17/71	-24.1	1.349	0.418	1.00	0.200	0.046	0.201	0.216	85.0	98.8
6/10/71	-24.0	1.341	0.418	1.25	0.200	0.046	0.200	0.218	85.8	101.8
6/10/71	-23.9	1.341	0.418	1.60	0.200	0.046	0.201	0.219	86.1	102.7
6/17/71	-23.9	1.349	0.410	1.25	0.200	0.046	0.201	0.217	87.0	104.0
6/24/71	-20.0	1.349	0.426	1.25	0.200	0.046	0.195	0.235	87.0	107.7
6/30/71	-20.0	1.355	0.421	1.25	0.200	0.046	0.196	0.235	87.9	110.0

TABLE A1-2

Physical Absorption Data with the 3/4 inch Sphere

Date	T _A °C	P _T atm	L cc/sec	h _{TL} cm	h _j cm	d _j cm	G x 10 ⁵ gm/sec	G (1 atm) x 10 ⁵ gm/sec	Percent Saturation	D x 10 ⁶ cm ² /sec
2/25/71	-27.8	1.347	0.336	1.25	0.170	0.046	0.149	0.149	75.6	102.1
2/11/71	-26.6	1.366	0.351	1.25	0.170	0.046	0.156	0.156	74.9	105.0
2/01/71	-25.9	1.360	0.349	1.25	0.190	0.046	0.154	0.157	75.6	106.3
2/04/71	-25.8	1.362	0.303	1.25	0.190	0.046	0.143	0.146	80.7	105.4
2/04/71	-25.2	1.362	0.350	1.25	0.190	0.046	0.156	0.161	76.8	110.9

APPENDIX B1

The following start-up and operating procedure may be used for the measurement of diffusivity of hydrogen in liquid aminomethane using the single sphere absorber.

- (1) Charge the system with hydrogen and make a few soap bubbles in the soap-meter to check for possible gas leaks in the system.
- (2) When the soap bubbles are stationary for about 30 minutes, charge the hydrogen saturator with pure aminomethane.
- (3) Open the solenoid valve S_1 between the hydrogen saturator and the gas absorption chamber.
- (4) Start the peristaltic (hydrogen circulation) pump and circulate hydrogen for about one hour. The system temperature will rise during this time.
- (5) Stop the peristaltic pump, close solenoid valve S_1 and allow system temperature to stabilize.
- (6) Immerse the aminomethane dump tank in liquid nitrogen.
- (7) Open the solenoid valve S_1 and the solenoid valve S_2 between the liquid distributor and the absorption chamber.
- (8) Introduce aminomethane to the system by opening the micrometer control feed valve. Maintain the flow rate at a level higher than the discharge rate of the nozzle. This will cause aminomethane to accumulate in the distributor.
- (9) Step 8 will cause the system pressure to increase substantially due to aminomethane vapour pressure. Vent the system periodically to ensure that the pressure remains above the setting of

the gas regulator.

- (10) When the aminomethane level appears in the take-off tube, open the valves in the liquid return line and adjust the micrometer control liquid return valve so as to maintain the liquid level in the take-off tube.
- (11) When the level of aminomethane in the liquid distributor reaches the glass tube above the distributor, close the solenoid valves S_1 and S_2 and adjust the feed control valve to maintain the desired flow rate as seen on the liquid rotameter.
- (12) Bring the pressure of the system to the value corresponding to the regulator setting by venting the excess pressure from the system.
- (13) Open solenoid valves S_1 and S_2 momentarily to balance system pressures and then close them again.
- (14) Wet the soap-meter wall with soap solution by allowing some hydrogen gas to bubble through it and go through the soap-meter.
- (15) Carry out the final adjustments on the aminomethane feed rate and liquid level in the take-off tube.
- (16) Open the hydrogen feed valve and allow the system to stabilize.
- (17) Record the readings of the four system thermocouples during this transient period. A steady temperature record indicates that the system is reaching stability.
- (18) After reaching a steady state with regard to the temperatures, form two soap films in the soap-meter and record the time taken by the bottom bubble to sweep a given volume (5.0 cc).
- (19) Control the liquid level in the take-off tube at the desired level for the entire duration of the run. A cathetometer should be

used for this purpose.

- (20) The liquid flow rate or take-off height may be changed during a run, but at least 20 minutes should be allowed for the system to stabilize after any change is made in the absorber conditions.
- (21) Upon completion of a run, close the hydrogen feed valve and drain the liquid aminomethane from the absorber flow lines and the liquid saturator into the dump tank. The remaining aminomethane in the feed tanks should also be drawn into the dump tank.
- (22) Isolate the dump tank from the absorber and evacuate the dump tank to a pressure of about 5 microns. Ascertain that sufficient liquid nitrogen is present around the dump tank.
- (23) Isolate the dump tank from the vacuum system and allow it to warm up to room temperature.
- (24) Evacuate the gas-absorption system so as to clear it of any residual aminomethane and hydrogen.
- (25) On the day following the run, immerse the feed tanks in liquid nitrogen and evacuate them. Isolate the vacuum system and feed aminomethane, under its own vapour pressure, from the dump tank to the feed tanks.
- (26) When all the aminomethane is transferred, isolate the dump tank and evacuate the feed tanks so as to degas the aminomethane further. A pressure of about 1 micron should be maintained in the feed tanks for about four or five hours. This requires that the liquid nitrogen level around the feed tanks be kept high during this time.
- (27) Isolate the feed tanks and allow to warm up to room temperature. A period of about forty hours should be allowed for this purpose.

APPENDIX C1

The equations used for the analysis of the errors in the data obtained for the determination of the diffusivity of hydrogen in amino-methane may be developed as follows.

The error of a number of measured quantities may be expressed in terms of a standard error defined as

$$\alpha^* = \frac{\sigma}{N^{\frac{1}{2}}} \quad (C1-1)$$

where

σ = standard deviation of the measured quantity

and N = the total number of observations.

For any function

$$G = f(A, B, C, D)$$

The standard error α_G in \bar{G} is given by

$$\alpha_G^2 = \left(\frac{\partial f}{\partial A}\right)^2 \alpha_A^2 + \left(\frac{\partial f}{\partial B}\right)^2 \alpha_B^2 + \left(\frac{\partial f}{\partial C}\right)^2 \alpha_C^2 + \left(\frac{\partial f}{\partial D}\right)^2 \alpha_D^2 \quad (C1-2)$$

where \bar{G} is the mean of G and $\alpha_A, \alpha_B, \alpha_C, \alpha_D$ are the standard errors in the means of A, B, C and D .

The rate of gas absorption on the sphere absorber is represented by the high depth of penetration model of Davidson and Cullen [3]. Neglecting the last two exponential terms in $f(\alpha)$ the equation may be written as

$$G_s = L(C_i - C_o) [1 - 0.7857 \exp(-3.414\alpha) - 0.1001 \exp(-26.21\alpha)] \quad (C1-3)$$

$$\text{where } \alpha = 2 \times 1.68\pi \left[\frac{2\pi g}{3v}\right]^{1/3} \frac{R^{7/3}}{L^{4/3}} D \quad (1-29)$$

The contribution of the two exponential terms neglected in equation (C1-3) is negligible at the saturation levels involved in this study. Equation (C1-3) may be expressed in general as

$$G_s = f_1[L, (C_i - C_o), D, v] \quad (C1-4)$$

$$\begin{aligned} \therefore \alpha_{G_s}^2 &= \left(\frac{\partial G_s}{\partial L} \right)^2 \alpha_L^2 + \left(\frac{\partial G_s}{\partial (C_i - C_o)} \right)^2 \alpha_{(C_i - C_o)}^2 + \left(\frac{\partial G_s}{\partial D} \right)^2 \alpha_D^2 \\ &\quad + \left(\frac{\partial G_s}{\partial v} \right)^2 \alpha_v^2 \end{aligned} \quad (C1-5)$$

Representing

$$f(\alpha) = 1 - 0.7857 \exp(-3.414\alpha) - 0.1001 \exp(-26.21\alpha) \quad (C1-6)$$

the derivatives $\frac{\partial G_s}{\partial L}$, $\frac{\partial G_s}{\partial (C_i - C_o)}$, $\frac{\partial G_s}{\partial D}$ and $\frac{\partial G_s}{\partial v}$ may be represented as follows:

$$\begin{aligned} \frac{\partial G_s}{\partial L} &= (C_i - C_o) f(\alpha) + L(C_i - C_o) [-0.7857(-3.414) \exp(-3.414\alpha) \\ &\quad - 0.1001(-26.21) \exp(-26.21\alpha)] \frac{\partial \alpha}{\partial L} \end{aligned}$$

$$\begin{aligned} \text{or } \frac{\partial G_s}{\partial L} &= (C_i - C_o) f(\alpha) + L(C_i - C_o) [2.6824 \exp(-3.414\alpha) + 2.6234 \\ &\quad \exp(-26.21\alpha)] \frac{\partial \alpha}{\partial L} \end{aligned} \quad (C1-7)$$

Representing

$$\beta(\alpha) = 2.6824 \exp(-3.414\alpha) + 2.6234 \exp(-26.21\alpha) \quad (C1-8)$$

equation (C1-7) reduces to

$$\frac{\partial G_s}{\partial L} = (C_i - C_o) f(\alpha) + L(C_i - C_o) \beta(\alpha) \frac{\partial \alpha}{\partial L} \quad (C1-9)$$

The remaining derivatives are obtained in a similar manner:

$$\frac{\partial G_s}{\partial (C_i - C_o)} = L f(\alpha) \quad (C1-10)$$

$$\frac{\partial G_s}{\partial D} = L(C_i - C_o) \beta(\alpha) \frac{\partial \alpha}{\partial D} \quad (C1-11)$$

$$\frac{\partial G_s}{\partial v} = L(C_i - C_o) \beta(\alpha) \frac{\partial \alpha}{\partial v} \quad (C1-12)$$

The partial derivatives of ' α ' may be obtained from equation (1-29) as

$$\frac{\partial \alpha}{\partial L} = -4/3 \frac{\alpha}{L} \quad (C1-13)$$

$$\frac{\partial \alpha}{\partial D} = \frac{\alpha}{D} \quad (C1-14)$$

$$\frac{\partial \alpha}{\partial v} = -1/3 \frac{\alpha}{v} \quad (C1-15)$$

Substituting from equations (C1-9) to (C1-15) in equation (C1-5), α_{G_s} may be written as

$$\begin{aligned} \alpha_{G_s}^2 = & \left\{ (C_i - C_o)^2 [f^2(\alpha) + \frac{16}{9} \alpha^2 \beta^2(\alpha) - \frac{8}{3} f(\alpha) \beta(\alpha) \alpha] \right\} \alpha_L^2 \\ & + L^2 f^2(\alpha) \alpha^2 (C_i - C_o) + L^2 (C_i - C_o)^2 \beta^2(\alpha) \alpha^2 \left[\left(\frac{\alpha D}{D} \right)^2 \right. \\ & \left. + \left(\frac{\alpha v}{3v} \right)^2 \right] \end{aligned} \quad (C1-16)$$

Considering the fractional errors to be all additive (thus representing the worst situation), α_D may be expressed as

$$\left(\frac{\alpha_D}{D}\right)^2 = \left[\left\{ \left(\frac{f(\alpha)}{\alpha\beta(\alpha)}\right)^2 + \frac{16}{9} - \frac{8}{3} \left(\frac{f(\alpha)}{\alpha\beta(\alpha)}\right) \right\} \left(\frac{\alpha_L}{L}\right)^2 + \left(\frac{f(\alpha)}{\alpha\beta(\alpha)}\right)^2 \right. \\ \left. \left[\left(\frac{\alpha C_i - C_o}{C_i - C_o}\right)^2 + \left(\frac{f(\alpha)}{\alpha\beta(\alpha)}\right)^2 \left(\frac{\alpha G_s}{G_s}\right)^2 + \frac{1}{9} \left(\frac{\alpha_v}{v}\right)^2 \right] \right] \quad (C1-17)$$

Representing

$$Z = \frac{f(\alpha)}{\alpha\beta(\alpha)} \quad (C1-18)$$

equation (C1-17) reduces to

$$\left(\frac{\alpha_D}{D}\right)^2 = (Z - 4/3)^2 \left(\frac{\alpha_L}{L}\right)^2 + Z^2 \left[\left(\frac{\alpha C_i - C_o}{C_i - C_o}\right)^2 + Z^2 \left(\frac{\alpha G_s}{G_s}\right)^2 \right. \\ \left. + \frac{1}{9} \left(\frac{\alpha_v}{v}\right)^2 \right] \quad (C1-19)$$

The total measured hydrogen absorption rate in gms/sec into the absorber may be written as:

$$G_H = \frac{2.016}{22414.6} \left[\frac{273.15}{T_H} \right] \left(\frac{P}{1} \right) Q_H \quad (C1-20)$$

where

T_H = hydrogen soap-meter temperature (sec)

Q_H = volumetric flow rate of hydrogen (cc/sec)

Following a similar pattern of analysis as shown for α_{G_s} , the following equation may be written:

$$\left(\frac{\alpha_{G_H}}{G_H} \right)^2 = \left(\frac{\alpha_{T_H}}{T_H} \right)^2 + \left(\frac{\alpha_{P_T}}{P_T} \right)^2 + \left(\frac{\alpha_{Q_H}}{Q_H} \right)^2 \quad (C1-21)$$

$$\text{Also } Q_H = \frac{V_{SFM}}{t} \quad (C1-22)$$

where V_{SFM} = vol. of hydrogen swept in soap-meter (cc)

t = time for sweeping volume V_{SFM} (sec)

$$\therefore \left(\frac{\alpha_{Q_H}}{Q_H} \right)^2 = \left(\frac{\alpha_{V_{SFM}}}{V_{SFM}} \right)^2 + \left(\frac{\alpha_t}{t} \right)^2 \quad (C1-23)$$

$$\therefore \left(\frac{\alpha_{G_H}}{G_H} \right)^2 = \left(\frac{\alpha_{T_H}}{T_H} \right)^2 + \left(\frac{\alpha_{P_T}}{P_T} \right)^2 + \left(\frac{\alpha_{V_{SFM}}}{V_{SFM}} \right)^2 + \left(\frac{\alpha_t}{t} \right)^2 \quad (C1-24)$$

The total measured hydrogen absorption rate may be considered to consist of the following:

$$G_H = G_A + G_j + G_T + G_{TL} \quad (C1-25)$$

where

G_H = total measured gas absorption rate $\left(\frac{\text{gms}}{\text{sec}} \right)$

G_A = actual absorption rate on sphere $\left(\frac{\text{gms}}{\text{sec}} \right)$

G_j = gas absorbed on jet $\left(\frac{\text{gms}}{\text{sec}} \right)$

G_T = hydrogen absorption rate due to a change in absorber temperature during a run $\left(\frac{\text{gms}}{\text{sec}} \right)$

G_{TL} = hydrogen absorption rate due to a change in the take-off level during a run $\left(\frac{\text{gms}}{\text{sec}} \right)$

G_T and G_{TL} are assumed to have a mean of zero so that only the expected error due to their presence is considered. From equation (C1-25) the fractional error may be expressed as

$$\left(\frac{\alpha_{G_A}}{G_H} \right)^2 = \left(\frac{\alpha_{G_H}}{G_H} \right)^2 + \left(\frac{\alpha_{G_j}}{G_H} \right)^2 + \left(\frac{\alpha_{G_T}}{G_H} \right)^2 + \left(\frac{\alpha_{G_{TL}}}{G_H} \right)^2 \quad (C1-26)$$

The absorption rate on the jet is given by

$$G_j = 4.0 (C_i - C_o') \{h_j LD\}^{\frac{1}{2}} \quad (1-1)$$

Assume $C_o' = 0$

\therefore fractional error is given as

$$\left(\frac{\alpha_{G_j}}{G_j} \right)^2 = \left(\frac{\alpha_{C_i}}{C_i} \right)^2 + 1/4 \left(\frac{\alpha_{h_j}}{h_j} \right)^2 + 1/4 \left(\frac{\alpha_L}{L} \right)^2 + 1/4 \left(\frac{\alpha_D}{D} \right)^2 \quad (C1-27)$$

The effect of a change in the absorber temperature and the liquid take-off height may be determined from the equation describing the hydrogen partial pressure in the absorber.

$$P_2 = P_T - P_1 \quad (C1-28)$$

where P_2 = hydrogen partial pressure

P_T = total system pressure

P_1 = aminomethane vapour pressure

Assuming the gas law to hold

$$P_2 = \frac{nR^*T_A}{V} \quad (C1-29)$$

$$\therefore \frac{nR^*T_A}{V} = P_T - P_1 \quad (C1-30)$$

Also

$$G_T + G_{TL} = \left(\frac{\partial n}{\partial t} \right)_{P_T} \times 2.016 \quad (C1-31)$$

since the effect of G_T and G_{TL} is to change the number of moles at constant total pressure.

From equation (C1-30)

$$\begin{aligned} R^* \left(\frac{\partial n}{\partial t} \right)_{P_T} &= \frac{(P_T - P_1)}{T_A} \left(\frac{\partial v}{\partial t} \right)_{P_T} - \frac{V(P_T - P_1)}{T_A^2} \left(\frac{\partial T_A}{\partial t} \right)_{P_T} \\ &\quad - \frac{V}{T_A} \left(\frac{\partial P_1}{\partial t} \right)_{P_T} \end{aligned} \quad (C1-32)$$

Since G_{TL} is a change represented through a change in volume one might say that

$$\alpha_{G_{TL}} = 2.016 \frac{(P_T - P_1)}{T_A R^*} \left(\frac{\partial v}{\partial t} \right)_{P_T} \quad (C1-33)$$

and also as G_T is manifested through a temperature change

$$\alpha_{G_T} = -2.016 \frac{V}{T_A^2 R^*} \left\{ P_2 - T_A \left(\frac{\partial P_1}{\partial T_A} \right)_{P_T} \right\} \left(\frac{\partial T_A}{\partial t} \right)_{P_T} \quad (C1-34)$$

The change in absorber volume due to a change in the liquid take-off height may be evaluated as follows:

$$V = \frac{\pi d^2}{4} h_{TL} + V_s \quad (C1-35)$$

where d = diameter of the take-off tube

h_{TL} = take-off height

V_s = volume of the absorption chamber excluding the take-off tube

$$\therefore \left(\frac{\partial v}{\partial t} \right)_{P_T} = \frac{\pi d^2}{4} \left(\frac{\partial h_{TL}}{\partial t} \right)_{P_T} \quad (C1-36)$$

Approximating $\left(\frac{\partial h_{TL}}{\partial t} \right)$ by a linear relationship between h_{TL} and t

$$\left(\frac{\partial v}{\partial t} \right)_{P_T} \approx \frac{\pi d^2}{4} \frac{\Delta h_{TL}}{t} \quad (C1-37)$$

$$\therefore \alpha_{G_{TL}} = 2.016 \frac{P_2}{T_A R^*} \left(\frac{\pi d^2}{4} \right) \left(\frac{\Delta h_{TL}}{t} \right) \quad (C1-38)$$

Similarly, for α_{G_T} the derivative $\frac{\partial P_1}{\partial T_A}$ is required. This may be evaluated from the expression of P_1 as a function of T_A , namely

$$\ln P_1 = 100.90554 - \frac{5716.32506}{T_A} + 0.02248 T_A - 15.3 \ln T_A \quad (C1-39)$$

$$\therefore \frac{1}{P_1} \left(\frac{\partial P_1}{\partial T_A} \right) = \frac{5716.32506}{T_A^2} + 0.02248 - \frac{15.3}{T_A} \quad (C1-40)$$

Substituting for $\left(\frac{\partial P_1}{\partial T_A} \right)$ in equation (C1-34) and approximating $\left(\frac{\partial T_A}{\partial t} \right)$ by $\frac{\Delta T_A}{t}$

$$\alpha_{G_T} = \frac{-2.016}{R^* T_A^2} \left\{ P_2 - P_1 \left[\frac{5716.32506}{T_A} + 0.02248 T_A - 15.3 \right] \right\} \left(\frac{\Delta T_A}{t} \right) \quad (C1-41)$$

The actual hydrogen absorption rate over the sphere G_A is related to the rate G_s through the area correction accounting for the film thickness over the sphere.

$$G_s = \frac{G_A}{ACOR} \quad (C1-42)$$

$$\text{where } ACOR = \frac{A_A}{A_S} = 1 + 2.58 \frac{\Delta^+}{R} \quad (1-30)$$

$$\Delta^+ = \left(\frac{3vL}{2\pi Rg} \right)^{1/3} \quad (1-31)$$

This leads to the relation

$$\left(\frac{\alpha_{G_S}}{G_S} \right)^2 = \left(\frac{\alpha_{G_A}}{G_A} \right)^2 + \left(\frac{\alpha_{ACOR}}{ACOR} \right)^2 \quad (C1-43)$$

Using the definition of ACOR (equation 1-30) and equation (1-31), the following equation may also be written down:

$$\left(\frac{\alpha_{ACOR}}{ACOR} \right)^2 = \left(\frac{2.58\Delta^+}{3R(ACOR)} \right)^2 \left(\frac{\alpha_L}{L} \right)^2 + \left(\frac{2.58\Delta^+}{3R(ACOR)} \right)^2 \left(\frac{\alpha_v}{v} \right)^2 \quad (C1-44)$$

The bulk concentration C_o of hydrogen in aminomethane flowing over the sphere is given by

$$C_o = \frac{G_j}{L} \quad (1-2)$$

which leads to the relation

$$\left(\frac{\alpha_{C_o}}{C_o} \right)^2 = \left(\frac{\alpha_{G_j}}{G_j} \right)^2 + \left(\frac{\alpha_L}{L} \right)^2 \quad (C1-45)$$

Assuming Henry's Law to apply, the interfacial concentration C_i is given by

$$C_i = \frac{2.016}{M_1} p_1 \left[\frac{1}{\frac{H_2}{P_2} - 1} \right] \quad (C1-46)$$

where M_1 = molecular weight of aminomethane

ρ_1 = density of aminomethane

H_2 = Henry's Law coefficient

P_2 = partial pressure of hydrogen

Following the procedure outlined earlier, the fractional error in the interfacial concentration is given by

$$\left(\frac{\alpha_{C_i}}{C_i} \right)^2 = \left(\frac{\alpha_{\rho_1}}{\rho_1} \right)^2 + \left(\frac{\alpha_{H_2}}{H_2} \right)^2 + \left(\frac{\alpha_{P_1}}{P_T - P_1} \right)^2 + \left(\frac{\alpha_{P_T}}{P_T - P_1} \right)^2 + \left(\frac{\alpha_{T_A}}{\Lambda(T_A)} \right)^2 \quad (C1-47)$$

where

$$\frac{1}{\Lambda(T_A)} = \left[\frac{1}{\rho_1} \frac{\partial \rho_1}{\partial T_A} + \frac{1}{(P_T - P_1)} \frac{\partial P_T}{\partial T_A} - \frac{1}{(P_T - P_1)} \frac{\partial P_1}{\partial T_A} - \frac{1}{H_2} \frac{\partial H_2}{\partial T_A} \right]$$

Assuming P_T to be constant, thus neglecting $\frac{\partial P_T}{\partial T_A}$, the above equation reduces to

$$\frac{1}{\Lambda(T_A)} = \left[\frac{1}{\rho_1} \frac{\partial \rho_1}{\partial T_A} - \frac{1}{(P_T - P_1)} \frac{\partial P_1}{\partial T_A} - \frac{1}{H_2} \frac{\partial H_2}{\partial T_A} \right] \quad (C1-48)$$

The derivatives of ρ_1 , P_1 and H_2 with respect to temperature are obtained from the defining relations of ρ_1 , P_1 and H_2 as a function of T_A . The relations for P_1 and H_2 are given as equations (C1-39) and (I-32) respec-

tively. The variation of density ρ_1 with temperature is given as

$$\rho_1 = 0.90580 - 4.00947 \times 10^{-4} T_A - 1.45769 \times 10^{-6} T_A^2 \quad (C1-49)$$

From the relations of $\frac{\alpha C_i}{C_i}$ and $\frac{\alpha C_o}{C_o}$ the fractional error in the driving force $(C_i - C_o)$ may be obtained from

$$\left(\frac{\alpha C_i - C_o}{C_i - C_o} \right)^2 = \left(\frac{\alpha C_i}{C_i - C_o} \right)^2 + \left(\frac{\alpha C_o}{C_i - C_o} \right)^2 \quad (C1-50)$$

Using the relationships derived for the different variables used during an experiment (equations (C1-20) to (C1-50)) the error in the diffusion coefficient may be explicitly evaluated using equation (C1-19).

PART II

KINETICS OF HYDROGEN -
AMINOMETHANE EXCHANGE

CHAPTER 1

INTRODUCTION

The kinetics of the hydrogen-aminomethane exchange reaction have received limited attention in the past [1,2] and the data available do not conform to the operating conditions of interest to industry. Industrial contactors are expected to operate with a high concentration of the homogeneous potassium methyl amide catalyst and within a temperature range of -40°C to 70°C . The data of Bar-Eli and Klein [1] was restricted to very low lithium catalyst concentrations of less than 0.3 gms Li/kg solution and temperatures of less than -22°C , while Rochard [2] obtained her data at potassium methyl amide concentrations of less than 5 gms K/kg solution and temperatures not exceeding -62°C . The above mentioned investigations were both conducted in stirred type reactors and difficulties may have been encountered in eliminating mass transfer resistance at higher temperatures and catalyst concentrations.

The work reported here uses the single sphere absorber which allows the measurement of the rate constant at conditions of greater commercial significance.

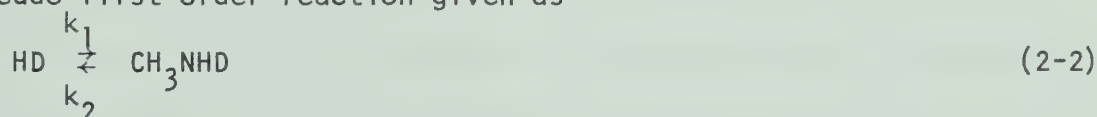
The exchange of isotopic hydrogen with aminomethane in the region of low deuterium concentrations can be described by the following reversible reaction:



which takes place in the liquid phase and is catalyzed by potassium

methyl amide. Bar-Eli and Klein [1] and Rochard [2] investigated the kinetics of the above reaction and concluded that the exchange process is of first order with respect to HD and CH_3NHD concentrations. They indicated that the reaction rate is substantially higher than for the analogous hydrogen-ammonia system. Since the latter reaction is known to be fast [3] it is reasonable to suggest that the hydrogen amine system also involves a fast reaction.

Assuming that the concentrations of CH_3NH_2 and H_2 are large and substantially invariant, the exchange process may be represented by a pseudo-first order reaction given as



The equilibrium constant for the reaction (2-2) may be written down as

$$K' = \frac{[\text{CH}_3\text{NHD}]_e}{[\text{HD}]_e} = \frac{k_1}{k_2} \quad (2-3)$$

where $[\text{CH}_3\text{NHD}]_e$ and $[\text{HD}]_e$ represent the concentrations of the deuterated species at equilibrium. The local rate of reaction 'r' may be expressed as

$$r = k_1[\text{HD}] - k_2[\text{CH}_3\text{NHD}] \quad (2-4)$$

which on substitution from (2-3) gives

$$\begin{aligned} r &= k_1[\text{HD}] - \frac{k_1}{K} [\text{CH}_3\text{NHD}] \\ &= k_1 \left([\text{HD}] - \frac{[\text{CH}_3\text{NHD}]}{K} \right) \end{aligned} \quad (2-5)$$

Equation (2-5) could also be written as

$$r = k_1(C - C_e) \quad (2-5a)$$

where 'C' is synonymous with $[HD]$ and C_e is a concentration of HD that would be in equilibrium with $[CH_3NHD]$. If the bulk volume of the liquid aminomethane used is such that the molar ratio of the liquid to hydrogen gas is large then the product concentration $[CH_3NHD]$ is essentially constant and C_e in equation (2-5a) would also be a constant value.

The rate constant, k_1 , of the exchange reaction can be simply measured by knowing the total liquid holdup and the absorption data, provided the resistance for transfer of deuterium in the liquid phase can be sufficiently reduced so that the reaction becomes the rate controlling process. This condition has been defined as the kinetic regime by Astarita [4]. When, however, the reaction is a fast one it becomes exceedingly difficult to reduce the mass transfer resistance sufficiently to operate in the kinetic regime. The data of Bar-Eli and Klein [1] and Rochard [2] was obtained in stirred type reactors which were provided with mechanical vibrators and stirrers so that mass transfer resistance may be reduced. In spite of this, their work was restricted to low catalyst concentrations and low temperatures because of difficulty in operating in the kinetic regime.

In contrast to operation in the kinetic regime there are a number of contactors which make it possible to conduct the exchange reaction in the fast reaction regime [4]. These include the wetted wall column, the laminar jet, the multiple sphere absorber, the single sphere absorber, the disc column absorber and the rotating drum absorber. The fast reaction regime is typified by high diffusion times as compared to the reaction times and a narrow reaction zone close to the gas-

liquid interface. For the pseudo-first order reaction (2-2) operating in this regime, the overall chemical absorption coefficient K_L is given by

$$K_L = \sqrt{k_1 D} \quad (2-6)$$

where k_1 is the pseudo-first order rate constant and D is the molecular diffusion coefficient of the solute in the liquid phase. The rate of absorption of the solute specie is represented as

$$G = K_L A (C_i - C_e) \quad (2-7)$$

where C_i and C_e are the interfacial and chemical equilibrium concentrations of the solute in the liquid phase. If K_L is known through experimental determination, then using the values of D estimated in the first part of this thesis, it is possible to evaluate the kinetic constant k_1 from equation (2-6).

In preference to the other contactors mentioned above, the single sphere absorber was used for this study. Its merits over the other absorbers may be summarized as follows:

- (i) It minimizes the end effects common to other gas liquid contactors.
- (ii) It provides longer contact times (0.1 sec to 1.0 sec) which is desirable for operation in the fast reaction regime.
- (iii) Relatively high liquid flow rates without surface rippling may be employed with this absorber.
- (iv) Its surface area exposed for absorption is large which makes it suitable for absorption of sparingly soluble gases such as hydrogen.

CHAPTER 2

LITERATURE SURVEY

A study of the kinetics of the exchange of hydrogen with ammonia or aminomethane involves an investigation of the manner in which the rate of exchange varies with the concentrations of hydrogen and of the catalyst in solution. The work of previous investigators [5,6,7,8] in this area is outlined below.

2.1 Hydrogen-Ammonia System

Aminomethane is a simple substituted derivative of ammonia and as such, exchange studies of the hydrogen-ammonia system with alkali metal amides as catalysts are pertinent and useful towards an assessment of the behavior of the hydrogen-aminomethane system.

Wilmarth and Dayton [5] used a stirred reactor to obtain exchange data for the hydrogen-ammonia system at -53°C using potassium amide as a catalyst in solution. Their work was restricted to very low catalyst concentrations ranging from 0 to 10 millimoles/litre (mm/l). The rate of exchange was reported to be proportional to the concentrations of hydrogen and the amide ion. A rate constant $k_1 = 1.3 \text{ min}^{-1}$ was obtained at a potassium amide concentration of 2.7 mm/l. Bar-Eli and Klein [6] also used a stirred reaction cell and extended the hydrogen-ammonia study to higher catalyst concentrations ranging from 5-200 mm/l. They covered a temperature range of -80°C to 0°C but their data of k vs. temperature appears to be inconsistent when compared with the data reported for k vs. catalyst concentration. Based on the data of k vs. temperature, however, they

indicate that an activation energy of 7.5 kcal/mole was obtained for the hydrogen-ammonia exchange reaction. Dirian et al. [7] investigated a fairly wide range of potassium amide catalyst concentrations extending from 0.4 to 1400 mm/l. They indicate that the mass transfer resistance in the liquid phase could not be eliminated at conditions of high catalyst concentrations and high temperatures inspite of stirrer speeds of about 9000 rpm. At -50°C the mass transfer resistance could be eliminated only for catalyst concentrations upto 60 mm/l. From a plot of the kinetic rate constant vs. the catalyst concentration at -50°C reported by them, it appears that $k_1 = 1.5 \text{ min}^{-1}$ at about 2.5 mm/l and $k_1 = 2.5 \text{ min}^{-1}$ at about 5.0 mm/l. This would indicate concurrence with the work of Wilmarth and Dayton [5]. An activation energy of 8.0 kcal/mole was reported for the reaction. Delmas et al. [8] also conducted a study of the exchange of the hydrogen-ammonia system using a stirred reactor. Their work was directed towards the evaluation of the dissociation coefficients of the potassium amide catalyst in solution and their conclusions have helped to identify the catalytically active specie. The study covered an investigation of amides of potassium, rubidium and cesium within a concentration range of 1 to 200 mm/l at -45.3°C , -59.3°C and -70°C . Typical values of the rate constant at -59.3°C and at potassium amide concentrations of about 5 mm/l and 150 mm/l are approximately 1.0 min^{-1} and 20.0 min^{-1} respectively. A value of 5.5 kcal/mole is reported for the activation energy of the reaction and the discrepancy with the value of 7.5 kcal/mole obtained by Bar-Eli and Klein [6] is attributed to different values used for the solubility of hydrogen. The work of Bourke and Lee [3] appears to be the only one

where the exchange reaction was conducted with contactors which allowed accounting for the diffusional resistance in the liquid phase. They used a wetted rod column and a disc column to obtain the dependence of the rate constant with temperature and catalyst concentration. They reaffirmed the first order dependence of the rate of reaction on the hydrogen concentration and indicated that the reaction zone in the liquid was very narrow, with the bulk of the reaction occurring within a depth of about 0.001 in. below the gas-liquid interface. Rate constants were found to lie in the range $10\text{--}500\text{ sec}^{-1}$ at potassium amide catalyst concentrations of $4\text{--}40\text{ gms KNH}_2/\text{l}$ ($73\text{--}730\text{ mm/l}$). The temperature range investigated was -40°C to 20°C , and an activation energy of 8.0 kcal/mole was reported. The above authors, however, used diffusivity values for hydrogen-deuteride in ammonia as predicted by the Wilke-Chang equation using an association parameter of unity. This equation, as indicated in the first section of this investigation, underestimates the diffusion coefficients for the hydrogen-ammonia system by as much as 100%. The data of Bourke and Lee [3] when corrected for diffusivity using equation (1-49) gave values of the rate constant in the range $10\text{--}160\text{ sec}^{-1}$ for the same temperatures and catalyst concentrations. The activation energy corresponding to the corrected data was found to be 5.8 kcal/mole . A plot of the corrected values of the rate constant k_1 vs catalyst concentration at 20°C indicated that k_1 varied linearly with catalyst concentration upto about 365 mm/l .

Values of the rate constant at two temperatures and catalyst concentrations as obtained by some of the authors mentioned above [3,6, 7,8] are compared in Table 1. In order to obtain a common basis for comparison the data had to be extrapolated linearly both for tempera-

ture and catalyst concentration wherever necessary. It may be noted from Table 1 that there is a reasonable agreement between the values obtained from the data of all the investigators at 163.7 mm/l and -59.3°C whereas at 655 mm/l and -23°C the value obtained from the data of Delmas [8] is significantly lower than that obtained from the data of the other authors [3,6,7]. This appears to be due to the fact that a linear extrapolation in catalyst concentration upto 655 mm/l underestimates the rate constant obtained from the data of Delmas [8] and this cannot be compensated for through a temperature extrapolation using an activation energy of 5.5 kcal/mole. The higher activation energies reported by Bar-Eli and Klein [6] and Dirian [7] seem to compensate for the underestimation and result in a better agreement with the measured value reported by Bourke and Lee [3].

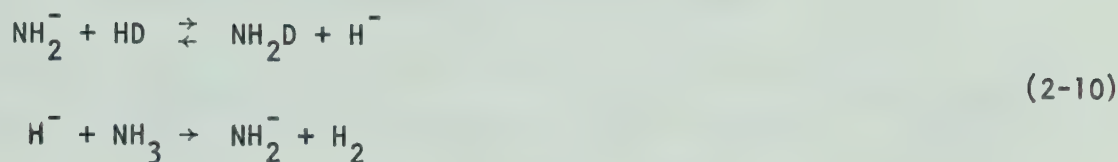
2.1.1 Effect of Catalyst Concentration. In order to understand the manner in which the catalyst concentration affects the rate constant k_1 , it is desirable to have some information regarding the catalytically active specie. Wilmarth and Dayton [5] reported that the rate of exchange of the hydrogen-ammonia reaction is first order with respect to the amide ion concentration $[\text{NH}_2^-]$ which implies that the amide ion is the catalytically active specie. The rate constant could thus be expressed as

$$k_1 = k_o [\text{NH}_2^-] \quad (2-8)$$

The authors suggested that the dissociation of potassium amide in solution occurs according to the equation



and that the reaction proceeds through the formation of a hydride ion i.e.



Bar-Eli and Klein [6], however, suggest that in addition to the amide ion, the undissociated potassium amide also catalyzes the reaction although its activity is 20 times lower than that of the amide ion. Their data indicates that the reaction rate is linear with catalyst concentration through the entire range of concentrations investigated (5-200 mm/l). The rate constant k_1 was expressed as

$$k_1 = k_o [\text{NH}_2^-] + k_o' [\text{KNH}_2] \quad (2-11)$$

Dirian and his coworkers [7] reported the catalytic effect of the alkaline cation and suggested the following equation for the rate constant:

$$k_1 = k_{o1} a_{\text{NH}_2^-} + k_{o1}' a_{\text{NH}_2^-} a_{\text{K}^+} \quad (2-12)$$

where $a_{\text{NH}_2^-}$ and a_{K^+} are the activities of the anion and the cation species respectively. The rate of exchange was found to depend linearly on catalyst concentration only up to a value of 20 mm/l after which the first order dependence was found to be invalid.

The apparent uncertainty about the catalytically active specie was due to the lack of information regarding the dissociation coefficients of amides and the activity coefficients of ions in liquid ammonia. Delmas et al. [8] conducted a kinetic study of the hydrogen-ammonia exchange reaction and carefully calculated the dissociation coefficients for amides of potassium, rubidium, and cesium. They conclude that the

TABLE 1

Comparison of the Reaction Rate
Constant for the Hydrogen-Ammonia System

Reference	Catalyst Concentration mm/l	Temperature °C	Rate Constant Min ⁻¹	Activation Energy kcal/mole
Bar-Eli & Klein [6]	163.7* 655.0*	-59.3 -23.0*	23.5 1570	7.4
Dirian et al. [7]	163.7* 655.0*	-59.3 -23.0*	22.8 1566	8.0
Delmas et al. [8]	163.7* 655.0*	-59.3 -23.0*	22.3 701	5.5
Bourke & Lee [3]	163.7 655.0	-59.3* -23.0	28.2 1428	5.8

* Indicates that the variable was extrapolated outside the reported range.

free amide ion is the only catalytically active specie and the rate of exchange is linear with the concentration of the amide ion of potassium upto a value of 5 mm/l. This corresponds to a potassium amide overall concentration of about 65 mm/l. They suggest that the deviation from the first order law above these concentrations is due to the presence of triple ions like $(K_2NH_2)^+$.

2.2 Hydrogen-Aminomethane System

(a) System Properties

The investigation of the hydrogen-aminomethane exchange system is of recent origin and as such the extent of data available on fundamental properties of the system is very limited. The properties of particular interest from the point of view of this investigation include:

- (i) The hydrogen solubility.
- (ii) The diffusivity of hydrogen-deuteride in aminomethane.
- (iii) The equilibrium constant of the exchange reaction.

Rochard [2] has reported data for the solubility of hydrogen in aminomethane at three specific temperature namely -62.2°C , -77.2°C and -90°C . These were the temperatures at which her exchange studies were conducted. Moore [9] undertook a study to measure the solubilities of hydrogen in amines over an extensive temperature range. His work for aminomethane covers a temperature range of -62°C to $+23^\circ\text{C}$. Assuming Henry's Law to apply the temperature dependence of the Henry's Law coefficient is reported as

$$\ln H_2 = 4.1403 + 1.6612\beta - 0.1160\beta^2 \quad (2-13)$$

$$\text{where } \beta = \frac{1000}{T(^{\circ}\text{K})} \quad (2-14)$$

$$\text{and } P_2 = x_2 H_2 \quad (2-15)$$

P_2 is the partial pressure of hydrogen in atmospheres and x_2 is the mole fraction of hydrogen in aminomethane. Equation (2-13) is used for estimation of the hydrogen deuteride solubility for this investigation.

The data obtained in the first part of this study is perhaps the only data available for the diffusivity of hydrogen in aminomethane. The diffusivity of hydrogen deuteride is estimated using the modified Ferrell and Himmelblau equation reported as equation (1-49) in this thesis.

The equilibrium constant for the hydrogen-aminomethane exchange reaction (2-1) may be written as

$$K_{eq} = \frac{[\text{CH}_3\text{NHD}][\text{H}_2]}{[\text{CH}_3\text{NH}_2][\text{HD}]} \quad (2-16)$$

where $[\text{CH}_3\text{NHD}]$, $[\text{H}_2]$ etc. represent the concentrations of the species at chemical equilibrium. The separation factor relating the deuterium concentrations in the amine and hydrogen at equilibrium is expressed as

$$\alpha_{eq} = \frac{[\text{D/H}]_{\text{amine}}}{[\text{D/H}]_{\text{hydrogen}}} \quad (2-17)$$

Rearranging equation (2-16) one obtains

$$K_{eq} = \frac{\frac{[\text{CH}_3\text{NHD}]}{[\text{CH}_3\text{NH}_2]}}{\frac{[\text{HD}]}{[\text{H}_2]}} = \frac{m^* \left[\frac{\text{D}}{\text{H}} \right]_{\text{amine}}}{n^* \left[\frac{\text{D}}{\text{H}} \right]_{\text{hydrogen}}} \quad (2-18)$$

$$\text{or } K_{eq} = \frac{m^*}{n^*} \alpha_{eq} \quad (2-19)$$

where m^* and n^* are the number of exchangeable hydrogen atoms per molecule of the amine and hydrogen respectively. Since aminomethane and hydrogen both have two exchangeable atoms per molecule m^* is equal to n^* for the hydrogen-aminomethane system. This implies that

$$K_{eq} = \alpha_{eq} \quad (2-20)$$

AECL [10] have conducted some studies to measure the separation factor for the hydrogen aminomethane system. Their present conclusions indicate that the separation factor for this system may be taken to be equal to that for the hydrogen-ammonia system. The expression for the change of the separation factor with temperature for the hydrogen-ammonia system is given as

$$\lg_{10} \alpha_{eq}^* = -0.2422 + \frac{237.59}{T} \quad (2-21)$$

where T is the temperature in $^{\circ}\text{K}$. In the absence of indications to the contrary α_{eq} is taken equal to α_{eq}^* for this investigation also.

(b) Exchange Studies

Kenyon and Pepper [11] noticed in 1961 that small additions of certain amines to the hydrogen-ammonia system enhanced the rate of reaction. Bar-Eli and Klein [1] undertook to measure the rate of exchange of hydrogen-deuteride, tritium hydride and deuterium with aliphatic amines in the presence of lithium and potassium alkyl amide catalysts. Their study was conducted in a stirred reactor in a manner very similar to the study of the hydrogen-ammonia system [6]. The data for $\text{HD-CH}_3\text{NH}_2$ in presence of LiNHCH_3 indicates the rate constant

to be about 6.5 min^{-1} at -29°C and about 3.5 min^{-1} at -46°C . The maximum lithium amide concentration studied appears to be about 30 mm/l. A comparison of the rates of exchange of deuterium in amino-methane and in ammonia indicated that the rate in the amine was up to 35 times higher at -66°C . Based on the kinetic data obtained for the $\text{HD-CH}_3\text{NH}_2$ system an estimated value of the activation energy was reported to be 3.6 kcal/mole.

The work of Rochard [2] also conducted in a stirred reactor investigated the exchange of the hydrogen-aminomethane system between -62°C and -90°C and a potassium methyl amide catalyst concentration of 0 to 70 mm/l. For a catalyst concentration of about 9 mm/l a rate constant of 55 min^{-1} was observed at -62.2°C . In contrast to the value of the activation energy reported by Bar-Eli and Klein [1], Rochard [2] estimates the activation energy to be 6.8 kcal/mole and attributes the discrepancy to a different value of hydrogen solubility used by Bar-Eli and Klein [1].

2.2.1 Effect of Catalyst Concentration. The works of Bar-Eli and Klein [1] and Rochard [2] are the only ones dealing with the effect of catalyst concentration on the exchange of the hydrogen-aminomethane system.

Bar-Eli and Klein [1] noted that at -22°C the rate of the reaction became invariant to increases in catalyst concentration beyond a value of 10 mm/l. This effect was attributed to the saturation of the amino-methane with lithium methyl amide at 10 mm/l. A linear variation of the rate constant k_1 with catalyst concentration was observed up to the suggested saturation value. Rochard [2] also observed a linear dependence of k_1 with catalyst concentration upto a value of about 20 mm/l at -90°C and suggested that the subsequent levelling off might be

due to the variation of the degree of dissociation with catalyst concentration. By analogy with the work of Delmas [8] for hydrogen-ammonia, Rochard suggests that the free alkylamide ion $[\text{CH}_3\text{NH}^-]$ may be the only catalytically active specie. Additional work is, however, required to determine the degree of dissociation of the alkyl amide catalyst in the hope of establishing whether the alkylamide ion is in fact the only catalytically active specie.

2.3 Catalyst Solubility

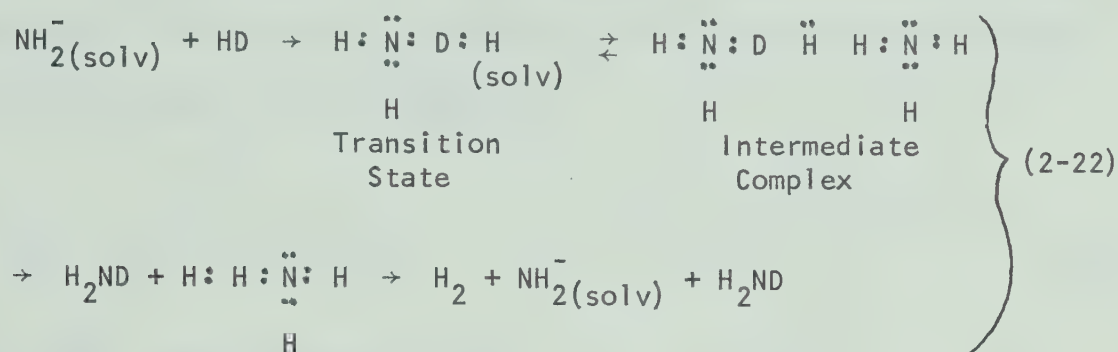
Since catalyst concentration is an important variable for the kinetic study of the hydrogen-aminomethane exchange reaction it is desirable that the limits of solubility of the alkyl amide catalyst in the liquid be known.

Hayashitani [12] conducted a study to determine the solubility of potassium alkyl amide in amines over a temperature range of -78°C to $+40^\circ\text{C}$. His work indicates that the solubility of potassium methyl amide in aminomethane decreases with increasing temperature. Typical values of the solubility reported are 40 gms K/kg amine at -78°C and 25 gms K/kg amine at 25°C .

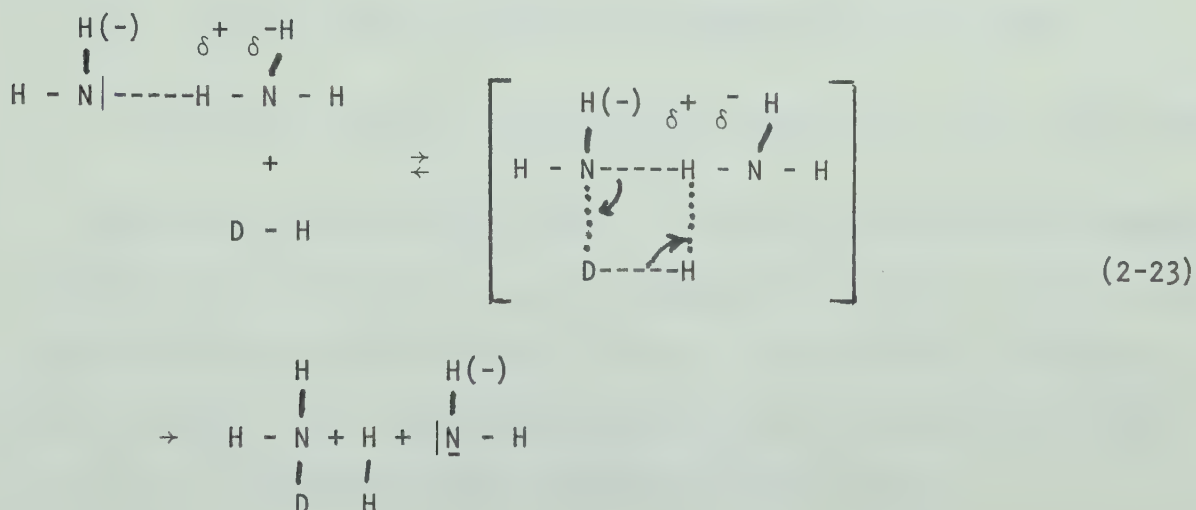
2.4 Reaction Mechanism

The reaction mechanism for the hydrogen-aminomethane exchange is derived from the mechanism of the analogous hydrogen-ammonia reaction. Wilmarth and Dayton [5] suggested that hydride ions were formed in liquid ammonia solution as a reaction intermediate but this was contested by Bar-Eli and Klein [6] on the basis that lithium hydride failed to

catalyze the reaction. They believe that the free electron pair in the catalyst ion or ion pair initiates the exchange. This, they suggest, is done by stretching the D-H bond and partially forming a N-D bond. The solvent molecule then supplies a hydrogen atom and the exchange is completed by the transfer of charge as shown below.



Delmas et al. [8] suggest that the exchange occurs between a HD molecule and the solvated NH_2^- ion. A N-H bond of the solvated ammonia molecule is polarized by NH_2^- and then weakened. A four center mechanism is involved, i.e.



Rochard [2] suggests that the above mechanism proposed by Delmas [8] is the most plausible one for the hydrogen-aminomethane exchange.

CHAPTER 3

ANALYSIS OF MASS TRANSFER AND CHEMICAL REACTION OVER A SPHERE

In order to obtain a theoretical support to the experimental study of mass transfer with chemical reaction in a liquid flowing over a sphere it is necessary to solve the equation which describes the above phenomena. In essence this equation is the equation of continuity of the solute specie and is written as

$$\frac{\partial C}{\partial t} + \underline{v} \cdot \nabla C = D \nabla^2 C - r \quad (2-24)$$

where $\frac{\partial C}{\partial t}$ = The accumulation term

$\underline{v} \cdot \nabla C$ = The convective transfer term

$D \nabla^2 C$ = The molecular diffusion term

r = The rate of reaction (disappearance of the specie)

D = The diffusion coefficient of the solute in the liquid phase.

Equation (2-24) may be written in spherical coordinates to represent a solute mass balance in a liquid flowing over a sphere. With reference to the set of coordinates given in Figure 1 and neglecting convective terms in the R and ϕ directions and the diffusion terms in the θ and ϕ directions, equation (2-24) may be simplified to give

$$DR \frac{\partial^2 C}{\partial x^2} - 2D \frac{\partial C}{\partial x} = v_{\psi} \left(\frac{\partial C}{\partial \theta} \right)_{\psi} + Rr + \frac{\partial C}{\partial t} \quad (2-25)$$

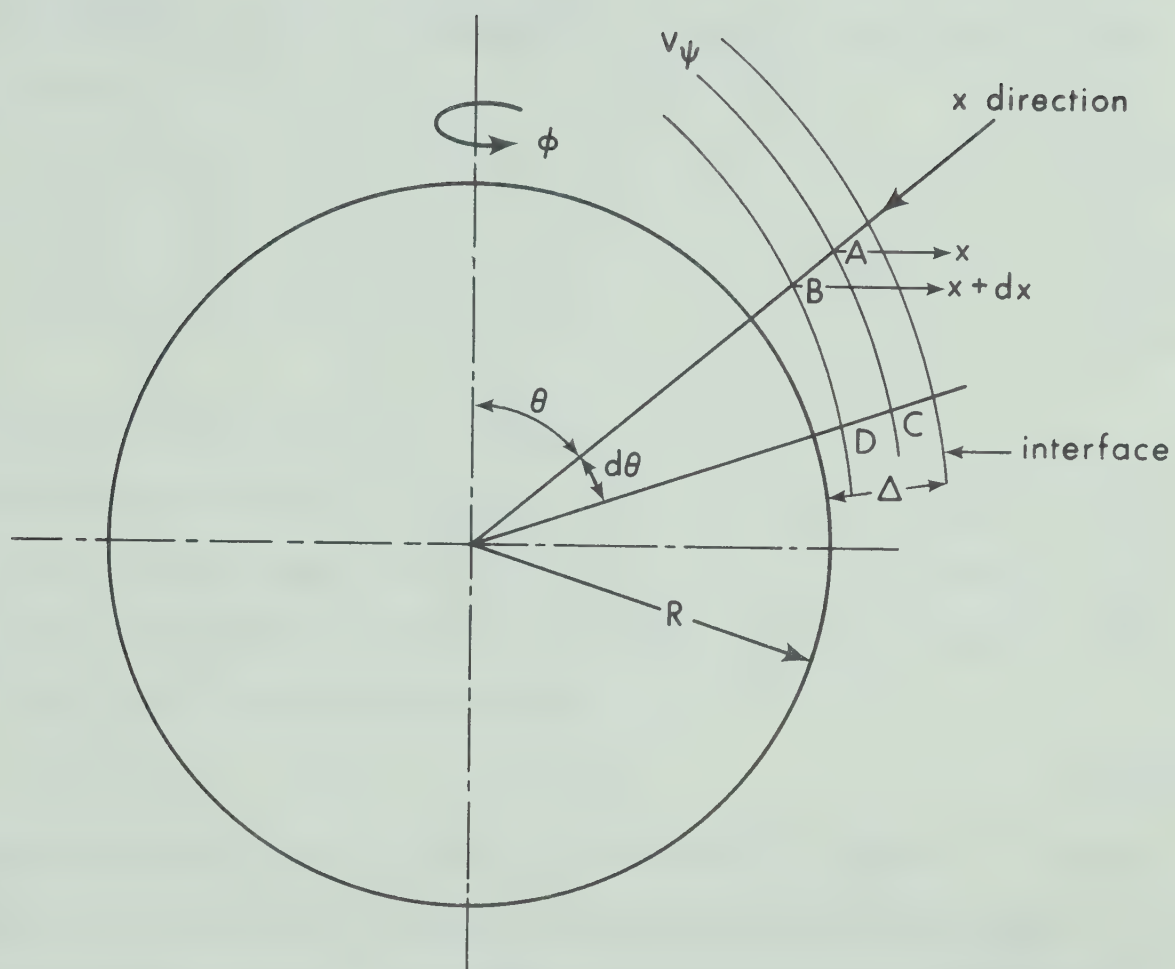


FIGURE 1

Co-ordinate Representation of Flow Over a
Sphere Absorber

Under steady state conditions and assuming a first order or pseudo-first order reaction, equation (2-25), becomes

$$DR \frac{\partial^2 C}{\partial x^2} - 2D \frac{\partial C}{\partial x} = v_{\psi} \left(\frac{\partial C}{\partial \theta} \right)_{\psi} + R k_1 (C - C_o) \quad (2-26)$$

The boundary conditions associated with equation (2-26) may be stated as follows:

$$C = C_i \quad x = 0 \quad \theta > 0 \quad (2-27a)$$

$$\frac{\partial C}{\partial x} = 0 \quad x = \Delta \quad \theta > 0 \quad (2-27b)$$

$$C = C_o \quad x > 0 \quad \theta = 0 \quad (2-27c)$$

where Δ is the liquid film thickness.

The boundary condition given by (2-27b) is used when the depth of penetration of the solute in the film is high so that the presence of the sphere influences the concentration profile. When the depth of penetration is small (2-27b) may be replaced by

$$C = C_o \quad x = \infty \quad \theta > 0 \quad (2-27d)$$

which considers the film to be infinitely deep as compared to the depth of penetration. The low and high depth of penetration cases were reported for the case of pure physical absorption in a liquid flowing over a sphere by Davidson and Cullen [13].

When the reaction rate is such that the concentration in the bulk of the liquid is at chemical equilibrium then C_o may be replaced by C_e in (2-27d). A fast reaction, in fact, has the effect of reducing the concentration level to C_e very close to the interface thus steepening the concentration gradient in the film. This also implies that when a

chemical reaction occurs simultaneously with gas absorption the depth of penetration of the solute species is lower than the case for pure physical absorption. For higher rates of reaction this effect is more pronounced. The boundary condition (2-27d) would thus apply in most cases where a fast reaction was involved.

Ratcliff and Holdcroft [14] presented a solution to a simplified form of equation (2-26) wherein R was assumed much larger than Δ and $\frac{\partial C}{\partial x}$ was neglected in comparison to $R \frac{\partial^2 C}{\partial x^2}$. Their solution was asymptotic to the equation for physical absorption of Davidson and Cullen [13] but failed to approach the equation describing the gas absorption rate at high values of the rate constant namely

$$G = 4\pi R^2 \sqrt{k_1 D} (C_i - C_e) \quad (2-28)$$

where $(4\pi R^2)$ is the interfacial area for absorption on a sphere. Astarita [15] pointed out this anomaly and assuming no stretching effect of the liquid film obtained the following solution to the original differential equation of Ratcliff and Holdcroft [14].

$$G = 2R^2 \sqrt{D\pi} C_i \int_0^\pi \left(\sqrt{k_1 \pi} \operatorname{erf}(\sqrt{k_1 t}) + \frac{\exp(-k_1 t)}{\sqrt{t}} \right) \sin \theta d\theta \quad (2-29)$$

$$\text{where } t = \frac{R}{V_o^+} \int_0^\theta \sin^{1/3} \theta d\theta \quad (2-30)$$

and V_o^+ is the interfacial velocity at the sphere equator. The boundary conditions used for equation (2-29) correspond to conditions (2-27a), (2-27c) and (2-27d) with C_o and C_e assumed equal to zero.

For a fast reaction when $k_1 t$ or $\frac{k_1 R}{V_o^+}$ is $\gg 1$, $\operatorname{erf}(\sqrt{k_1 t})$ and

$\frac{\exp(-kt)}{\sqrt{t}}$ approach 1 and 0 respectively, and equation (2-29) reduces to equation (2-28). It is important to note that equation (2-28) is independent of liquid flow rate which implies that at high reaction rates the hydrodynamics over the sphere do not affect the rate of gas absorption. This, however, is only true as long as the surface area of contact can be estimated by the expression $4\pi R^2$. For values of $k_1 t$ or $\frac{kR}{V_o} \ll 1$ equation (2-29) degenerates to

$$G = 2(C_i - C_e) R^2 \sqrt{D\pi V_o} \int_0^\pi \frac{\sin\theta d\theta}{\left(\int_0^\theta \sin^{\frac{1}{3}} \alpha d\alpha\right)^{\frac{1}{2}}} \quad (2-31)$$

For $k_1 t = 0$, which corresponds to the case of pure physical absorption, C_e the equilibrium concentration in equation (2-31) may be replaced by C_o the bulk liquid concentration to give an equation which is identical to the one given by Lynn et al. [16]. In developing equation (2-31), however, Astarita [15] followed the approach of Lynn et al. [16] who neglected the stretching effect of the spherical liquid film. Wild and Potter [17] indicate that when the stretching effect is neglected the solution given by (2-31) for low reaction rates is about 18% in error. For high reaction rates the effect is indeed negligible. They solved equation (2-26) numerically for low depths of solute penetration and reported different equations representing the absorption rate in different ranges of k_1 . Defining

$$d\psi = \frac{RD}{V_o \Delta^2} d\theta = \frac{4\pi R^2 D}{3L\Delta^2} \sin^{5/3} \theta d\theta \quad (2-32)$$

where V_o , the interfacial velocity, and Δ , the film thickness over the

sphere, are given by equations (1-5) and (1-3) respectively, in the first part of this thesis. Δ^+ is the film thickness measured at the sphere equator and is given by equation (1-31). The maximum value of ψ for the sphere is given as

$$\psi_2 = \int_{4^\circ}^{\pi} d\psi \quad (2-33)$$

and t_{\max} the maximum contact time is expressed as

$$t_{\max} = \frac{R}{V_o} + \int_0^{\pi} \sin^{1/3} \theta d\theta \quad (2-34)$$

The solutions obtained by Wild and Potter [17] may thus be written as:

(i) $k_1 t_{\max} = 0$ (physical absorption)

$$\frac{G}{L(C_i - C_o) \sqrt{\psi_2}} = \left(\frac{9}{\pi} \right)^{1/2} \quad (2-35)$$

(ii) $k_1 t_{\max} < 1.0$

$$\frac{G}{L(C_i - C_e) \sqrt{\psi_2}} = 0.455 k_1 t_{\max} + 1.693 \quad (2-36)$$

(iii) $1.0 < k_1 t_{\max} < 5.0$

$$\frac{G}{L(C_i - C_e) \sqrt{\psi_2}} = 1.428 \sqrt{k_1 t_{\max}} + \frac{0.689}{\sqrt{k_1 t_{\max}}} \quad (2-37)$$

(iv) $5.0 < k_1 t_{\max} < 25.0$

$$\frac{G}{L(C_i - C_e) \sqrt{\psi_2}} = 1.428 \sqrt{k_1 t_{\max}} + \frac{0.54}{\sqrt{k_1 t_{\max}}} \quad (2-38)$$

and

$$(v) \quad k_1 t_{\max} > 25.0$$

$$\frac{G}{L(C_i - C_e) \sqrt{\psi_2}} = 1.428 \sqrt{k_1 t_{\max}} \quad (2-39)$$

It may be noted that for equations (2-36) to (2-39) it is assumed that the reaction rate is high enough to keep the bulk liquid concentration at the chemical equilibrium value C_e .

Wild and Potter [17] also indicated that their numerical solution could be closely approximated over the entire range of $k_1 t_{\max}$ by the equation

$$\frac{G}{L(C_i - C_e) \sqrt{\psi_2}} = 0.714 \sqrt{k_1 t_{\max}} \int_0^\pi \left(\operatorname{erf} \sqrt{\eta} + \frac{e^{-\eta}}{\sqrt{\pi \eta}} \right) \sin \theta d\theta \quad (2-40)$$

where

$$\eta = \frac{k_1 t_{\max}}{2.58} \sin^{-4/3} \theta \int_0^\theta \sin^{5/3} \theta d\theta \quad (2-41)$$

Equation (2-39) is representative of high values of $k_1 t_{\max}$ and is in fact identical to equation (2-28). Using equations (2-35) and (2-40) one may express the enhancement factor ϕ due to chemical reaction as

$$\phi = 0.421 \sqrt{k_1 t_{\max}} \int_0^\pi \left(\operatorname{erf} \sqrt{\eta} + \frac{e^{-\eta}}{\sqrt{\pi \eta}} \right) \sin \theta d\theta \quad (2-42)$$

Danckwerts [18] obtained a solution for ϕ for a semi-infinite slab model (i.e. neglecting the stretching effect of the film) which is expressed as

$$\phi = \frac{\sqrt{\pi}}{2} \left\{ \left[\sqrt{k_1 t_{\max}} + \frac{1}{2\sqrt{k_1 t_{\max}}} \right] \operatorname{erf}(\sqrt{k_1 t_{\max}}) + \frac{\exp(-k_1 t_{\max})}{\sqrt{\pi}} \right\} \quad (2-43)$$

Wild and Potter [17] compared equations (2-42) and (2-43) for various values of $k_1 t_{\max}$ and indicated that for low reaction rates neglecting the stretching effect predicted absorption rates about 18% lower than the values obtained by considering the sphericity of the liquid film.

CHAPTER 4

EXPERIMENTAL4.1 Apparatus

4.1.1 General. The mechanics of the hydrogen-aminomethane exchange experiment involve contacting the aminomethane flowing over the ball absorber with hydrogen gas which is enriched in deuterium. The hydrogen-deuteride (HD) transfers from the gas phase to the liquid where it dissolves and reacts. The reaction transfers the deuterium atom (D) to the aminomethane in exchange for a hydrogen atom (H) which combines with the remaining H atom of the HD resulting in a slight supersaturation of the aminomethane liquid with H_2 . This excess hydrogen gas then diffuses back to the gas phase. The consequence of the exchange is therefore to deplete the gas phase of its deuterium content.

The solubility of HD in liquid aminomethane is very low and consequently the driving force for mass transfer in the liquid phase is small resulting in low gas absorption rates. This implies that if the gas phase were contacted with the liquid on a single pass basis the depletion of the deuterium in the gas phase would be very small which in turn would cause difficulties in detection of the small change. In order to alleviate this problem the gas phase was contacted with the liquid on a recirculating basis making the depletion of deuterium cumulative with time. A gas sample drawn from the circulating gas phase at a suitable time would indicate a deuterium content which is sufficiently lower than that of the previous sample to make the analysis

reliable.

The potassium methyl amide-aminomethane (PMA) solution is hazardous to work with and certain general precautions should always be observed to ensure adequate safety. These precautions may be briefly summarized as follows:

(i) Potassium methyl amide reacts violently with water liberating hydrogen which ignites creating explosive conditions in an air atmosphere. Moisture must therefore be kept out of the system at all times and contact with air must always be avoided.

(ii) When handling PMA solution in a refrigerated condition care should be taken to allow for volume expansion in case a warm up should occur or become necessary. Cold PMA solution should therefore, not be left trapped between valves.

(iii) Aminomethane is toxic and a powerful irritant. Continued exposure to it can cause eye irritation and respiratory problems. Adequate ventilation and purge fans should be available when working with this system.

(iv) The equipment used to feed and to store PMA solution must be protected against possible pressure buildup by providing pressure relief valves.

(v) Amyl alcohol and methyl alcohol can be used to destroy the PMA solution and must be available at hand when required. Adequate fire fighting equipment should also be available.

(vi) Face protection shields should be worn when handling PMA solution to avoid severe burns of the skin and eye damage from possible splashes.

The materials of construction used in the design of the hydrogen-aminomethane exchange equipment were limited to 316 stainless steel and glass due to the corrosive nature of the PMA solution. The stainless steel equipment was designed for 500 psig pressure and temperatures lower than -200°C . Operating pressures and temperatures in the steel equipment during an experiment were in the range of 40-50 psig and -40°C . The glass equipment was used where visual observation was desired. It was designed for a pressure of 50 psig although the most severe operating conditions were limited to 15 psig and -30°C . Neoprene rubber was used for most gaskets and O-rings. Polyethylene gaskets were used only where liquid PMA solution contact was anticipated and polypropylene glands were used for all valve packings. Polypropylene tubing was used in place of 316 ss tubing where flexible lines were considered desirable.

4.1.2 Hydrogen-Aminomethane Exchange Apparatus. The basic purpose of the hydrogen-aminomethane exchange system was to contact a circulating stream of enriched hydrogen with PMA solution flowing over the sphere absorber on a once through basis. An adequate volume of liquid feed was available to allow the liquid to flow on a once through basis and yet provide a sufficient time for the experiment. The planned temperature range of investigation was between -10°C and -30°C and to achieve this the entire exchange apparatus was enclosed in a refrigerated air bath whose temperature could be controlled between -5°C and -30°C with a sensitivity of about $\pm 1^{\circ}\text{C}$. The refrigeration was provided by a "York" unit model F62C-502E, six cylinder, two stage internally compounded refrigerant 502 compressor, with a capacity of 7920 BTU/hr. at -100°F saturated suction temperature. Methyl hydrate was used as the external

heat transfer medium. Auxiliary refrigeration units of smaller capacity were used to service the feed and catalyst wash sections of the apparatus. Details of the equipment that constitutes the exchange system are shown in Figure 2.

Pre-cooled liquid feed (PMA solution) from the liquid feed section (III) came into the absorption system through a "Whitey 21RS4" 316ss feed control valve (6) provided for accurate flow control. Any solid particles that might have been carried over by the liquid stream from the feed section were retained in a 60 μ size 316ss filter (15). The feed was then passed through a temperature stabilizing coil (16) and its flow rate was measured with a rotameter (18). A distributor (19) was provided in line to dampen any fluctuations in liquid flow before it was admitted on to the sphere absorber (23). The PMA solution passed over the sphere absorber through a jet nozzle (20) and the return liquid was collected in a take-off tube (24) from where it was led out of the air bath. Care was taken to keep the return liquid outside the air bath cold by installing concentric pipe heat exchangers (7,8) in the return line. This was done to ensure that no inverse pressure gradients, created by a possible fluid warm up, would impede the flow of the liquid to the receiving tanks (IV). A flow control valve (5) similar to the one in the feed line (6) was provided for accurate regulation.

Details of construction of the distributor, the nozzle, the ball absorber and the absorption chamber (25) have been included in the section on the diffusivity of hydrogen in aminomethane.

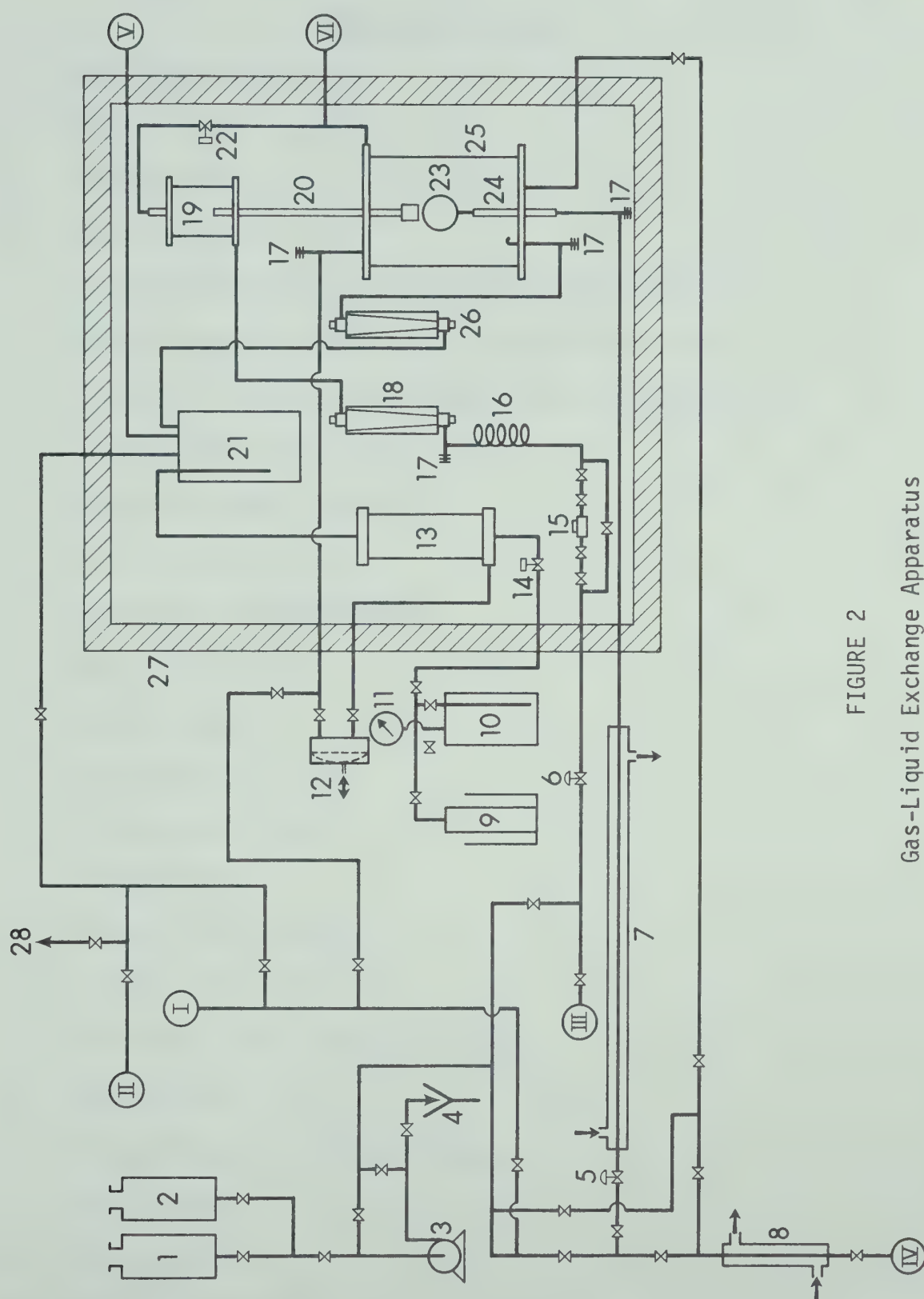


FIGURE 2
Gas-Liquid Exchange Apparatus

Symbols for Figure 2

1. Amyl Alcohol Container
2. Methyl Alcohol Container
3. Alcohol Pump
4. Drain
5. "Whitey" Control Valve on PMA Solution Return Line
6. "Whitey" Control Valve on PMA Solution Feed Line
- 7,8. Concentric Tube Heat Exchangers on Liquid Return Line
9. Saturator Amine Retrieving Tank
10. Saturator Amine Feed Tank
11. Pressure Gauge
12. Gas Phase Circulation Pump
13. Gas Saturator
14. Solenoid Valve
15. 316 SS Micron Filter
16. In Line Cooling Coil
17. Thermocouples
18. Liquid Feed Rotameter
19. Liquid Distributor
20. Jet Nozzle and its Approach Tube
21. Gas Reservoir
22. Pressure Balance Solenoid Valve
23. Ball Absorber
24. Take-Off Tube
25. Absorption Chamber
26. Gas Rotameter

- 27. Refrigerated Air Bath Enclosure
- 28. Gas Vent Line
 - I. To Vacuum System
 - II. To Enriched Hydrogen Feed Tank
 - III. To Liquid Feed System
 - IV. To Liquid Return Tanks and Catalyst Wash Tank
 - V. To Gas Sampling System
 - VI. To Mercury Manometer for System Pressure Record.

Enriched hydrogen was introduced into the exchange system at the beginning of an experiment and then was kept circulating through the absorption chamber with the aid of a diaphragm pump (12). The diaphragm was constructed from neoprene rubber and had to be replaced periodically due to wear. In order to prevent evaporation of aminomethane from the surface of the sphere absorber the circulating hydrogen was kept saturated with aminomethane. This was accomplished by passing the gas through a column of pure, dry, catalyst free liquid kept in the saturator (13). It was introduced into the saturator from a separate feed tank (10) through a solenoid valve (14). If necessary this aminomethane could be retrieved through the same line into a chamber (9) immersed in liquid nitrogen. From the saturator the circulating hydrogen passed into a tank volume (21) where flow fluctuations were dampened and the gas was led into the absorption chamber through a rotameter (26). The volume of the gas phase is a parameter to which the time taken to deplete a given fraction of the deuterated specie is proportional. The tank volume was thus suitably selected so that sufficient time for exchange might be available. Gas samples for analysis were taken from this tank through the gas sampling section (V).

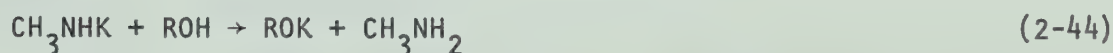
In order to achieve a smooth gravity flow of the liquid over the sphere absorber it was necessary to balance the pressures in the liquid distributor and the absorption chamber. This was accomplished through a solenoid valve (22) connecting the vapor spaces of the two chambers. The pressure in the absorption chamber was measured through this line by a mercury manometer (VI).

At the end of an experimental run the lines of the gas-liquid

exchange system had some residual PMA solution that could not be retrieved into the receiving tanks. In order to avoid plugging of the lines and the jet nozzle with solid catalyst due to evaporation of the amine from the PMA solution, this trapped liquid had to be disposed of in a suitable manner. This was achieved through the catalyst wash and destruction systems. The wash system as shown in Figure 3 was used to dilute the trapped PMA solution in the lines with pure aminomethane until the straw yellow color of the solution could no longer be seen.

The remaining catalyst in the diluted PMA solution was destroyed using the catalyst destruction system as shown in Figure 2. In order to destroy the catalyst, methyl hydrate was pumped through the lines and the reaction products were led into the drain or waste disposal area.

Potassium methyl amide reacts with alcohols to give a non-reactive alkoxide and aminomethane. The reaction is given by



where R is an alkyl radical. With an excess of the alcohol the products of reaction can be taken out of the system without difficulty. The reaction (2-44) generates substantial amounts of heat the magnitude of which depends on the alcohol being used. Higher alcohols give a mild reaction but are disadvantageous from the standpoint of subsequent system evacuation because of their low vapour pressures.

During an experiment, hydrogen gas samples were taken at suitable intervals from the tank volume of the exchange apparatus into a line

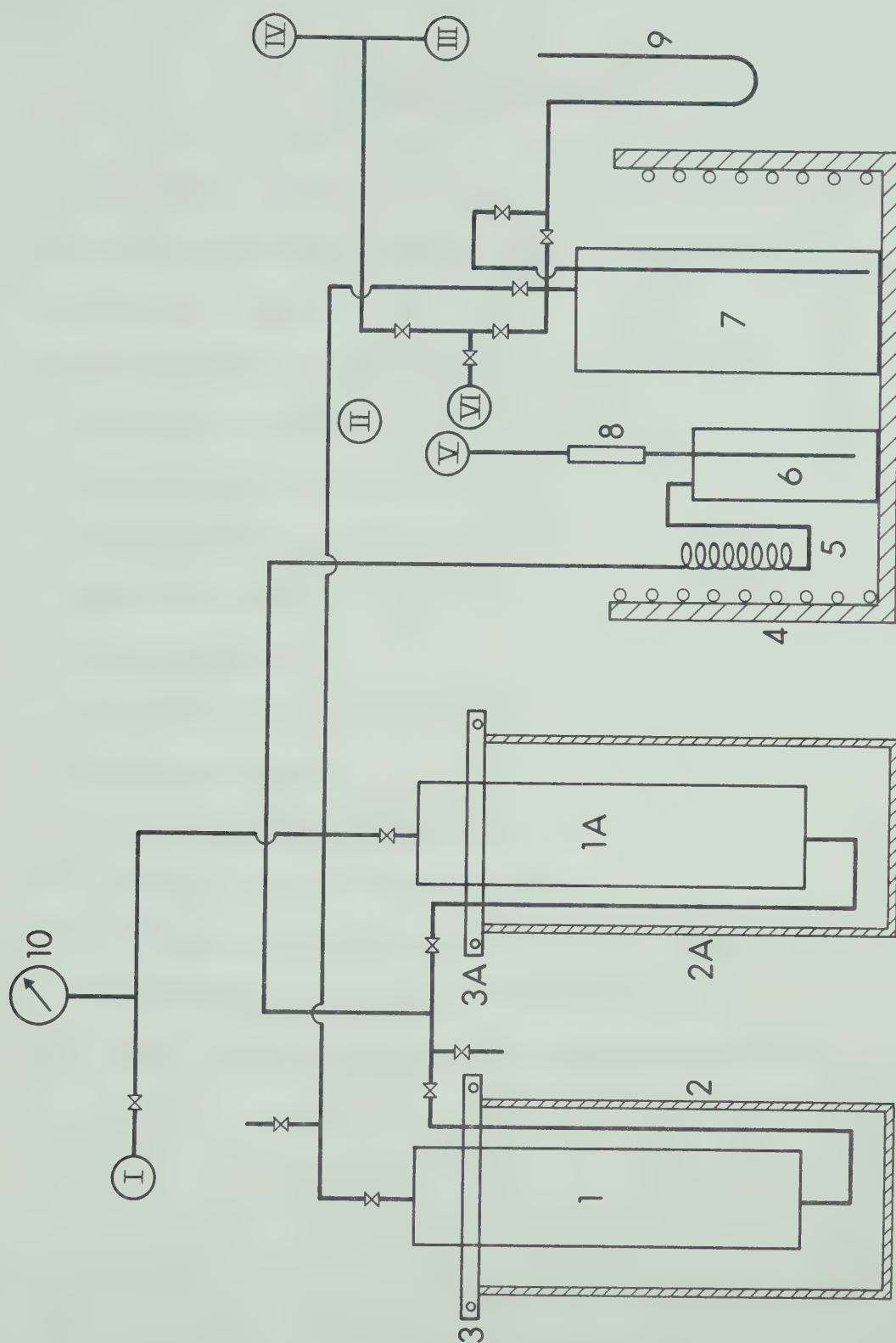


FIGURE 3
The Catalyst Wash System

Symbols for Figure 3

- 1, 1-A Aminomethane Holding Tanks
- 2, 2-A Mild Steel Drums to hold liquid nitrogen when required
- 3, 3-A Steel Straps
4. Cooling Bath with Ethylene Glycol-Water Mixture
5. In Line Cooling Coil
6. Intermediate Holding Tank
7. Catalyst Wash Receiving Tank
8. Glas Wool Filters
9. Mercury Manometer
10. Pressure Gauge
- I. To Vacuum System
- II. To Liquid Feed-Receiving Tank System
- III. From Gas-Liquid Exchange Apparatus
- IV. To Catalyst Destruction System (Alcohol Lines)
- V. Aminomethane Wash Feed to Exchange Apparatus
- VI. Alcohol to Drain during Catalyst Destruction Cycle.

whose volume was about 5cc. The sample was then expanded into sample bombs. The aminomethane vapours in the gas sample were condensed in chilled traps. At the end of a run the samples were analyzed using mass spectrometry.

In order to characterize the data completely it was necessary to take PMA solution samples and analyze them for concentration of potassium. This sampling was not done as a regular feature at the end of every experiment but was done frequently to ensure that the catalyst concentration was well established. The analysis was done on an atomic absorption spectrophotometer.

Additional equipment used to carry out the various operations outlined above, for a hydrogen-aminomethane exchange experiment, is described below.

4.1.3 Liquid Feed System. The liquid feed system as shown in Figure 4 was made up of two parallel trains which served as the feeding tanks (1-1A) and receiving tanks (2-2A) on an alternating basis. Each set of tanks was made from two 6 inch diameter, 316 SS chambers immersed in a bath of ethylene glycol-water mixture (11,12). The temperature of the bath around the feeding tanks was controlled at 25°C and the bath around the receiving tanks was kept refrigerated at -40°C. Methyl hydrate was used as the heat exchange medium. A constant vapour pressure of the PMA solution at 25°C was thus used to feed the liquid to the gas absorption chamber. Liquid was fed from the feeding tanks through two dip tubes and was cooled en route to the absorption chamber by concentric pipe heat exchangers (13, 14, 15 16) and an intermediate cooling bath (10) also containing ethylene glycol-water. Adequate residence time was provided in the cooling bath by introducing an in-line cooling coil

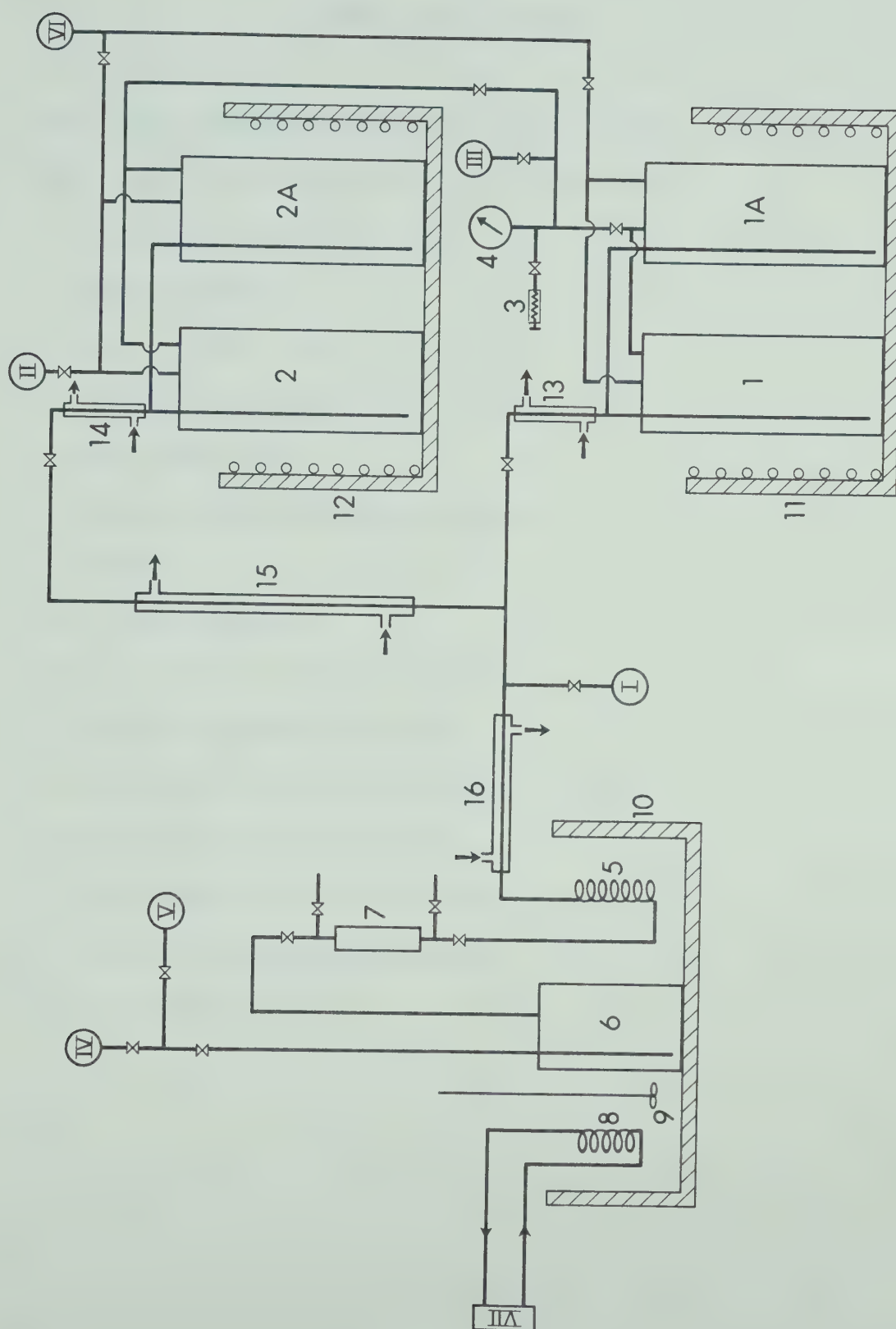


FIGURE 4
The Liquid Feed System

Symbols for Figure 4

- 1-1A. Liquid (PMA) Feed/Return Tanks (1st Set)
- 2-2A. Liquid (PMA) Feed/Return Tanks (2nd Set)
- 3. Pressure Relief Valve
- 4. Pressure Gauge
- 5. In Line Cooling Coil
- 6. Intermediate Holding Tank
- 7. Glass Wool Filter
- 8. Cooling Coil carrying Refrigerant
- 9. Stirrer
- 10-12. Cooling Baths
- 13-16. Concentric Tube Heat Exchangers
- I. To PMA Solution Storage Tank
- II. PMA Solution Feed Line from Storage Tank
- III. To Argon Pressure Cylinder
- IV. To Alcohol Lines for Catalyst Destruction
- V. To Gas-Liquid Exchange System
- VI. To Vacuum System

(5) and an intermediate tank (6). Secondary filtering of the PMA solution was achieved through a glass wool filter (7). Each set of tanks was provided with vacuum, argon blanketing, pressure measuring and pressure relief services.

4.1.4 Catalyst Wash System. Two stainless steel holding tanks (1,1A) (Fig.3) containing pure aminomethane were supported on the edge of two outer mild steel drums (2,2A) by steel straps (3,3A). The holding tanks were connected in parallel to ensure an adequate supply of aminomethane and to balance pressures. The aminomethane was pre-cooled by passing it through a cooling coil (5) and a tank volume (6) both immersed in a refrigerated bath (4) of ethylene glycol-water. The wash amine was then filtered through a glass wool filter (8) before being finally led to the gas-liquid exchange section. The diluted PMA solution was returned into a mild steel refrigerated holding tank (7). After three or four experiments the bulk of the amine in tank (7) was flash distilled into the original holding tanks (1,1A) for re-use. The flash distillation was achieved by filling the mild steel drums (2-2A) surrounding the holding tanks with liquid nitrogen and connecting the vapour spaces of the holding tanks (1,1A) with tank (7) which was brought to room temperature before initiating the distillation procedure.

4.1.5 Catalyst Destruction System. Two glass bottles (1,2) (Fig.2) containing amyl alcohol and methyl alcohol respectively, were connected to the gas-liquid exchange system through a centrifugal pump (3). The amyl alcohol was kept stocked as a standby in case of an emergency situation. The methyl alcohol was used to destroy the remaining catalyst in diluted PMA solution left in the lines of the gas-liquid

exchange system after the wash operation was completed. The alcohol was pumped into the absorption chamber through the PMA feed line, return line and the drain line. These were the only lines that come in contact with the liquid. The same pump was then used to pump the liquid out of the chamber into a drain (4). The above procedure was followed only when some PMA solution spillage had occurred during an experiment. If such was not the case then the alcohol was simply pumped through the liquid feed line and out through the return line into the drain.

4.1.6 Catalyst Make-up Section. Potassium methyl amide catalyst was made by contacting freshly cut potassium metal with dry aminomethane in a 10 inch diameter 316 SS storage tank (1) (Fig. 5) of about 35 litres total capacity.

The potassium metal was cut into small pieces, washed in n-pentane and introduced into the tank through a 1/2 inch bore under a blanket stream of argon. This was done to prevent contact of air and moisture with the highly reactive metal. The storage tank was then evacuated through the main vacuum system (IV) to eliminate traces of air, argon and n-pentane. When a vacuum of the order of $1-5\mu$ was obtained, the required amount of dry aminomethane was flash distilled into the storage tank (V) by cooling the latter in a bath of liquid nitrogen. The frozen aminomethane was then allowed to thaw out and on doing so the potassium metal began dissolving in the liquid. This could be seen by observing the blue color of the solution through a sight glass (9). The solution of potassium in aminomethane is a slow step in the preparation of the PMA solution. In order to enhance the rate of solution the aminomethane was circulated in and out of the storage tank by a 316 SS

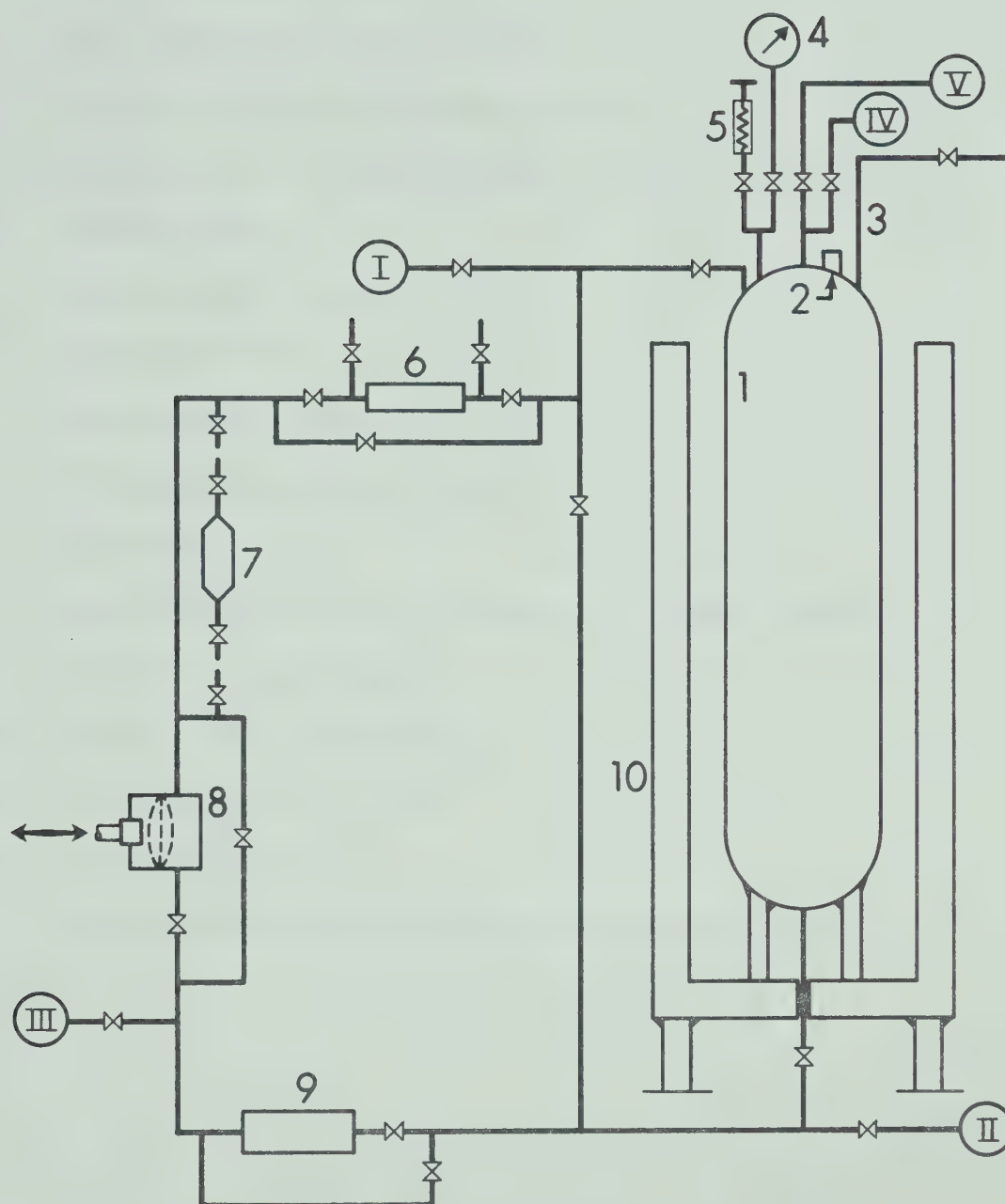


FIGURE 5

The Catalyst Make-up and Liquid Sampling Section

Symbols for Figure 5

1. PMA solution Bulk Storage Tank
2. Port for Introducing Potassium Metal
3. Alternate Line for Removing Feed from Tank
4. Pressure Gauge
5. Pressure Relief Valve
6. Glass Wool Filter
7. Sampling Bomb Assembly
8. Polypropylene Diaphragm Pump
9. Sight Glass
10. Outer Vessel for holding Liquid Nitrogen When required
- I. Return from Feed System
- II. Liquid Feed to Feed System
- III. To Argon Pressure System
- IV. To Vacuum System
- V. Feed Line for Flash Distilled Dry Aminomethane Vapour

positive displacement pump with a polypropylene diaphragm (8). Any solids foreign to the system were retained in a glass wool filter (6) installed in the circulation loop. A by-pass was installed so that liquid samples could be drawn from the circulating stream by introducing a pre-assembled sample bomb (7) in line with the system. Other by-passes were installed to isolate any piece of equipment from the PMA circulation line, should any replacement or maintenance become necessary.

Potassium metal reacted with aminomethane forming the amide and liberating hydrogen. The liberated hydrogen resulted in an increase in the total pressure of the storage vessel. This could be monitored on a pressure gauge (4). A pressure relief valve (5) was provided to bleed off any pressure in excess of a safe limiting value. A dip tube (3) was also installed so that the entire charge could be dumped if necessary. This was done as an extra safety measure.

4.1.7 Gas Sampling System. Gas samples were drawn from the gas-liquid exchange system during a run, into an evacuated line of about 5cc volume. This sample was then expanded through a set of liquid nitrogen chilled traps (1) (Fig. 6) into an evacuated sample bomb. Aminomethane vapours carried over with the gas sample were condensed in the chilled traps. A mercury manometer (3) was used to measure the pressure in the sample bomb. After the sample was obtained, the lines were completely evacuated in readiness for the next sample.

The pressure in the absorption chamber was measured by a mercury manometer (9). In order to know the pressure at which the sample was drawn from the exchange system it was necessary to know the drop of pressure in the absorption chamber after each sample was drawn. This

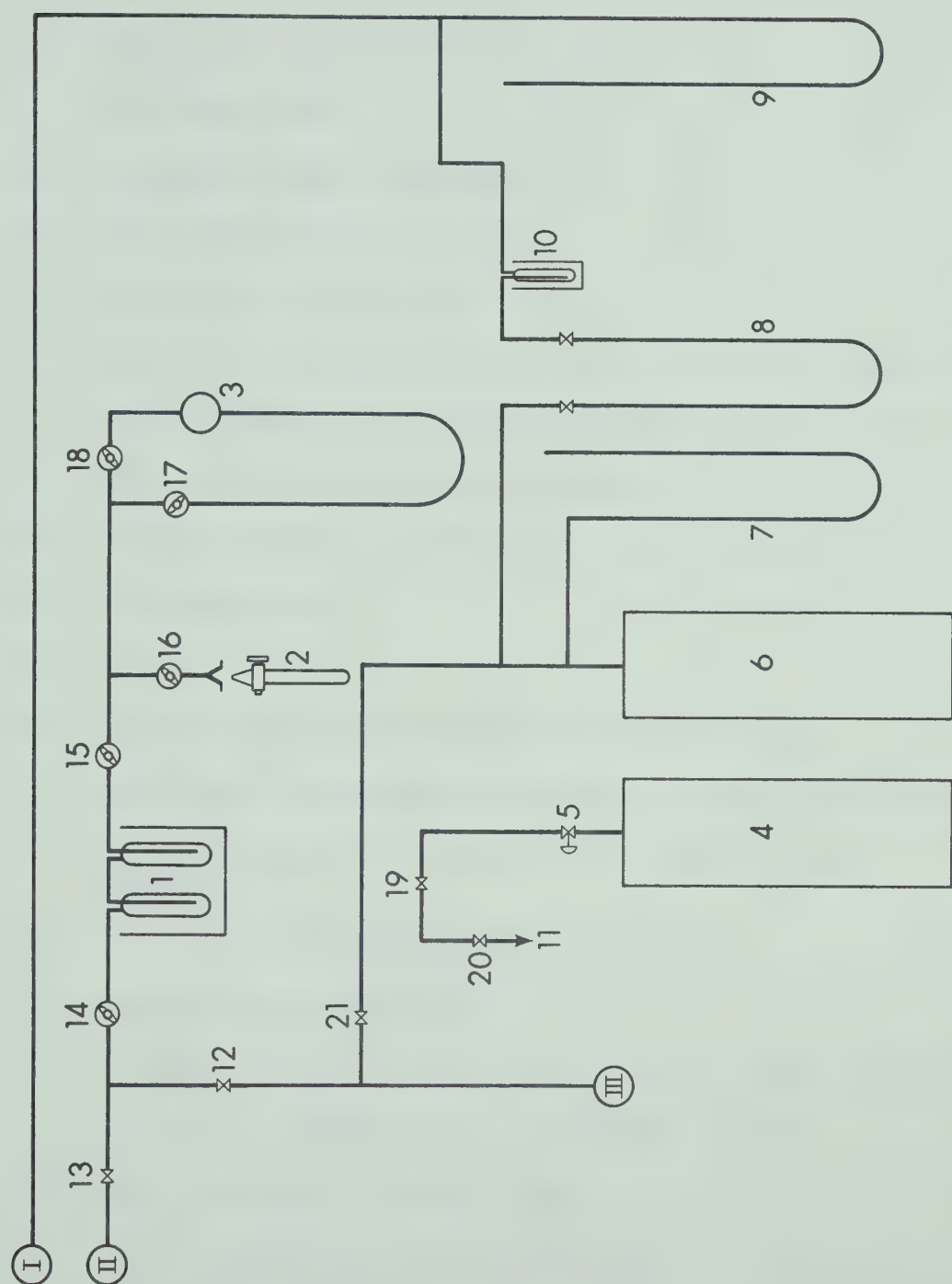


FIGURE 6

The Gas Sampling Apparatus

Symbols for Figure 6

1. Aminomethane Vapour Traps
2. Gas Sample Bomb
3. Sampling Pressure Manometer
4. Ultra Pure Hydrogen Cylinder
5. Pressure Regulator Valve
6. 15 Litre Tank Capacity filled with Ultra Pure Hydrogen
7. Mercury Manometer to measure pressure in (6)
8. Differential Pressure Oil Manometer
9. Mercury Manometer on the Gas Absorption Chamber
10. Oil Vapour Trap
11. To Vent
12. Valve isolating Sample Volume from Vacuum Pump.
13. Valve isolating Sample Volume from the Gas-Liquid Exchange Apparatus
14. Glass Valve isolating Sample Volume from the rest of the Sampling Apparatus
15. Glass Valve to Sample Pressure Manometer
16. Glass Valve to Sample Bomb
- 17,18 Glass Valves on either leg of Sample Pressure Manometer
19. Valve to introduce ultra pure Hydrogen in (6).
20. Valve for Excess Pressure Bleed
21. Valve isolating (6) from Vacuum Pump
- I. To Gas Absorption Chamber
- II. From Gas Reservoir in the Gas-Liquid Exchange System
- III. To Vacuum Pump

drop was small enough to go undetected on the mercury manometer (9) and was thus measured with an oil manometer (8). Octoil-S, a high vacuum diffusion pump oil was used as a manometric fluid. This oil has a very low vapour pressure which is desirable to prevent contamination of the exchange system. A small ice chilled trap (10) was also used between manometers (8) and (9) to reduce the risk of contamination.

One leg of the oil manometer was hooked to the absorption chamber along with the mercury manometer (9). The other limb was attached to a large fifteen litre tank (6) which contained pure hydrogen. The pressure in this tank was measured by another mercury manometer (7). At the beginning of an experiment the pressure in the tank (6) was set to the starting pressure of the absorption system by matching manometers (7) and (9). This was accomplished by adjusting the pressure in (6) so that both limbs of the oil manometer (8) read zero. A hydrogen supply cylinder (4) was used to introduce gas into tank (6) if required.

4.1.8 Analysis.

(a) Gas Samples

The gas samples taken from the exchange system during an experiment were analyzed for deuterium content by a mass spectrometer.

The instrument, designed and built by Buckley [19] is a 90° sector analyzer with a radius of 2.5 inches and employs dual collection of the isotopes D and H. The sample is introduced into the instrument as a gas and the signal from the collection cup for each isotope is amplified and read on vibrating reed electrometers. The electrical signal of the electrometers is also sampled on-line by an IBM 1800 process computer which processes the data and computes the results in accordance with pre-programmed instructions.

(b) Liquid Samples

Liquid samples of the PMA solution were taken occasionally from the feed tanks for analysis of total potassium. Atomic absorption spectrophotometry was used to estimate the concentration of the catalyst. The sample was weighed, hydrolyzed and diluted to known volumes. A set of potassium standards ranging from 0.0 to 5.0 mg K/litre solution were prepared and analyzed on the Atomic Absorption Spectrophotometer (AAS) to generate the calibration curve. The sample was then analyzed and its potassium content was estimated from the calibration curve. The catalyst concentration was computed from the potassium content of the sample and the known dilution procedure. The AAS was a model 290-B "Perkin-Elmer" unit which employs a hollow cathode type "Intensitron Lamp" #566-M. The cathode of the lamp contains the element which has to be analyzed. The sample is aspirated and burnt through a flame which breaks the chemical bonds of the compound and the individual atoms of the element of interest float freely in the absorption area of the instrument. Light emitted from the element of hollow cathode lamp is passed through the flame and depending on the concentration of the sample a certain proportion of the light is absorbed. The instrument measures the amount of absorption.

4.1.9 Hydrogen Make-Up and Purification. A Milton-Roy hydrogen generator was used to produce a supply of hydrogen enriched with deuterium. The feed to the generator was enriched water which was electrolyzed to give hydrogen. The enriched gas was passed through a series of three beds to remove impurities before entering the gas absorption chamber. The beds consisted of activated charcoal for hydrocarbon

impurities, palladium supported on alumina for oxygen and silica gel for water.

4.2 Operating Procedures

4.2.1. The Exchange Experiment. The operating procedure used for conducting the hydrogen-aminomethane exchange experiment was similar to the procedure for the measurement of diffusivity of hydrogen in aminomethane as far as control of liquid flow rate, take-off level and system temperature of the gas-liquid exchange section was concerned. However, some basic differences between the exchange and diffusivity experiments introduced important changes in the running of the equipment. A step by step operating procedure for a typical experimental run is outlined in Appendix A2.

One inch and one and one half inch diameter sphere absorbers were used for the exchange experiments. The large ball was found to be useful in effectively reducing the time taken for a given fractional depletion and thus improved the chances of reaching chemical equilibrium during the period of the experiment. A jet diameter of 0.046 cms and jet lengths of 0.2 to 0.265 cms were used to obtain the entire data set. In concurrence with the findings of the diffusivity work, a take-off length of 1.25 cms was always maintained and it was assumed that for this value of the take-off length the stagnant layer mentioned in the first part of this thesis was always at the junction of the sphere and the take-off rod. The take-off rod was 1/16 inch in diameter.

Pre-cooled liquid feed was introduced into the refrigerated, controlled temperature exchange apparatus to contact with enriched

hydrogen which had been previously saturated with aminomethane and which was kept circulating at a rate of about 100 cc/sec. The total gas volume of the system was about 2500 cc which meant that the turn around time for the gas was about 25 seconds. A liquid flow rate of about 0.3 cc/sec was maintained by controlling the feed rate with the "Whitey" control valve. This flow rate was adequate to ensure that there was minimal enrichment of a liquid element during its residence over the sphere absorber. At the above mentioned liquid flow rate there was no visual evidence of any ripples being present on the sphere absorber. Minor disturbances of the liquid were, however, observed on the take-off tube level and were perhaps indicative of some activity on the take-off rod. Since the diameter of the sphere absorber was 24 times larger than the rod some activity on the latter could be expected. This only emphasized the importance of keeping the take-off level well controlled at 1.25 cms.

A gas sample was taken before the liquid PMA solution was introduced into the system and subsequent gas samples were generally taken at 10 minute intervals during the exchange experiment. This was achieved by expanding a 5 cc sample into an evacuated glass sample bomb. Aminomethane vapours in the sample were condensed in a trap immersed in liquid nitrogen. Before allowing a sample into the sample bomb, the equivalent of one sample volume (~5cc) was discarded. This was done to eliminate the effect of dead volume in the line up to the tank from which the sample was drawn.

In order to justify the assumption of an essentially constant composition of the liquid with respect to the deuterated specie the

minimum molar ratio of liquid to gas in the system during operation was about 300. This could be achieved by running the experiment at a hydrogen partial pressure of about 1.2 atmospheres with a maximum total system pressure of about 2.0 atmospheres at -10°C .

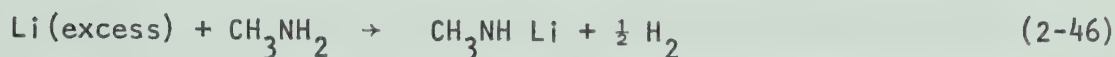
After the desired number of samples were obtained, the feed was stopped and the PMA solution in the system was drained into the receiving tanks. Any left over solution in the lines was diluted with pure aminomethane and the wash was separately stored. Finally the system was washed with methyl hydrate to destroy any remnants of catalyst in the system. The outgoing methyl hydrate, aminomethane and potassium methoxide mixture was drained.

4.2.2 PMA Solution Make-Up. The handling of potassium or lithium metal requires adherence to safe working procedures so that a hazardous situation might be avoided. The most prominent one of these is the necessity of keeping the metals out of contact with air or moisture at all times. The work of Hayashitani [12] has outlined details of the methods recommended when working with potassium metal. These methods were followed quite rigidly.

A high catalyst concentration in the PMA solution results in high rates of exchange which is a desirable feature from an industrial standpoint. Catalyst concentrations upto 15.8 gms K/kg Amine were prepared for this study.

Aminomethane was obtained in cylinders from Matheson of Canada Ltd. Its analysis report indicated a maximum of 0.8% moisture content which was removed by contacting the required aminomethane charge (about 28 litres) with a slight excess of lithium metal in the absence of air. The reaction of lithium with water produced lithium hydroxide

and hydrogen. The equations that describe the reactions of lithium with aminomethane containing moisture are:



The hydrogen produced from these reactions increases the pressure of the system which in turn inhibits the reaction. The gas was bled off periodically and the pressure kept at about 30 psig at room temperature. The reaction was assumed to have gone to completion when no further increase of pressure was observed. The entire process of removing water from the aminomethane took about 48 hours.

The PMA catalyst solution was prepared in much the same manner as the drying of aminomethane. The amount of potassium metal required for a charge of about 28 litres of PMA solution was cleaned, cut and contacted with dry aminomethane in a 316 SS storage vessel in absence of air or moisture. The aminomethane was flash distilled into the vessel by immersing the latter in a bath of liquid nitrogen. On thawing out, the aminomethane reacted with the potassium according to the following equation.



This reaction is catalyzed by traces of iron which were supplied by the walls of the stainless steel vessel.

Potassium metal dissolves in aminomethane giving a blue color to the solution. It then reacts to form the amide and on completion of the reaction the color changes to straw yellow. The solution step is

however, the slower of the two and as such the liquid of the make-up vessel was kept circulating so as to improve the rate of dissolution. As in the case of the lithium drying of aminomethane, the hydrogen pressure buildup was continually relieved to keep the reaction progressing. In spite of these measures, however, the reaction may still take a week or more to go to completion. A detailed sequential procedure for the make-up of PMA solution is included in Appendix A2.

4.2.3 Analysis

(a) Gas Samples

The mass spectrometer used for the analysis of gas samples was calibrated using hydrogen standards containing 1.5, 99, 365 and 471 ppm deuterium.

The 1.5 ppm standard was prepared by collecting the hydrogen gas evolved by contacting a water standard of 1.5 ppm deuterium concentration with calcium metal. The water standard was supplied by the Chalk River Nuclear Laboratory (CRNL) of AECL. The other three standards were prepared by diluting a high deuterium concentration volume of hydrogen obtained from the hydrogen generator with ultra pure hydrogen of natural concentrations obtained from Matheson of Canada Ltd. These three standards were analyzed at CRNL relative to the 1.5 ppm water standard and the resulting values reported above were taken to be the absolute deuterium concentrations of the samples.

The mass spectrometer was calibrated before and after the analysis of a set of samples belonging to an exchange experiment. The current ratios (I_3/I_2) obtained from the mass spectrometer for the standards were compared with the absolute D/H ratios through the following relationships.

$$\delta_{DI} = \left(\frac{R^*}{R_{st}} - 1 \right) 1000 \quad (2-48)$$

$$\delta_{st} = \left(\frac{C_1^*}{C_{st}} - 1 \right) 1000 \quad (2-49)$$

where R^* = The ratio of mass three (HD) to mass two (H_2) currents (I_3/I_2) for the sample at a fixed value of I_2 (also described as a fixed value of hydrogen pressure). The ratio I_3/I_2 is uncorrected for H_3^+ contribution.

R_{st} = The ratio I_3/I_2 for the principal standard at the same value of I_2 .

C_1^* = Absolute value of the sample in ppm deuterium.

C_{st} = Absolute value of the principal standard in ppm deuterium.

The principal standard chosen for this study was the 365 ppm deuterium sample but in principle any of the 99, 365 or 471 ppm standards could be chosen as the principal standard. I_3 and I_2 are respectively, the current signals generated by the HD and H_2 beams bombarding the collector caps of the mass spectrometer. A plot of δ_{DI} and δ_{st} was considered to be the calibration curve of the mass spectrometer. The plot was essentially a straight line whose equation was determined by standard least square techniques. A typical example of this curve with the plotted points representing the standards is shown in Figure 7. The values 'R' obtained from the mass spectrometer for each of the samples taken during a run, were converted to the corresponding δ_{DI} 's using equation (2-48). The least square equation was then used to determine the δ_{st} 's from which the absolute values ' C_1^* ' were obtained by equation (2-49).

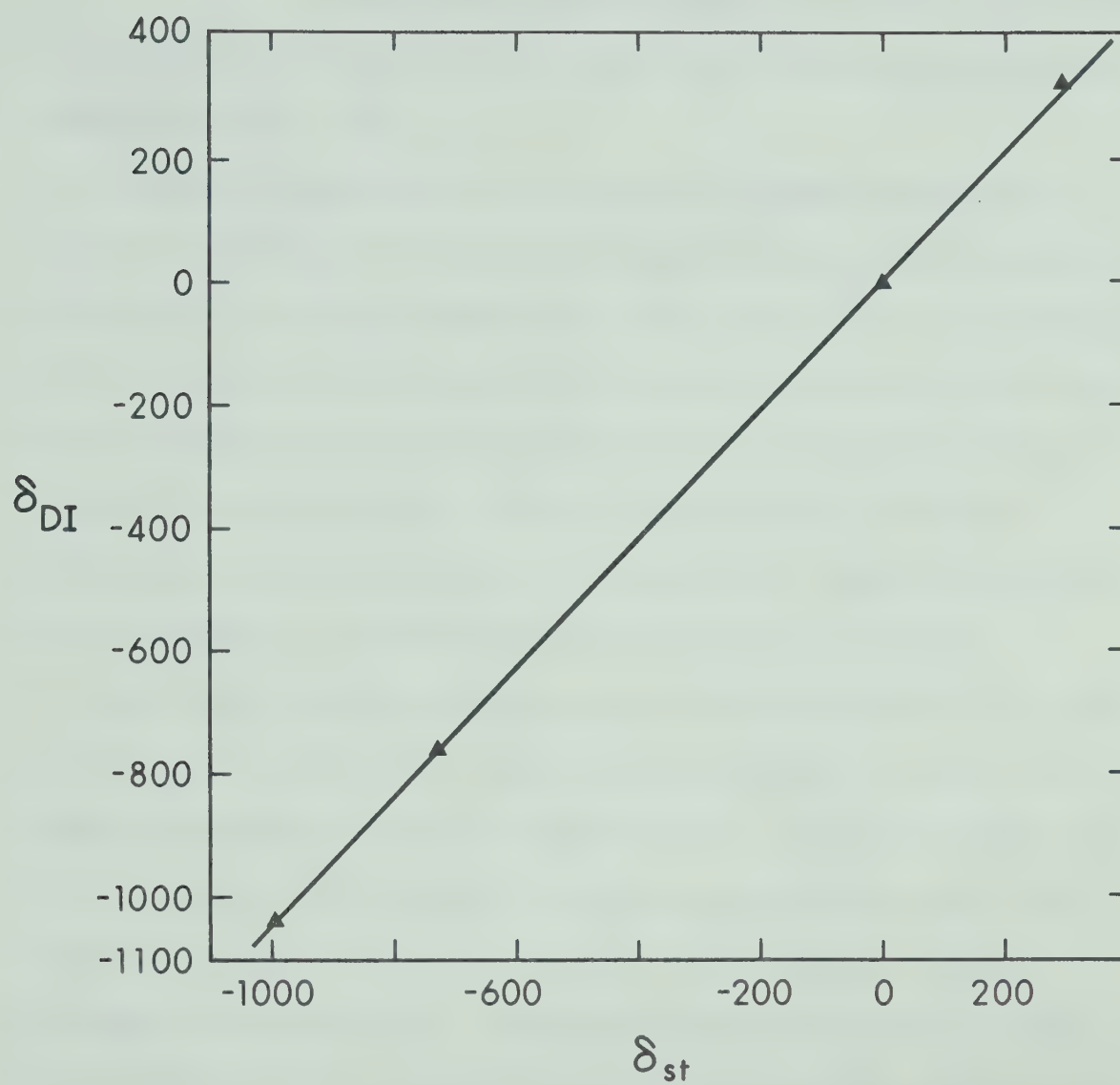


FIGURE 7

A Typical Mass Spectrometer Calibration Curve

(b) Liquid Samples

Liquid samples were taken from the system periodically and analyzed for potassium methyl amide using the atomic absorption spectrophotometer (AAS).

Two 316 SS sample bombs consisting of a sample volume and an expansion volume were thoroughly evacuated and then used to sample the PMA in line. An average sample was in the range of 4 to 6 gms and was taken in duplicate. The sampled PMA was then hydrolzed in distilled water and the resulting solution was heated in an oven at 200°F to drive off the aminomethane. On most occasions the solution was evaporated to dryness but this is not essential. Usually heating for about four hours is sufficient to drive off the aminomethane.

Six liquid standards containing 0.0 (distilled water), 1.0, 2.0, 3.0, 4.0 and 5.0 mgms K/litre solution were prepared by dissolving appropriate amounts of KCl in distilled water. The dried sample was re-dissolved in distilled water to make up a volume such that its estimated concentration of potassium was between 0.0 and 5.0 mgms K/litre solution. The standards and the samples were then analyzed on the AAS. A calibration curve of potassium concentration vs AAS reading was prepared by using the standards. The AAS reading obtained from the samples was then converted to potassium concentration by using the calibration curve. The concentrations thus obtained were interpreted to give PMA concentrations in gms K/kg amine by using the dilution procedure and the weight of the samples. A typical calibration curve for the AAS is shown in Figure 8.

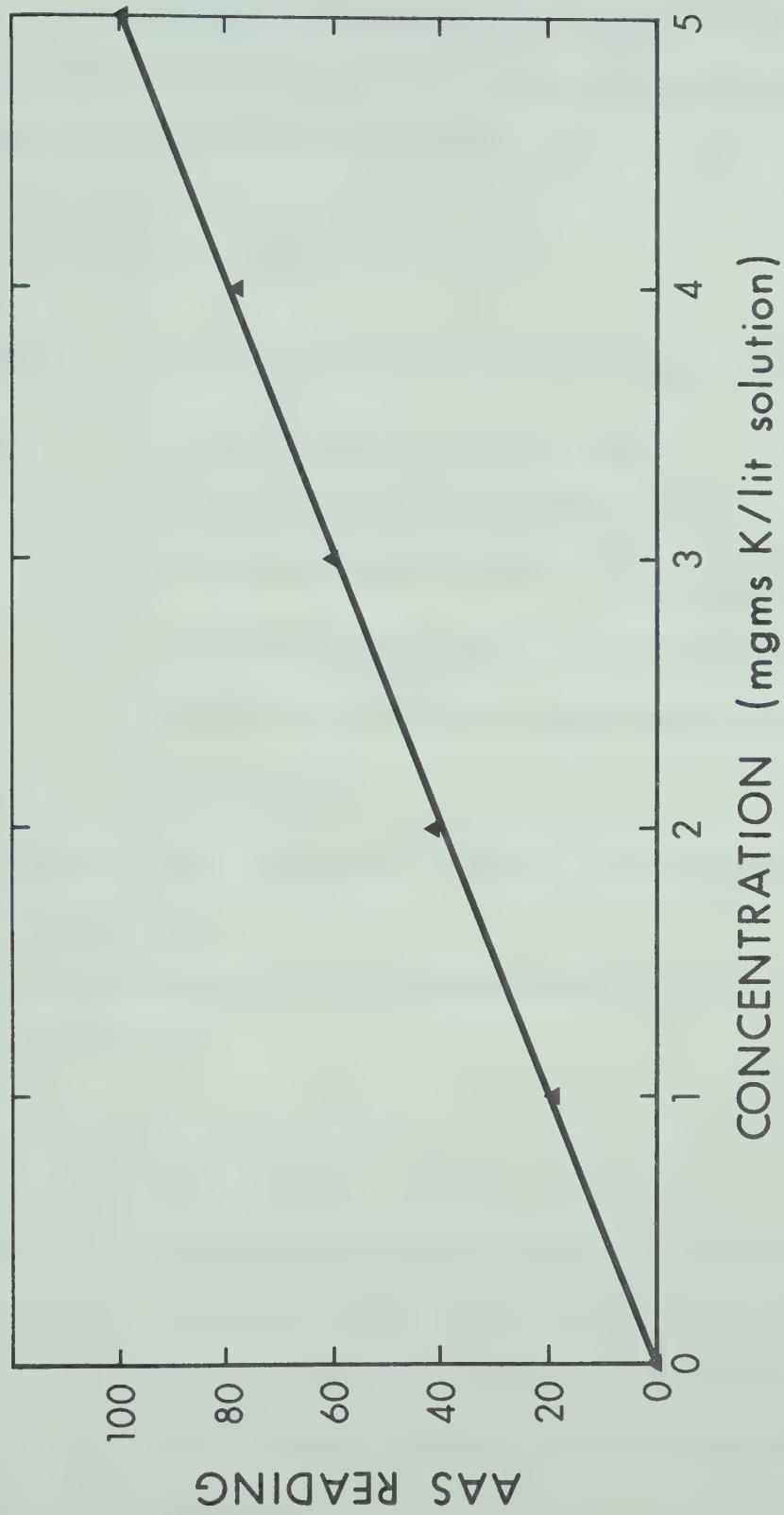


FIGURE 8

A Calibration Curve for the Atomic Absorption Spectrophotometer

4.2.4 Method of Interpretation of Data. The number of moles of HD in the circulating gas phase deplete cumulatively with time. This depletion rate may be expressed as

$$-n_{H_2} \frac{dy}{dt} = - \frac{PV}{R_g T} \frac{dy}{dt} = G_i \quad (2-50)$$

where n_{H_2} = Total number of moles of hydrogen gas.

P = The partial of hydrogen (atm)

V = Total volume of the system occupied by the gas (cc)

R_g = Universal gas constant = $\frac{82.06(cc)(atm)}{(gm\ mole)(^{\circ}K)}$

T = Absolute temperature of the circulating hydrogen ($^{\circ}K$)

y = Mole fraction of hydrogen deuteride (HD) in hydrogen (H_2)

t = time (sec)

The negative sign indicates a decreasing concentration y of HD with time in the gas phase.

A mass balance of the hydrogen deuteride across the gas-liquid interface yields

$$- \frac{PV}{R_g T} \frac{dy}{dt} = K_L A_s (C^* - C_e) \quad (2-51)$$

where A_s = The surface area of contact for the dry sphere (cm^2)

K_L = The overall mass transfer coefficient (cm/sec)

C^* = The concentration of HD in the liquid phase in physical equilibrium with the HD concentration in the bulk gas phase

$\frac{gm\ moles}{cc}$

C_e = The concentration of HD in the liquid in chemical equilibrium with the concentration of CH_3NHD in the bulk liquid $\frac{gm\ moles}{cc}$

Since the molar ratio of the liquid to gas used was always very high the value of CH_3NHD in the bulk liquid was essentially constant which implies that C_e is a constant for a given experiment. Assuming that the total resistance to mass transfer can be represented by a two film theory concept one can say that

$$\frac{1}{K_L} = \frac{1}{k_L} + \frac{\rho_L}{H_2 k_g} \quad (2-52)$$

where ρ_L = molar density of the liquid $\frac{\text{gm moles}}{\text{cc}}$

H_2 = The Henry's Law coefficient $\frac{\text{atm}}{\text{mole fraction}}$

k_L = Liquid phase mass transfer coefficient $\frac{\text{cm}}{\text{sec}}$

k_g = Gas phase mass transfer coefficient $\frac{\text{gm moles}}{\text{cm}^2 \text{sec atm}}$

Since the solubility of hydrogen in aminomethane is very low (i.e. H_2 is very high) the resistance to mass transfer is essentially in the liquid phase and therefore

$$\frac{1}{K_L} \approx \frac{1}{k_L} \quad (2-52a)$$

and C^* corresponds to the interfacial concentration as well and may be replaced by C_i . Representing the solubility of HD in aminomethane by the Henry's Law as

$$yP = P_2 = H_2 x_2 \quad (2-53)$$

$$\therefore x_2 = \frac{yP}{H_2} \quad (2-54)$$

where P_2 = Partial pressure of hydrogen deuteride

x_2 = Mole fraction of HD in the liquid phase.

Noting that

$$\left. \begin{aligned} c_i &= \rho_L x_i \\ \text{and } c_e &= \rho_L x_e \end{aligned} \right\} \quad (2-55)$$

Equation (2-51) may be expressed as

$$- \frac{PV}{R_g T} \frac{dy}{dt} = K_L A_s \rho_L \frac{P}{H_2} (y_i - y_e) \quad (2-56)$$

Assuming that the concentration of HD in the gas at time $t=0$ is given by y_{in} , and replacing y_i by y , integration of equation (2-56) between 0 and t leads to

$$\ln \left(\frac{y - y_e}{y_{in} - y_e} \right) = - \frac{K_L A_s \rho_L R_g T}{V H_2} t \quad (2-57)$$

If the interfacial area of contact for the sphere is corrected for the thickness of the film then A_s in equation (2-57) may be replaced by

A_A where

$$\frac{A_A}{A_s} = 1 + \frac{2.58 \Delta^+}{R} \quad (2-58)$$

A_s being the surface area of the dry sphere and Δ^+ the liquid film thickness at the sphere equator.

A plot of $\ln \left(\frac{y - y_e}{y_{in} - y_e} \right)$ vs t yields a slope of

$$- \frac{K_L A_A \rho_L R_g T}{V H_2} \quad \text{from which } K_L \text{ the mass transfer coefficient may}$$

be obtained. For high values of the chemical rate constant k_1 (i.e.

in the fast reaction regime) equation (2-6) may then be used to determine k_1

$$\text{i.e. } K_L = \sqrt{k_1 D} \quad (2-6)$$

For lower values of k_1 equations (2-35) to (2-38) may be suitably rearranged to isolate K_L as a function of k_1 and known system properties.

CHAPTER 5

RESULTS

Experiments were conducted to measure the rate of exchange of hydrogen with PMA solution at four temperatures in the range of -10°C to -30°C . Both the 1 inch and the 1.5 inch diameter sphere absorbers were used to obtain the data. Three catalyst concentrations were investigated in the range of 5.0 to 16.0 gms K/kg amine. The rate constants and the mass transfer coefficients calculated from the data are given in Table 2. Equation (2-6) was used to relate K_L with k_1 and the surface area exposed by the sphere absorber and the jet was considered to be the interfacial area of contact. A detailed sample calculation showing the procedure used is given in Appendix B2.

Figure 9 is a typical plot of $\ln \left(\frac{y-y_e}{y_{in}-y_e} \right)$ vs time and indicates the pseudo-first order nature of the exchange reaction. The ratio $\left(\frac{y-y_e}{y_{in}-y_e} \right)$ is indicative of the cumulative depletion of hydrogen deuteride in the gas phase. The equilibrium value y_e was estimated either by direct gas analysis or from the liquid concentration of deuterium and the separation factor defined by equation (2-17). Equation (2-21) was used to represent the separation factor as a function of temperature. For cases where the experiment was allowed to reach equilibrium, y_e was obtained directly by gas analysis and the corresponding liquid phase equilibrium concentration was estimated using equation (2-17). Once known, the liquid phase concentration was suitably adjusted to account for liquid enrichment at the end of each experiment. This was achieved by a simple mass balance of deuterium between the gas and the liquid

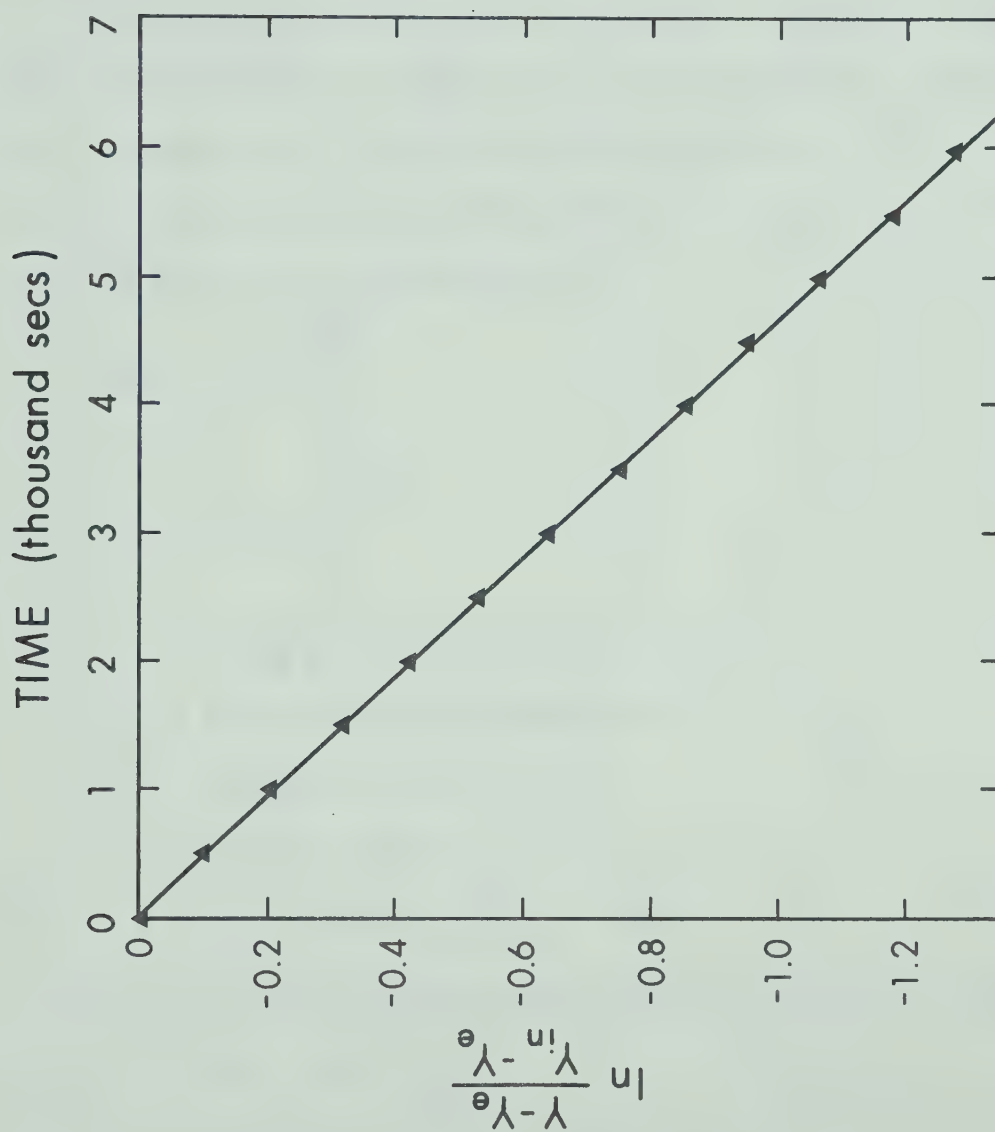


FIGURE 9

The Cumulative Depletion of Hydrogen-Deuteride in the Gas Phase with Time

phases. Details of this calculation are given in Appendix B2. Owing to the very large molar ratio of liquid to gas (~300) the enrichment of the liquid for each experiment was seldom above 1 ppm which meant a change in the gas phase equilibrium value of about 0.2 ppm.

The logarithm of the rate constant k_1 is plotted vs the reciprocal absolute temperature in Figure 10. The relation of k_1 with temperature may be expressed by (a) the Arrhenius Equation, or (b) the Transition State or Absolute Reaction Rate Theory. The temperature dependency for the two cases is expressed as

$$\text{a) } k_1 = k_o e^{-\frac{E_a}{R_g T}} \quad (2-59)$$

and

$$\text{b) } k_1 = k_o' T e^{-\frac{E_a}{R_g T}} \quad (2-60)$$

where

k_o = pre-exponential constant (sec^{-1})

k_o' = pre-exponential constant ($\text{sec}^{-1} \cdot \text{K}^{-1}$)

E_a = Activation energy $\frac{\text{cal}}{\text{mole}}$

T = absolute temperature ($^{\circ}\text{K}$)

R_g = gas constant $\frac{\text{cal}}{\text{mole}^{\circ}\text{K}} = 1.987$

Taking natural logs of equations (2-59) and (2-60) one obtains

$$\text{a) } \ln k_1 = \ln k_o - \frac{E_a}{R_g T} \quad (2-61)$$

$$\text{and b) } \ln k_1 = \ln k_o' + \ln T - \frac{E_a}{R_g T}$$

$$\text{or } \ln \frac{k_1}{T} = \ln k_o' - \frac{E_a}{R_g T} \quad (2-62)$$

A linear model fit to equations (2-61) and (2-62) suggests the following parameters based on a least square estimation

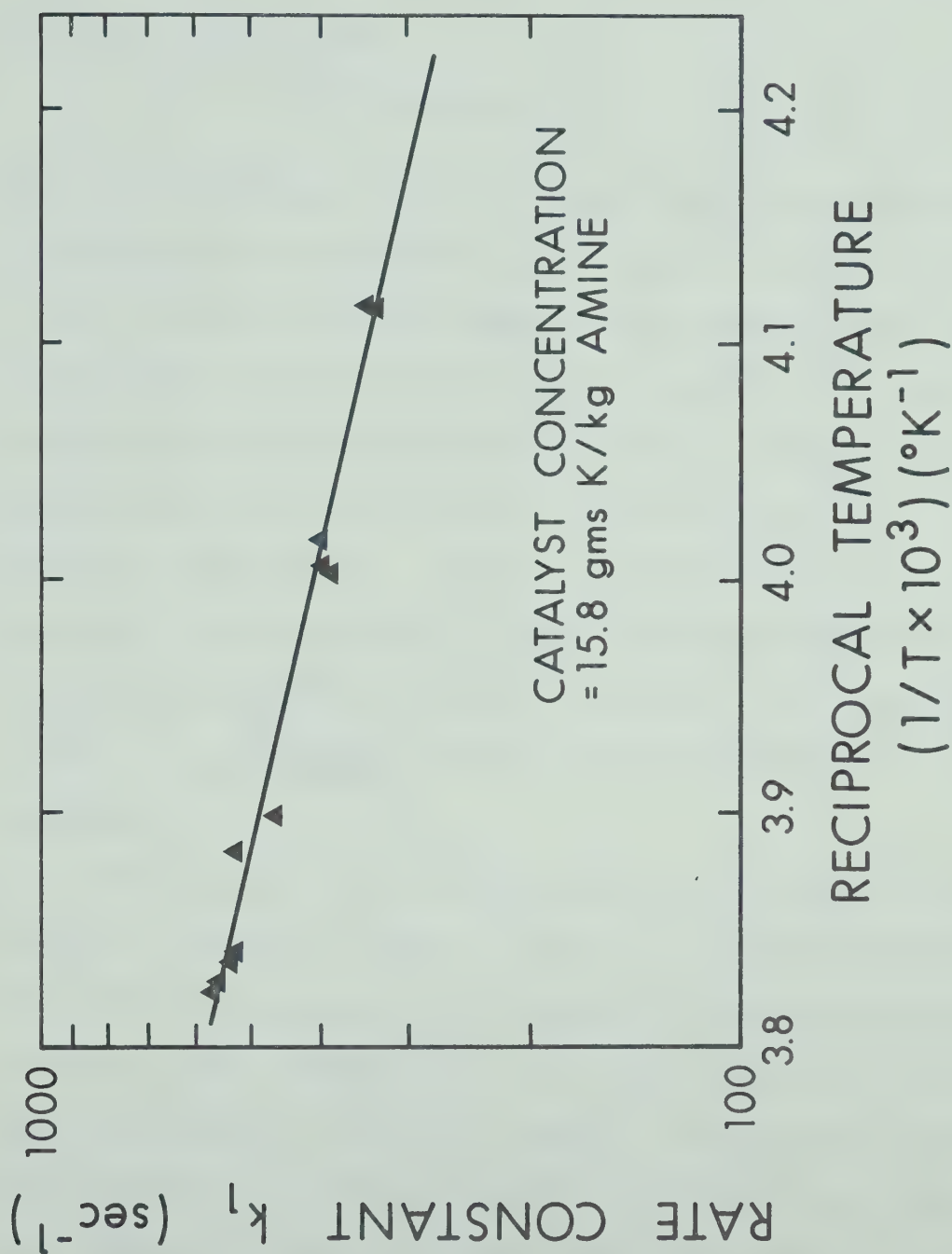


FIGURE 10

The Variation of the Kinetic Rate Constant with Temperature
(Hydrogen-Aminomethane System)

$$a) \ln k_o = 13.172$$

$$E_a = 3.554 \text{ kcal/s/gm.mole} \quad (2-63)$$

$$\text{and } b) \ln k_o^i = 6.641$$

$$E_a = 3.053 \text{ kcal/s/gm.mole} \quad (2-64)$$

The activation energy of 3.6 kcal/mole reported by Bar-Eli and Klein [1] was apparently determined using the model represented by equation (2.59). Rochard [2] on the other hand used equation (2-60) to calculate the activation energy of 6.8 kcal/mole reported in her work. She attributed the discrepancy between the values obtained by her and by Bar-Eli and Klein [1] to different values used for the solubility of hydrogen in aminomethane. This is in contradiction to the fact that the Henry's Law coefficient at -62.2°C calculated from equation (2-13) and the value reported by Rochard [2] are $1.24 \times 10^4 \frac{\text{atm}}{\text{mole fraction}}$ and $1.28 \times 10^4 \frac{\text{atm}}{\text{mole fraction}}$ respectively and indicate a reasonable agreement.

The variation of the rate constant k_1 vs the catalyst concentration in the PMA solution is shown in Figure 11. The catalyst concentration was analyzed in duplicate and a mean of two such duplicates was taken to be the correct concentration. The maximum deviation of the samples about the mean was within $\pm 1\%$. Figure 11 indicates that the rate constant apparently increases almost linearly with catalyst concentration for values of 'c' less than about 5.0 gms K/kg amine and subsequently levels off and appears to become independent of 'c' at values larger than about 20.0 gmsK/kg amine.

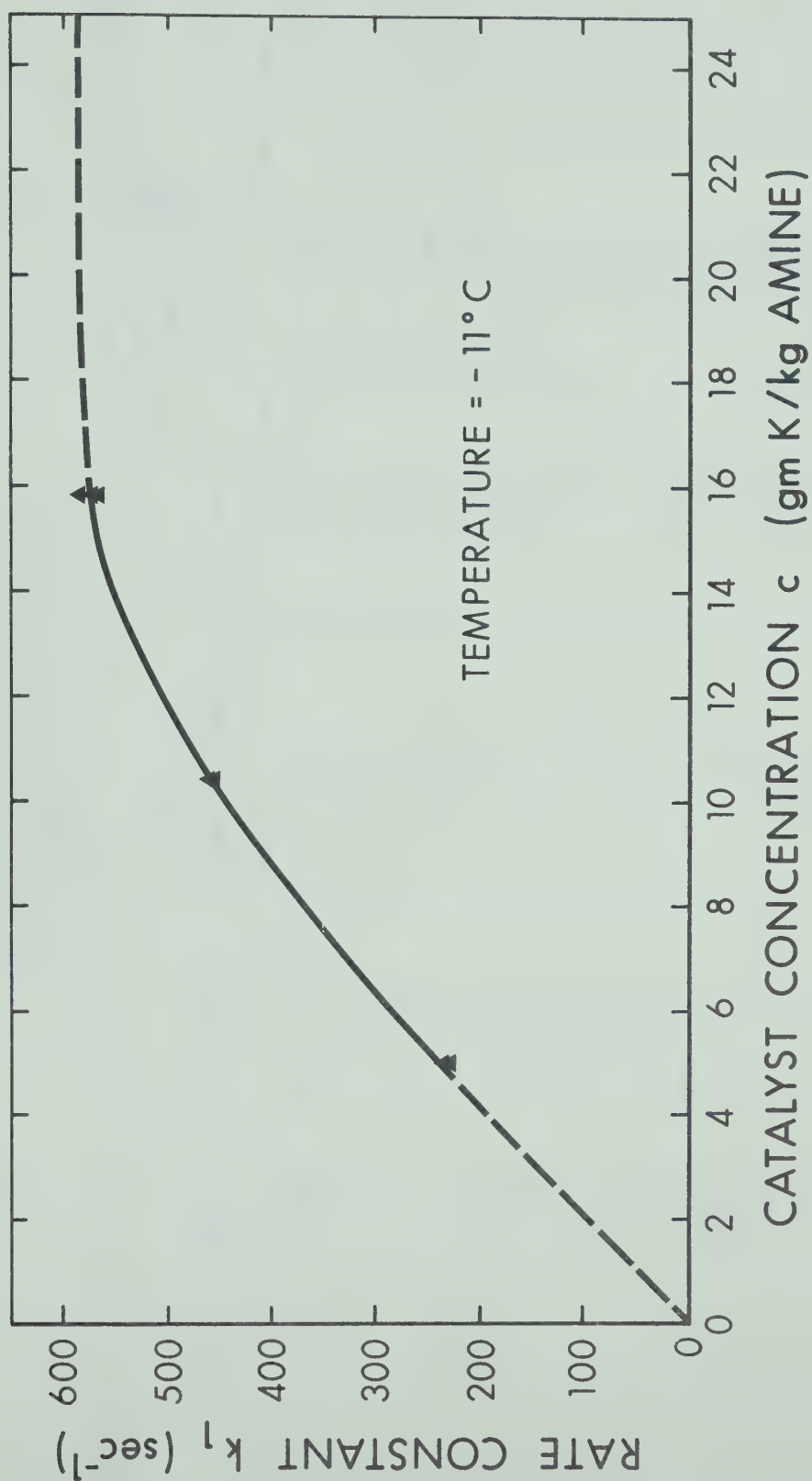


FIGURE 11

The Variation of the Kinetic Rate Constant with Catalyst Concentration in Solution (Hydrogen-Aminomethane System)

TABLE 2

Kinetic Rate Constant Data for
The Hydrogen-Aminomethane System

Date	Sphere size (cms)	Residence time t_{\max} (sec)	Temperature ($^{\circ}\text{C}$)	Catalyst Concentration (gmsK/kg amine)	Rate Constant k_1 (sec^{-1})	Mass Transfer Coefficient K_L (cm/sec)	$k_1 t_{\max}$
23/3/72	2.54	0.3944	-30.1	15.80	333.2	0.1672	131.4
5/4/72	2.54	0.3949	-30.2	15.80	342.1	0.1694	135.1
17/4/72	2.54	0.3611	-12.0	15.80	563.3	0.2506	203.4
5/7/72	3.81	0.9748	-16.7	15.80	466.9	0.2204	455.1
7/7/72	3.81	0.9661	-15.6	15.80	522.1	0.2350	504.4
11/7/72	3.81	0.9574	-24.2	15.80	399.8	0.1924	382.8
26/7/72	3.81	0.9517	-23.5	15.80	400.7	0.1937	381.3
31/7/72	3.81	0.9507	-23.3	15.80	393.8	0.1922	374.4
2/8/72	3.81	0.9242	-12.8	15.80	530.4	0.2417	490.2
28/8/72	3.81	0.8918	-12.5	15.80	539.8	0.2445	481.4
14/9/72	3.81	0.8868	-11.7	15.80	572.3	0.2532	507.5
22/9/72	3.81	0.8857	-11.5	10.42	452.5	0.2255	400.8
30/9/72	3.81	0.8758	-11.4	10.42	454.4	0.2261	398.0
9/10/72	3.81	0.8785	-11.1	4.95	238.3	0.1641	209.3
11/10/72	3.81	0.8874	-11.8	4.95	229.0	0.1601	203.2

CHAPTER 6

DISCUSSION6.1 Gas Phase Resistance

It may be seen from Table 2 that the values of $k_1 t_{\max}$ for each experimental determination are larger than 25.0 which, in light of the theoretical development of chapter 3 indicates that the exchange reaction always took place in the fast reaction regime for both the 1 inch and the 1.5 inch diameter absorbers. When the rate of chemical reaction increases and becomes high, the resulting increase in the chemical absorption coefficient K_L implies that the resistance to mass transfer in the liquid phase has been reduced. Under such conditions it is not uncommon for the gas phase resistance to become important, in which case the absorption process would cease to be liquid phase controlling. Due consideration must therefore be given to ascertain whether the effect of the gas-phase resistance has to be accounted for when estimating the rate constant of the liquid phase reaction.

Froessling's equation [20] for forced convection mass transfer in gases around spheres was used to estimate the mass transfer coefficient in the gas phase. The liquid and gas phase resistances were compared on the basis of the two-film theory. Froessling's equation may be represented by the following expression.

$$\frac{k'_G d_s}{D_v} = 2.0 + 0.556 R_e^{1/2} S_c^{1/3} \quad (2-65)$$

where k'_G = the gas phase mass transfer coefficient $\frac{\text{cms}}{\text{sec}}$
 d_s = diameter of the sphere absorber (cm)
 D_v = diffusivity of HD in the gas phase $\frac{\text{cm}^2}{\text{sec}}$

R_e = Reynolds number based on sphere diameter $\frac{\rho_g v d_s}{\mu_g}$

S_c = Schmidt number = $\frac{v}{D_v}$

The diffusivity (D_v) of hydrogen-deuteride in hydrogen saturated with aminomethane vapour was estimated using the equation recommended by Hirschfelder, Bird and Spotz [21] which is given as

$$D_v = 1.492 \times 10^{-3} \frac{T_1^{3/2}}{P_T r_{12}^2 I_D} \sqrt{\frac{1}{M_A} + \frac{1}{M_B}} \quad (2-66)$$

where D_v = the diffusivity expressed in (ft²/hr)

T_1 = absolute temperature in (°R)

P_T = absolute gas pressure in (atm)

r_{12} = mean collision radius of species 1 and 2 (Å)

= $[(r_o)_1 + (r_o)_2] / 2$

$(r_o)_1$ = collision radius of species 1 (Å)

$(r_o)_2$ = collision radius of species 2 (Å)

I_D = collision integral for diffusion

I_D is expressed as a function of $\frac{k T_1}{\epsilon_{12}}$

where

$$\frac{\epsilon_{12}}{k} = \sqrt{\left(\frac{\epsilon_1}{k}\right) \left(\frac{\epsilon_2}{k}\right)} \quad (2-67)$$

and k = Boltzmann's constant (erg/°K)

ϵ_{12} = energy of molecular interaction (ergs)

Further details and tabulated values of I_D vs. $\frac{k T_1}{\epsilon_{12}}$ for the use of

equations (2-66) and (2-67) are given in Perry [22] where a modified form of equation (2-66) is reported.

Based on the two film theory, the overall liquid phase resistance may be expressed as

$$\frac{1}{K_L} = \frac{1}{k_L} + \frac{1}{k_G H'} \quad (2-68)$$

where K_L = the overall liquid phase mass transfer coefficient $\frac{\text{cms}}{\text{sec}}$

k_L = the liquid phase mass transfer coefficient $\frac{\text{cms}}{\text{sec}}$

k_G = the gas-phase mass transfer coefficient expressed per unit of partial pressure driving force $\frac{\text{gm moles}}{\text{cm}^2 \text{ sec atm}}$

H' = The Henry's Law constant expressed as $\frac{\text{cc atm}}{\text{gm moles}}$

The mass transfer coefficients k_G and k_G' may be related by the following expression

$$k_G = \frac{k_G'}{R_g T} \quad (2-69)$$

For a typical experiment the following values were obtained:

$$D_v = 2.1 \text{ cm}^2/\text{sec}$$

$$S_c = 0.038$$

$$R_e = 87.2$$

$$K_L = 0.245 \text{ cm/sec}$$

$$k_G' = 3.08 \text{ cm/sec}$$

$$T = -12^\circ\text{C} = 261.18^\circ\text{K}$$

Using the above values it may be seen that

$$\frac{1/k_L}{1/K_L} = 0.996 \quad (2-70)$$

This implied that the resistance to mass transfer was predominantly in the liquid phase under conditions where the highest reaction rates were

obtained and the assumption of a liquid phase controlled absorption was justified.

6.2 Effect of a Change in y_e on k_1

The manner in which an error in the estimated equilibrium value would affect the slope of the plot given in Figure 9 and consequently would alter the value of the rate constant k_1 determined from that slope needs to be investigated. It is important to realize that for a given value of temperature and catalyst concentration, the rate constant k_1 is fixed but an error in the estimate of y_e could lead to a misinterpretation of $\ln\left(\frac{y-y_e}{y_{in}-y_e}\right)$ vs. t data.

Re-writing equation (2-57) as

$$u = \ln\left(\frac{y-y_e}{y_{in}-y_e}\right) = -k^* t \quad (2-71)$$

and differentiating w.r.t. y_e one obtains

$$\frac{\partial u}{\partial y_e} = \left(\frac{1}{y-y_e}\right) \left\{ \frac{(y_{in}-y_e)(-1) - (y-y_e)(-1)}{(y_{in}-y_e)^2} \right\} = -\frac{\partial}{\partial y_e} (k^* t)$$

or

$$\frac{\partial u}{\partial y_e} = \left(\frac{y_{in}-y_e}{y-y_e}\right) \left(\frac{y-y_{in}}{(y_{in}-y_e)^2}\right) = -t \frac{\partial k^*}{\partial y_e}$$

which on rearranging terms gives

$$-\frac{\partial u}{\partial y_e} = \frac{y_{in}-y}{y_{in}-y_e} \frac{1}{y-y_e} = t \frac{\partial k^*}{\partial y_e} \quad (2-71a)$$

substituting for $\frac{1}{y-y_e}$ from (2-71)

$$-\frac{\partial u}{\partial y_e} = \frac{(y_{in}-y)e^{k^* t}}{(y_{in}-y_e)^2} = t \frac{\partial k^*}{\partial y_e} \quad (2-71b)$$

Consider the first part of equation (2-71b) i.e.

$$-\frac{\partial u}{\partial y_e} = \frac{(y_{in}-y)e^{k^* t}}{(y_{in}-y_e)^2}$$

At $t \rightarrow 0$ $y \rightarrow y_{in}$ and $e^{k^*t} \rightarrow 1$ which leads to the conclusion that $\frac{\partial u}{\partial y_e} \rightarrow 0$. This implies that the ordinate u is invariant with y_e at small times. Since the ordinate u is invariant with y_e the plot of u vs. t is fixed and hence k^* is invariant with y_e or $\frac{\partial k^*}{\partial y_e} \rightarrow 0$. This may be shown rigorously by considering the second part of equation (2-71b) i.e.

$$\frac{(y_{in}-y)e^{k^*t}}{(y_{in}-y_e)^2} = t \frac{\partial k^*}{\partial y_e}$$

or

$$\frac{1}{t} \frac{(y_{in}-y)e^{k^*t}}{(y_{in}-y_e)^2} = \frac{\partial k^*}{\partial y_e} \quad (2-71c)$$

Taking the expression (2-71c) to the limit $t \rightarrow 0$; $y \rightarrow y_{in}$ one obtains

$$\lim_{\substack{t \rightarrow 0 \\ y \rightarrow y_{in}}} \frac{(y_{in}-y)e^{k^*t}}{(y_{in}-y_e)^2 t} = \lim_{y \rightarrow y_{in}} \frac{(y_{in}-y)}{(y_{in}-y_e)^2} \frac{k^* e^{k^*t}}{1} = \frac{(y_{in}-y_{in})k^*}{(y_{in}-y_e)^2} = 0$$

In general, as long as (k^*t) is a small number, the derivatives $\frac{\partial u}{\partial y_e}$ and $\frac{\partial k^*}{\partial y_e}$ and also the resulting error due to a change in y_e are small. The magnitude of k^* is usually small (the maximum value obtained was of the order of $3.3 \times 10^{-4} \text{ sec}^{-1}$) and as a result low errors in y_e would not affect the results appreciably if the data obtained in the earlier part of the experiment are used. Generally, the error in estimating y_e is not expected to be larger than ± 1 ppm and this was found to have a negligible effect on the final value of the rate constant k_1 . An analysis was conducted wherein the equilibrium value was changed from 22.0 to 25.0 ppm for a set of experimental data obtained at -11.7°C .

The corresponding values of the rate constant obtained are given in Table 3.

With the above arguments in mind, if a plot of $\ln\left(\frac{y-y_e}{y_{in}-y_e}\right)$ vs. t for an experiment indicated a deviation from linearity after a time 't', the data prior to that time was used to estimate the rate constant k_1 .

6.3 Modelling the Data of k_1 vs. t and k_1 vs. c

Two models were tested for the data of k_1 vs. T and three models were proposed and tested for the k_1 vs. c data. The best model for each set of data was selected on the basis of the Bayesian expected likelihood criteria which utilizes the Bayesian interpretation of probability. This approach to model discrimination has been used with considerable success by Singh [23]. The selected models were then combined to give a joint model incorporating both temperature and concentration and the best parameters for the model were determined by a non-linear estimation technique suggested by Marquardt [24].

6.3.1 The Bayesian Approach to Model Discrimination. Consider that a set of m models which contain the true model describing the observed data is selected after preliminary screening. Let the set of m models be represented as

$$\begin{aligned} y_1 &= \phi_1(\underline{x}, \underline{a}_1) + \varepsilon_1 \\ &\vdots \\ y_1 &= \phi_k(\underline{x}, \underline{a}_k) + \varepsilon_k \\ &\vdots \\ y_1 &= \phi_m(\underline{x}, \underline{a}_m) + \varepsilon_m \end{aligned} \tag{2-72}$$

where

\underline{x} = the vector of independent variables

\underline{a}_k = the vector of unknown parameters for the k th model

TABLE 3

Effect of a Change in y_e
on the Rate Constant k_1

y_e ppm	22.0	23.0	24.0	25.0
Rate Constant $k_1 (\text{sec})^{-1}$	557.0	562.4	567.9	573.5

y_1 = the dependent variable

ε_k = the error term in the k th model.

The truth (or conversely the uncertainty) of any model form k may be expressed quantitatively by a discrete probability p_k . The set of p_k 's then satisfy the following relationships

$$0 \leq p_k \leq 1.0 \text{ and } \sum_{k=1}^m p_k = 1.0 \quad (2-73)$$

The Bayesian probabilities p_k are indicative of the current state of information about a certain quantity and are subject to updating with the acquisition of additional information by the use of the Baye's Theorem which states that given n sets of observations $(y_{1i}, x_i; i=1, 2, \dots, n)$ the posterior probability for the j th model p_j'' is expressed as

$$p_j'' = \frac{p_j' L(y_1 | \phi_j)}{\sum_j p_j' L(y_1 | \phi_j)} \quad ; \quad (j = 1, 2, \dots, m) \quad (2-74)$$

p_j' is the probability prior to observing the data y_1 and $L(y_1 | \phi_j)$ is the expected likelihood of observing the data, given that the model form ϕ_j is the correct one.

In absence of any conclusive prior information it is generally assumed that all models are equally likely which implies that the prior probabilities are taken to be all equal. Similarly, the prior parameter values are assumed to be represented by an improper uniform distribution implying that they are distributed over the range $-\infty$ to $+\infty$. For the case where the parameter prior is represented by an improper uniform distribution the expected likelihood for the j th model may be represented by the following expression derived by Singh [23].

$$L(y_1 | \phi_j) = (2\pi\sigma_j^2)^{-n/2} \left(\frac{1}{2}\right)^{r^*/2} \exp \left\{ - \frac{\hat{S}_j^2}{2\sigma_j^2} \right\} \quad (2-75)$$

where r^* = the number of parameters in the j th model.

\hat{S}_j^2 = the minimum sum of errors squared.

$$= \sum_{i=1}^n (y_{\text{observed } i} - y_{\text{calculated } i})^2 \Bigg|_{\text{minimum}}$$

\hat{a}_j = the parameter vector which minimizes the sum of errors squared.

$\sigma_j^2 = \frac{\hat{S}_j^2}{(n-r^*)}$ = the unbiased estimate of the error variance.

The 95% confidence interval for the estimated parameters may be expressed

as

$$a_{j,k} = \hat{a}_{j,k} \pm 2 \sqrt{c_{j,kk}} \quad (2-76)$$

where $\hat{a}_{j,k}$ = the k th element of the least square estimated vector \hat{a}_j for the j th model.

$c_{j,kk}$ = the k th diagonal element of the variance covariance matrix for the j th model.

The variance co-variance matrix may be computed from the following relationships

$$\underline{C}_j = \sigma_j^2 \underline{A}_j^{-1} \quad (2-77)$$

where \underline{A}_j is defined by

$$\underline{A}_j = \underline{X}_j^T \underline{X}_j \quad (2-78)$$

and \underline{X}_j is the $(n \times r)$ design matrix given by

$$\underline{X}_j = x_{j,ik} \quad (i = 1, 2, \dots, n; k = 1, 2, \dots, r) \quad (2-79)$$

The elements of the design matrix are simply the first derivatives of

the model with respect to the parameters evaluated at the least square estimate $\hat{\underline{a}}_j$. They are represented as

$$x_{j,ik} = \left. \frac{\partial \phi_j(\underline{x}_i, \underline{a}_j)}{\partial a_{jk}} \right|_{\underline{a}_j = \hat{\underline{a}}_j} \quad (2-80)$$

6.3.2 The Models

k_1 vs. Temperature. The models attempted for a fit to the data represented as $\ln k_1$ vs. $\frac{1}{T}$ were

$$1) \quad k_1 = k_o e^{-E_a/R_g T} \quad (2-59)$$

$$\text{or} \quad \ln k_1 = \ln k_o - \frac{E_a}{R_g T} \quad (2-61)$$

Equation (2-59) is the Arrhenius equation

$$2) \quad k_1 = k_o' T e^{-E_a/R_g T} \quad (2-60)$$

$$\text{or} \quad \ln k_1 = \ln k_o' + \ln T - \frac{E_a}{R_g T}$$

$$\text{i.e.} \quad \ln \frac{k_1}{T} = \ln k_o' - \frac{E_a}{R_g T} \quad (2-62)$$

which corresponds to the Transition State Theory with an exponent of 1 on T. The data was fit to equations (2-61) and (2-62). The values of k_o , k_o' and E_a obtained for the two models are reported as equations (2-63) and (2-64). The posterior probabilities of the two models, the 95% confidence limits for the parameters and the standard deviation of the fit are given in Table 4. The parameter estimates have also been included.

The posterior probabilities of the models indicate that in the

TABLE 4

Model Estimates for Rate
Constant vs Temperature Data

	$\ln k_o (\text{sec}^{-1})$ or $\ln k_o'$ ($\text{sec}^{-1} \text{ } ^\circ\text{K}^{-1}$)	E_a $\frac{\text{k.cal}}{\text{gm.mole}}$	P''	$\pm 2\sigma$ (Parameters)		σ (Model Fit)
				$\ln k_o$ or $\ln k_o'$	E_a	
MODEL 1 EQUATION (2-59)	13.088	3.515	0.49	0.614	0.309	0.0277
MODEL 2 EQUATION (2-60)	6.557	3.014	0.51	0.611	0.308	0.0275

range of the data the transition state theory equation is only marginally superior to the Arrhenius equation. This implies that the $\ln T$ term in the second model contributes very little to the overall representation of the data. A variance equal to the variance of the model fit was used to estimate the posterior probabilities.

k_1 vs. Concentration. The models selected to represent the data of k_1 vs. concentration were limited to those that satisfied some of the basic criteria observed by previous investigators and during the course of this investigation. These criteria may be stated as follows:

a) The curve of k_1 vs. c should pass through the point (0,0) since no reaction was observed in absence of the catalyst.

b) At very low catalyst concentrations, the dependency of k_1 vs. c should become almost linear [1,2].

c) As the concentration of the catalyst is increased the curve of k_1 vs. c should level off, eventually tending to become independent of concentration [1,2].

The data obtained during this investigation also suggests that all three of the above criteria hold. There is evidence however, (Fig. 11) that at low concentrations the plot of k_1 vs. c is not quite linear. Based on the above criteria the following models were proposed.

$$(i) \quad k_1 = a_{11}c + a_{21}c^2 \quad (2-81)$$

$$(ii) \quad k_1 = a_{12}(1 - e^{-a_{22}c}) \quad (2-82)$$

$$(iii) \quad k_1 = a_{13}(1 - e^{-a_{23}c^{a_{33}}}) \quad (2-83)$$

It may be noted that model (i) satisfies only criteria (a) and (b) but not (c); it was however selected so that a polynomial fit of the data

over the concentration range of this investigation may be analyzed. Model (ii) satisfies all the three criteria while model (iii) satisfies criteria (a) and (c) but suggests that at very low 'c' the rate constant would be approximated by

$$k_1 = a_1 a_2 a_3 c^{a_{33}} \quad (2-83a)$$

This was introduced to ascertain whether the linear relationship was valid for the data obtained during the course of this work. If the linearity did indeed hold the constant a_{33} was expected to be 1.0.

The k_1 vs. c data was all obtained in the temperature range of -11.0°C to -12.5°C . It was all reduced to -11.0°C using the transition state theory model. The resulting values of the least square parameter estimates, the 95% confidence intervals, the standard deviations of the fits and the posterior probabilities of the models are given in Table 5.

In order to compute the posterior probabilities of the models the variance of the data experimentally observed should be used. This is in general smaller than the variance predicted by the model fit because the latter incorporates uncertainties due to the model form. Based on all the data taken for k_1 vs. T and k_1 vs. c , a variance of 56.25 was used which corresponds to a 2σ value of 15.0 or a $\pm 2\sigma$ limit (95% confidence) of 30.0.

It is interesting to note that as far as models (i) and (ii) are concerned the closeness of the fit reflected by the standard deviations is approximately the same, with model (i) faring somewhat better. The main deficiency of model (i) apparently is reflected in its inability to predict a levelling off with increase of concentration. Model (ii), however, is designed to level off but is apparently quite poor because

TABLE 5

Model Estimates for Rate
Constant vs. Catalyst Concentration Data

	a_1	a_2	a_3	P''	$\pm 2\sigma(\text{Parameters})$			σ (Model Fit)
					a_1	a_2	a_3	
MODEL 1 EQUATION (2-81)	56.269	-1.274	-	0.0188	3.846	0.261	-	12.911
MODEL 2 EQUATION (2-82)	863.61	0.0689	-	0.0004	143.84	0.0189	-	15.550
MODEL 3 EQUATION (2-83)	637.41	0.0528	1.357	0.9808	61.964	0.0159	0.2176	10.163

it does not level off as fast as is required by the data. The posterior probabilities indicate that model (iii) is 98.08% probable while models (i) and (ii) have a 1.88% and 0.04% chance respectively, of being the correct models to represent the data. Model (iii) is therefore clearly the most likely one from the set of models chosen to represent the data. Its standard deviation also is the least of three with a 95% confidence interval for the data of about $\pm 3\%$. It may also be noticed that the value of $a_{33} = 1.357$ indicates a slight departure of the model from linearity at low catalyst concentrations.

An investigation of equations (2-60) and (2-83) suggests that if a joint model form was selected to represent the data so that the effect of temperature and concentration could be predicted from one equation, it becomes apparent that the parameter a_{13} of equation (2-83) could be the only temperature dependent term. With this in mind the following model form may be proposed.

$$k_1 = a_{14} T e^{-\frac{E_a}{R_g T}} (1 - e^{-a_{24} c^{a_{34}}}) \quad (2-84)$$

The above equation incorporates four parameters that need to be estimated namely a_{14} , E_a , a_{24} and a_{34} . A non-linear least square estimation based on the method of Marquardt [24] led to the following values of the parameters and their 95% confidence limits.

$$a_{14} = 883.09 \pm 593.34$$

$$E_a = 3.072 \frac{\text{k cal/s}}{\text{gm mole}} \pm 0.325$$

$$a_{24} = 0.0529 \pm 0.0190$$

$$a_{34} = 1.3588 \pm 0.2581$$

Standard deviation of the fit = 11.943.

The above given standard deviation of the fit corresponds to a 95% confidence interval of about $\pm 4\%$

It may be noticed that the parameter a_{14} has a very high band width whereas its counterpart in the linearized equation (2-62) namely k'_0 can be estimated with much better confidence. This may be attributed to the fact that the amount of data available for estimation of a four parameter non-linear model is limited. A larger number of points would improve the confidence level of the parameters.

Equation (2-84) was used to calculate k_1 vs. T data at a catalyst concentration of 15.80 gms K/kg amine and also k_1 vs. c data at a temperature of -11.0°C . The experimental data is compared with calculated values in Tables 6 and 7 respectively. Figure 12 is a series of plots of k_1 vs. c as predicted by equation (2-84) over a concentration range of 0 to 30 gms K/kg amine and a temperature range of -10°C to -30°C .

6.4 Comparison with Existing Data

The investigations of Rochard [2] and Bar-Eli and Klein [1] are the only ones to date dealing with hydrogen amine systems in the presence of metal alkali amide catalysts. Bar-Eli and Klein [1] used lithium methyl amide to measure the rates of exchange of the deuterium-amino-methane reaction. Since the effect of the cation on the rate of exchange of hydrogen-amine systems is not known it is not possible to compare the results of Bar-Eli and Klein [1] with the data of this investigation. The above authors [1], however, quote an Arrhenius activation energy of 3.6 k cal/gm mole obtained for the $\text{D}_2\text{-CH}_3\text{NH}_2\text{-LiNHCH}_3$ system. This

TABLE 6

Comparison of Calculated vs. Observed Data
of Rate Constant vs. Temperature using the Joint Model

Catalyst Concentration $c = 15.80$ (gms K/kg Amine)

Date	T(°C)	$k_{1P}(\text{sec}^{-1})$ Eqn. (2-84)	$k_{1E}(\text{sec}^{-1})$ (Experimental)	% Error $\left(\frac{k_{1E} - k_{1P}}{k_{1E}} \right) \times 100$
23/3/72	-30.1	331.8	333.2	+0.42
5/4/72	-30.2	331.3	342.1	+3.16
17/4/72	-12.0	554.2	563.3	+1.62
5/7/72	-16.7	488.8	466.9	-4.69
7/7/72	-15.6	503.8	522.1	+3.51
11/7/72	-24.2	395.9	399.8	+0.98
26/7/72	-23.5	403.9	400.7	-0.80
31/7/72	-23.3	405.3	393.8	-2.92
2/8/72	-12.8	542.4	530.4	-2.26
28/8/72	-12.5	547.5	539.8	-1.43
14/9/72	-11.7	558.9	572.3	+2.34

TABLE 7

Comparison of Calculated vs. Observed Data
of Rate Constant vs. Catalyst Concentration using the Joint Model

Temperature = -11.0°C

Date	C (gms K/kg Amine)	$k_{IP}(\text{sec}^{-1})$ Eqn. (2-84)	$k_{IE}(\text{sec}^{-1})$ (Experimental)	% Error $\frac{k_{IE} - k_{IP}}{k_{IE}} \times 100$
17/4/72	15.80	569.0	578.4	+1.63
2/8/72	15.80	569.0	556.5	-2.25
28/8/72	15.80	569.0	561.0	-1.43
14/9/72	15.80	569.0	582.7	+2.35
22/9/72	10.42	458.7	458.4	-0.07
30/9/72	10.42	458.7	459.1	+0.09
9/10/72	4.95	236.3	238.9	+1.09
11/10/72	4.95	236.3	233.7	-1.11

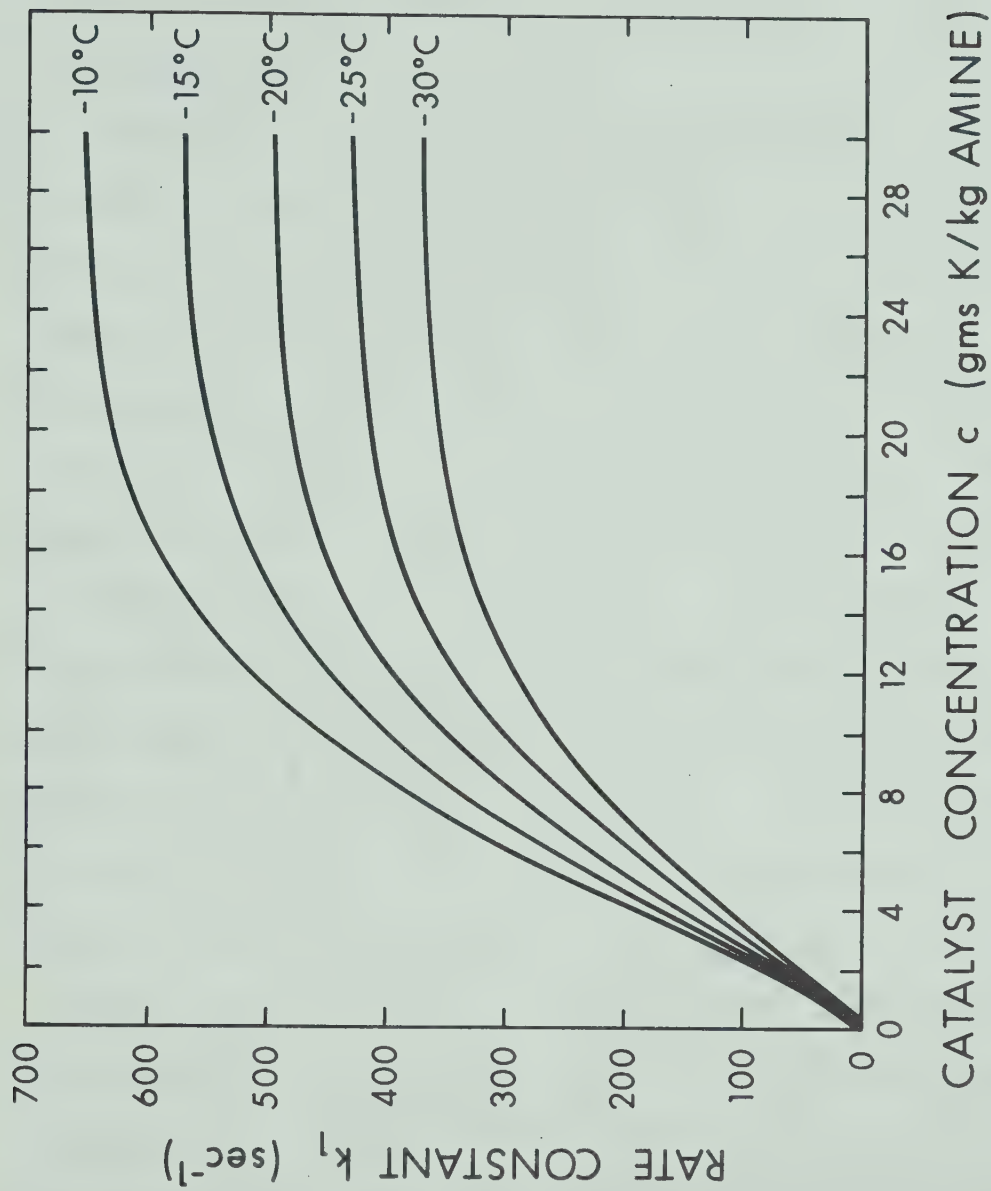


FIGURE 12

Estimation of the Variation of the Rate Constant with

Catalyst Concentration and Temperature

value compares quite closely with the value of 3.5 k cal/gm mole obtained from this investigation but the values of the rate constant k_1 are substantially higher than the corresponding values obtained by Bar-Eli and Klein [1].

The data of Rochard [2] for the hydrogen deuteride-aminomethane exchange was obtained in a stirred reaction vessel at temperatures of -62.2°C , -77.2°C and -90.0°C and potassium methyl amide concentrations ranging from 0 to 70 mm/l (0 to 3.5 gms K/kg amine). The low temperature and the low catalyst concentrations were apparently necessary because of difficulties encountered in eliminating liquid phase mass transfer resistance. This difficulty was particularly felt for the $\text{HD}-\text{CH}_3\text{NH}_2$ system wherein stirrer speeds had to be increased beyond 3000 rpm as a result of which temperature instabilities were also encountered. Rochard's data suggests that the rate constant k_1 varies linearly with catalyst concentration only up to about 20 mm/l at -90.0°C and about 10 mm/l at -77.2°C . Subsequently, the curve of k_1 vs. c levels off suggesting an invariance of k_1 with c for higher catalyst concentrations. This effect was attributed to the variation of the degree of dissociation of the PMA catalyst with total catalyst concentration. The values of the rate constant k_1 reported by Rochard are up to 25 times lower than the corresponding values obtained by extrapolating the data of this investigation in temperature and concentration. In light of the fact that the present data indicates a linear dependence of k_1 with c up to about 5.0 gms K/kg amine the curves of k_1 vs. c obtained by Rochard [2] were linearly extrapolated from 0.45 and 1.0 gms K/kg amine at -77.2°C and -90.0°C respectively to 5.0 gms K/kg amine and the resulting values of k_1 were plotted as $\ln \frac{k_1}{T}$

vs. $\frac{1}{T}$. The slope of this plot suggests an activation energy of 6.0 k cal/gm mole as compared to the value of 6.8 k cal/gm mole obtained by the above authors [2] through analysis of the data without extrapolation. Table 8 shows a comparison of the values of k_1 obtained by extending the above plot to a temperature range of -10°C to -30°C with the values calculated by the joint model represented as equation (2-84). It may be noted that the discrepancy in the two sets of data has been reduced to a factor ranging from 1.3 to 2.2. This could be attributed to the different values of the activation energy used and insufficient knowledge of the variation of the degree of dissociation of the amide catalyst with total catalyst concentration and with temperature. This analysis, however, suggests that in addition to the above mentioned uncertainties the liquid phase mass transfer resistance might not have been eliminated from the work of Rochard [2]. Additional work is required to relate the dissociation of the catalyst with temperature and total catalyst concentration in order to interpret the data on a more sound basis.

The rates of exchange of the hydrogen-aminomethane system have been reported to be an order of magnitude higher than those for the analogous hydrogen-ammonia exchange [1,2]. Bar-Eli and Klein [1] used an indirect method to compare the rates of the two exchange

processes and indicate that

$$\frac{[k_1]_{\text{CH}_3\text{NH}_2}}{[k_1]_{\text{NH}_3}}$$

are in the range of 10 to 35 at temperatures ranging from -48°C to -66°C respectively. The above authors however, could not adequately characterize the catalyst for the aminomethane exchange process but suggest that the

TABLE 8

Comparison of the Rate Constant k_1 predicted by the Joint Model with k_1 obtained by a Linear Extrapolation of Rochard's [2] Data

Catalyst Concentration = 5.0 gms K/kg Amine			
T (°C)	k_1 This Work Eqn(2-84) (sec^{-1})	k_1 Rochard[2] sec^{-1}	$\frac{k_1 \text{ This Work}}{k_1 \text{ Rochard}}$
-10	245.2	181.6	1.35
-15	214.7	140.7	1.53
-20	187.1	108.9	1.72
-25	162.1	83.9	1.93
-30	139.8	64.4	2.17

reported ratios are perhaps the lower limits of the expected values. At -59°C in the linear range of catalyst concentration Rochard [2] indicates that the ratio of the rate constants for the two exchange processes is about 25. The catalysts used were KNHCH_3 and KNH_2 for the aminomethane and ammonia reactions respectively. The data of Bourke and Lee [3] corrected for diffusivity and corresponding to 5.2

gms K/kg ammonia (i.e. 4.5 gms KNH_2 /lit.ammonia) and 20°C was extrapolated to -10°C using an activation energy of 5.8 kcal/gm mole.

The rate constant thus obtained was compared to the value obtained from this investigation as calculated by equation (2-84) at similar conditions of temperature and catalyst concentration. A similar comparison was also made at a catalyst concentration of 20.9 gms K/kg ammonia (18.0 gms KNH_2 /lit. ammonia) and -10°C . The ratio $\frac{[k_1]_{\text{CH}_3\text{NH}_2}}{[k_1]_{\text{NH}_3}}$

was found to vary from 56 at the lower to 37 at the higher concentrations. This decline was due to the fact that the linear increase of k_1 with c extends to higher values of c for ammonia than for aminomethane. It is estimated that these ratios will increase if similar comparisons were made at lower temperatures because of the difference between the activation energies of the two exchange processes.

6.5 Accuracy of the Data

An error analysis of the data based on the method of interpretation used for this study is given in Appendix C2. The above analysis indicated that the accuracy of the values of the rate constant is dependent largely on the accuracy with which the diffusivity of HD in aminomethane, the hydrogen solubility and the gas analysis are known. Aminomethane density, total gas volume and the time of sampling are also significant factors. Based on the accuracies of the above mentioned data it is estimated that the data obtained for the rate constant k_1 is reliable to within $\pm 10\%$.

CHAPTER 7

CONCLUSIONS

The use of a single sphere absorber for measuring diffusivities and reaction rate data for the hydrogen-aminomethane and the hydrogen deuteride-aminomethane-potassium methyl amide systems respectively, has been successfully demonstrated.

Experience has been gained in the handling of the above systems and suitable operating techniques have been developed after overcoming difficult experimental problems. Information has been obtained on the acceptable materials of construction for use with the aminomethane-potassium methyl amide solution.

The sphere absorber was operated in the fast reaction regime to obtain pseudo-first order rate constants for the hydrogen deuteride-aminomethane exchange between -10°C and -30°C , in the presence of potassium methyl amide as catalyst. The accuracy of the reported data is expected to be within $\pm 10\%$ and is dependent upon the accuracy of the diffusivity, the hydrogen solubility and the gas analysis of the data.

The data obtained was found to be an order of magnitude higher than similar data obtained in a stirred type reactor [2] where mass transfer effects are expected to be limiting. In addition, the rate constants obtained were found to be at least 35 times the corresponding values reported for the hydrogen-ammonia exchange reaction.

Additional work is required to relate the degree of dissociation of the PMA catalyst with temperature and total catalyst concentration before the data can be interpreted on a firm footing.

The experimental rate constants were correlated with temperature and catalyst concentration through a model which may be expressed as

$$k_1 = 883.09 T e^{-\frac{3072}{R T}} (1 - e^{-0.0529 C^{1.3588}}) \quad (2-85)$$

This model can be used to calculate the experimental rate data to within $\pm 4\%$ and is recommended for the estimation of rate constants where data is not yet available.

The information obtained on the diffusivity and the rate constants can be employed to predict transfer coefficients and thus tray efficiencies that may be expected in low temperature contacting towers used in the heavy water industry.

NOMENCLATURE

a_1, a_2, a_3	Constants in equation (2-83a)
a_{11}, a_{21}	Constants in equation (2-81)
a_{12}, a_{22}	Constants in equation (2-82)
a_{13}, a_{23}, a_{33}	Constants in equation (2-83)
a_{14}, a_{24}, a_{34}	Constants in equation (2-84)
$\underline{a}_{1\dots m}$	Vector of unknown parameters for models 1 to m.
$\hat{\underline{a}}_j$	The parameter vector which minimizes the sum of errors square for the jth model
$a_{\text{NH}_2^-}$	Activity of the amide ion
a_{K^+}	Activity of the potassium ion
A	Interfacial area (cm^2)
\underline{A}	Matrix defined by equation (2-78)
A_A	Interfacial area of the sphere absorber corrected for the film thickness (cm^2)
A_s	Surface area of the dry sphere (cm^2)
c	The catalyst concentration in PMA-aminomethane solution $\left(\frac{\text{gms K}}{\text{kg Amine}} \right)$
C	Concentration of HD in aminomethane liquid $\left(\frac{\text{gm moles}}{\text{cc}} \right)$
C_e	Concentration of HD in liquid aminomethane in equilibrium with CH_3NHD $\left(\frac{\text{gm moles}}{\text{cc}} \right)$
C_i	Interfacial concentration of HD in liquid aminomethane $\left(\frac{\text{gm moles}}{\text{cc}} \right)$
C_o	Bulk concentration of HD in the liquid phase $\left(\frac{\text{gm moles}}{\text{cc}} \right)$

C^*	The concentration of HD in the liquid in physical equilibrium with the HD concentration in the bulk gas phase $\left(\frac{\text{gm moles}}{\text{cc}}\right)$
C_l^*	Absolute concentration of (D/H) in the gas sample (ppm)
C_{st}	Absolute concentration of (D/H) in the principal standard (ppm)
\underline{C}	The variance-covariance matrix
[cat]	The concentration of catalyst in solution $\left(\frac{\text{gm moles}}{\text{cc}}\right)$
d_s	Diameter of the sphere absorber (CM)
D	Molecular diffusion coefficient of HD in liquid amino- $\left(\frac{\text{cm}^2}{\text{sec}}\right)$
D_v	Molecular diffusion coefficient of HD in a gas mixture of hydrogen and aminomethane $\left(\frac{\text{cm}^2}{\text{sec}}\right)$
E_a	Activation energy of the reaction $\left(\frac{\text{k cal}}{\text{gm mole}}\right)$
G	The total gas absorption rate $\left(\frac{\text{gm moles}}{\text{sec}}\right)$
G_i	The instantaneous gas absorption rate $\left(\frac{\text{gm moles}}{\text{sec}}\right)$
H_2	Henry's Law coefficient expressed as $\left(\frac{\text{atm}}{\text{mole fraction}}\right)$
H^1	Henry's Law coefficient expressed as $\left(\frac{\text{cc atm}}{\text{gm moles}}\right)$
I_2	Current signal corresponding to the H_2 concentration in the gas sample (amperes)
I_3	Current signal corresponding to the HD concentration in the gas sample (amperes)
I_D	Collision integral for diffusion

k_1	Pseudo-First Order rate constant for the forward reaction (sec^{-1})
k_2	Pseudo-First Order rate constant for the reverse reaction (sec^{-1})
k_o	Specific reaction rate constant ($[\text{cat}]^{-n} (C_i - C_e)^{1-m} \text{sec}^{-1}$)
k_o	Pre-exponential factor for equation (2-59) (sec^{-1})
k_o^i	Specific rate constant corresponding to the undissociated $[\text{KNH}_2]$ specie $\frac{\text{gm moles}}{\text{cc}}^{-1} \text{sec}^{-1}$
k_o^i	Pre-exponential factor for equation (2-60) ($\text{sec}^{-1} \text{ } ^\circ\text{K}^{-1}$)
k_{o1}	Specific rate constant based on the activity $a_{\text{NH}_2^-}$ (sec^{-1})
k_{o1}^i	Specific rate constant based on the activity product $a_{\text{NH}_2^-} a_{\text{K}^+}$ (sec^{-1})
k	Boltzmann's Constant ($\text{erg}/^\circ\text{K}$)
k^*	Defined by equation (B2-5)
k_G^i	The gas phase mass transfer coefficient (cm/sec)
k_G	The gas phase coefficient expressed per unit of partial pressure driving force $\frac{\text{gm moles}}{\text{cm}^2 \text{sec atm}}$
K_L	The overall chemical absorption coefficient (cm/sec)
K_{eq}	Chemical equilibrium constant defined by equation (2-16)
L	Liquid flow rate over the sphere absorber $\frac{\text{cc}}{\text{sec}}$
L	The likelihood function expressed as equation (2-75)
m^*	Number of exchangeable hydrogen atoms per molecule of amine

n^*	Number of exchangeable hydrogen atoms per molecule of hydrogen
n_{H_2}	Number of moles of hydrogen in the gas phase
$[NH_2]^-$	Concentration of the amide ion in solution $\frac{\text{gm moles}}{\text{cc}}$
$p_{1..m}$	Discrete probabilities for models 1 to m
p_j	Prior probability of the jth model
p_j''	Posterior probability of the jth model
P	Partial pressure of hydrogen (atm)
P_2	Partial pressure of hydrogen-deuteride (atm)
P_T	Total absolute gas pressure (atm)
r	The rate of chemical reaction $\frac{\text{gm moles}}{\text{cc sec}}$
r^*	The number of parameters in the jth model
$(r_o)_1$	Collision radius of species 1 (\AA)
$(r_o)_2$	Collision radius of species 2 (\AA)
r_{12}	Mean collision radius of species 1 and 2 (\AA) = $[(r_o)_1 + (r_o)_2]/2$
R	Radius of the sphere absorber (cm)
R^*	Ratio of currents (I_3/I_2) corresponding to HD and H_2 concentrations uncorrected for H_3^+ contribution (i.e. measured at a value of I_2 other than zero)
R_{st}	Ratio of (I_3/I_2) for the principal standard measured at the same value of I_2 as R^*
R_g	Universal gas constant $\frac{\text{cc atm}}{\text{gm mole } ^\circ\text{K}}$ or $\frac{\text{cal}}{\text{gm mole } ^\circ\text{K}}$
R_e	Reynolds number based on the sphere diameter $\frac{\rho_g v d_s}{\mu_g}$

S_c	Schmidt number $\frac{\nu}{D_v}$
\hat{S}_j^2	The minimum sum of errors squared
t	Time (sec)
t_{\max}	Maximum contact time (sec)
T	Absolute temperature ($^{\circ}\text{K}$)
T_1	Absolute temperature ($^{\circ}\text{R}$)
u	Expression defined by equation (2-69)
v	Velocity of the circulating gas $\frac{\text{cm}}{\text{sec}}$
\underline{v}	The velocity vector representing velocities of fluid elements flowing in the three coordinate directions over the sphere absorber $\frac{\text{cm}}{\text{sec}}$
v_{ψ}	Velocity of a fluid element along a stream line $\frac{\text{cm}}{\text{sec}}$
V	Total volume of the system occupied by gas (cc)
V_o	Interfacial velocity of the fluid $\frac{\text{cm}}{\text{sec}}$
V_o^+	Interfacial velocity of the fluid at the sphere equator $\frac{\text{cm}}{\text{sec}}$
x	Coordinate representing distance into the liquid film flowing over the sphere absorber (cm)
\underline{x}	Vector of independent variables.
x_2	Mole fraction of hydrogen deuteride in aminomethane
x_i	Mole fraction of hydrogen deuteride in aminomethane at the gas-liquid interface
x_e	Mole fraction of hydrogen deuteride in aminomethane in equilibrium with CH_3NHD
\underline{X}	The design matrix

y	Mole fraction of hydrogen deuteride in hydrogen
y_1	Dependent variable for equation set (2-72)
y_e	Mole fraction representing the equilibrium concentration of hydrogen deuteride in the hydrogen gas
y_{in}	Mole fraction of hydrogen deuteride in hydrogen at time $t = 0$

Greek Symbols

α_{eq}	The separation factor of D to H between aminomethane liquid and hydrogen gas at equilibrium
θ	Coordinate defined in Fig. 1 (radians)
ϕ	Coordinate defined in Fig. 1 (radians)
ϕ	Dimensionless expression defined by equation (2-43)
$\phi_{1..m}$	Representation of model forms for models 1 to m
Δ	Total thickness of the liquid film (cm)
Δ^+	Liquid film thickness measured at the sphere equator (cm)
δ_{DI}	Dimensionless ratio of gas phase concentrations of HD/H ₂ defined by equation (2-48)
δ_{st}	Dimensionless ratio for gas standards defined by equation (2-49)
ψ	Dimensionless variable defined by equation (2-32)
ψ_2	Maximum value of ψ for the sphere
η	Dimensionless expression defined by equation (2-41)
ρ_L	Molar density of liquid aminomethane $\frac{\text{gms moles}}{\text{cc}}$
ρ_g	Gas density $\frac{\text{gms}}{\text{cc}}$
μ_g	Gas viscosity (poise)

ν	Kinematic viscosity of the gas $\frac{\text{cm}^2}{\text{sec}}$
ϵ_{12}	Energy of molecular interaction (erg/°K)
$\epsilon_{1\dots m}$	Error terms in models 1 to m
σ_j^2	The unbiased estimate of the error variance of the jth model

REFERENCES

1. Bar-Eli, K., and Klein, F.S., J. Chem. Soc. (London), 36, 3083 (1962).
2. Rochard, E., CEA-R-3835 (1969).
3. Bourke, P.J., and Lee, J.C., Trans. Instn. Chem. Engrs., 39, 280 (1961).
4. Astarita, G., "Mass Transfer with Chemical Reaction", Elsevier Publishing Co., Amsterdam (1967).
5. Wilmarth, W.K., and Dayton, J.C., J. Amer. Chem. Soc., 75, 4553 (1953).
6. Bar-Eli, K., and Klein, F.S., J. Chem. Soc. (London), 36, 1378 (1962).
7. Dirian, G., Botter, F., Ravoire, J., and Grandcollot, P., J. Chim. Phys., 60, 139 (1963).
8. Delmas, R., Courvoisier, R., and Ravoire, J., Advances in Chemistry, 89, 25 (1969).
9. Moore, R.G., Ph.D. Dissertation, University of Alberta, 1971.
10. Atomic Energy of Canada Ltd., Report No. CRNL-207-18, p. 19, February 1970.
11. Kenyon, A.R., and Pepper, D., J. Appl. Chem., 14, 399 (1964).
12. Hayashitani, M., M.Sc. Thesis, University of Alberta, 1971.
13. Davidson, J.F., and Cullen, E.J., Trans. Instn. Chem. Engrs., 53, 113 (1957).
14. Ratcliff, G.A., and Holdcroft, J.G., Chem. Eng. Sci., 15, 100 (1961).
15. Astarita, G., Chem. Eng. Sci., 15, 708 (1961).
16. Lynn, S., Straatemeier, J.R., and Kramers, H., Chem. Eng. Sci., 4, 63 (1955).
17. Wild, J.D., and Potter, O.E., Tripartite Chemical Engineering Conference, Symposium on Mass Transfer with Chemical Reaction, September 23, 34 (1968).
18. Danckwerts, P.V., Trans. Faraday Soc., 46, 300 (1950).
19. Buckley, L.P., M.Sc. Thesis, University of Alberta, 1971.
20. Froessling, N., Gerlands Beitr Geophys., 32, 170 (1938).

21. Hirschfelder, J.O., Bird, R.B., and Spotz, E.L., Trans. Amer. Soc. Mech. Engrs., 71, 921 (1949).
22. Perry, J.H., "Chemical Engineer's Handbook", Sec. 14-20, 4th Edition, McGraw Hill Book Co., (1963).
23. Singh, H., M.Sc. Thesis, University of Alberta (1971).
24. Marquardt, D.W., J. Soc. Indust. Appl. Math., 11 (2), 431 (1963).

APPENDIX A2Detailed Operating ProceduresA2.1 The Exchange Experiment

The detailed operating procedure for conducting a typical hydrogen aminomethane exchange experiment using the single sphere absorber is outlined below:

- (1) Evacuate the entire gas-liquid exchange section and its connecting lines to a vacuum of better than 5μ .
- (2) Pressure the exchange system between the "Whitey" feed and liquid return valves with enriched hydrogen to a pressure of about 25 cms Hg (gauge)
- (3) Close the lid of the refrigerated air bath and begin refrigerating the system. As the temperature of the system falls the pressure in the absorption chamber will also fall as noticed on the mercury manometer attached to the chamber.
- (4) Also start refrigerating the ethylene glycol-water baths around the receiving tanks, the intermediate tank and the catalyst wash return tank. Steps (3) and (4) should be done on the day prior to the experiment because it takes about 12 to 16 hours to attain steady temperatures.
- (5) About one hour before the experiment start pumping the methyl hydrate coolant through the shell side of the concentric pipe heat exchangers. This ensures that the lines which carry the liquid are cold when the experiment is started.
- (6) Check the pressure on the absorption chamber manometer, if the pressure reads less than 12 cms Hg, add some more enriched hydrogen; if in excess of 12 cms Hg, bleed off some gas so as

to set the pressure to the above mentioned value.

- (7) Start the hydrogen circulator, the gas rotameter float should indicate a flow rate. The hydrogen circulator is driven by an air motor. The gas circulation rate can be controlled by adjusting the speed of the air motor. This in turn may be accomplished by varying the air pressure to the motor. Adjust the hydrogen circulation rate till the rotameter reads between 15 to 20% of full scale which corresponds to an approximate flow rate of about 100 cc/sec at the conditions of the system.
- (8) Introduce some pure dry aminomethane into the saturator from the dry aminomethane tank. The liquid would come in under a vapour pressure differential when the saturator solenoid valve is opened. Hydrogen gas will be seen bubbling through the aminomethane column in the saturator.
- (9) Open the distributor solenoid valve. The pressure of the system will be seen rising due to an increase of aminomethane partial pressure in the circulating hydrogen and due to a slight temperature rise due to the heat of the distributor solenoid valve.
- (10) Open all the valves in the return line downstream of the "Whitey" liquid return valve upto and including the valve isolating the receiving tanks. This ensures that the return line downstream of the "Whitey" valve is at the pressure of the receiving tanks which should be the pressure corresponding to the vapour pressure of the aminomethane at the temperature of the receiving tanks.
- (11) Start the vacuum pump serving the gas-sampling section and evacuate its lines including the traps and the sample manometer (3) (Fig. 6).

- (12) Surround the traps of the glass section (1) (Fig. 6) with liquid nitrogen and immerse the trap between the oil manometer and the gas absorption chamber manometer in a mixture of ice and water.
- (13) Turn on the power to the electric timer and the potentiometer which is used to measure temperatures of the exchange section. The temperatures are measured by copper-constantan thermocouples located as shown in Figure 2. The cold junction of these thermocouples is immersed in a mixture of ice and water.
- (14) Attach a gas sampling bomb at the sampling location (16) (Fig. 6) and evacuate it both on the bomb and on the valve side.
- (15) Approximately an hour after the hydrogen circulator is started, the manometer serving the gas absorption chamber should reach a steady pressure, indicating that the hydrogen is saturated with aminomethane.
- (16) Take the initial gas sample in the following manner. All numbers in parenthesis refer to equipment locations on Fig. 6.
 - (a) Isolate the vacuum pump of the gas-sampling section by closing the vacuum valve (12). Also isolate the sample bomb by closing the glass valve (14) between the steel sample line and the glass expansion lines.
 - (b) Open the sample valve (13) to introduce a gas sample into the steel line. Then close this valve.
 - (c) Open the vacuum pump valve (12). This would evacuate the gas sample trapped as in (b). One gas sample is discarded to eliminate gas in any dead volumes and thus obtain a representative sample. Then close vacuum valve (12) after about 30 sec.

- (d) Open the glass valve (14) and gradually crack open the sample valve (13) till the sample pressure manometer (3) records about 3 inches Hg pressure (absolute) in the sample bomb. Close sample valve (13).
- (e) Close the sample bomb glass valve (2) and then close valve (16).
- (f) Remove the sample bomb and open vacuum valve (12) to evacuate gas pressure in the glass line. The mercury limbs of the sample manometer (3) should come back to zero. The sampling section is now ready for the next sample. Attach a new sample bomb and open valves (2) and (16).
- (17) Open the liquid feed valve and introduce PMA solution into the exchange system. Maintain the flow rate at a level higher than the discharge rate of the nozzle. This will cause the PMA solution to accumulate in the distributor.
- (18) Step (17) will cause the system pressure to increase substantially since the entry of the liquid results in an effective compression of the vapour space.
- (19) When the jet (nozzle) starts flowing and the sphere absorber is completely wetted by the PMA solution, start the timer.
- (20) When the liquid level appears in the take-off tube, open the valves in the liquid return line and adjust the "Whitey" control valve so as to maintain the liquid level in the take-off tube.
- (21) When the level of the PMA solution in the liquid distributor reaches the glass tube above the distributor, close the distributor solenoid valve and adjust the feed control valve to maintain a flow rate of 7.0 to 7.5 on the liquid rotameter. This approximately corresponds to a liquid volumetric flow rate of

0.275 cc/sec.

- (22) Carry out the final adjustments with the liquid return control valve to set a take-off height of 1.25 cms. with the aid of a cathetometer.
- (23) Set the pressure in the reservoir tank of the gas sampling section equal to the system pressure. This may be done by first adjusting the pressure in the reservoir to within 1/2 cms Hg of the system pressure by visual inspection and then opening the valves connecting the oil manometer to the absorption chamber on one side and the reservoir on the other. The final adjustment may be done by balancing both the limbs of the oil manometer to zero.
- (24) Record the time at which all the adjustments for setting the conditions of the experiment have been completed. Since the system operation during this time did not conform to a fixed set of conditions, it may become necessary to shift the time axis by this amount during analysis of data.
- (25) Maintain the liquid flow rate and the take-off height at the desired values for the entire duration of the run.
- (26) After every 500 or 600 seconds take a gas sample in the following manner: Refer to Fig. 6.
 - (a) A sample bomb attached to the gas-sampling system should already have been evacuated.
 - (b) When the timer reads about 50 seconds less than the time at which a sample is desired, close valve (14) and the vacuum valve (12).
 - (c) Open sample valve (13) and note the oil manometer indicate a depletion of pressure in the absorption chamber. Close sample

valve (13).

- (d) Discard the sample by evacuating through vacuum valve (12).
Close this valve about five seconds before the desired sampling time.
 - (e) Open the sample valve (13) at the desired sampling time and introduce sample in the steel line. Close the sample valve (13).
 - (f) Open glass valve (14) to expand the sample into the sample bomb. The sample manometer will indicate the sample pressure.
 - (g) Close sample bomb valve (2) and valve (16).
 - (h) Remove sample bomb, open vacuum valve (12) and record the sample bomb number, the time at which sample was taken, the reading on the oil manometer and the temperatures of the gas and liquid leaving the absorption chamber.
 - (i) Attach a new sample bomb and open valves (2) and (16) so that the bomb is adequately evacuated at the next sampling time.
- (27) Continue taking gas samples according to step (26) till a sufficient number of samples are available. About 10 to 15 samples were taken for each experiment conducted during this investigation.
- (28) If an experimental measurement of the gas phase equilibrium value is desired, the time interval between samples after the first 10 samples should be increased to about 30 minutes and the experiment should be conducted for a total time of about 5 1/2 to 6 hours at -10°C .
- (29) Take the last gas sample in the same manner as the initial sample procedure outlined in step (16).
- (30) Close liquid feed valve and drain the PMA solution in the distributor

into the receiving tanks.

- (31) When the distributor is drained, open the valves leading to the wash return tank and isolate the receiving tanks.
- (32) Introduce aminomethane into the feed line and run the system in exactly the same fashion as for the PMA solution (steps (17), (19) and (20)). Continue feeding aminomethane till distributor is full.
- (33) Stop feeding aminomethane and drain the distributor into the wash return tank.
- (34) Repeat steps (32) and (33) till the liquid in the distributor and the take-off tube is colour less.
- (35) Stop the hydrogen circulator and record the level of the top of the saturator and the level of the aminomethane in the saturator using a cathetometer. These levels are required to estimate the vapour space in the saturator which must be included in the total gas volume of the system.
- (36) When the colour of the liquid in the distributor has faded, isolate the wash return tank and the aminomethane feeding tanks.
- (37) Introduce methyl hydrate into the liquid feed line and run the system with methyl hydrate in the usual fashion; the return alcohol should be sent to drain.
- (38) When alcohol is introduced into the system the chamber pressure will fall rapidly due to the reaction of the remaining catalyst in solution and the alcohol. The liquid in the system will turn milky initially but will start clearing up as the product of reaction are taken out of the system.
- (39) When the alcohol in the distributor and the take-off tube appears clear, the feed may be stopped and the system should be completely

drained till the absorption chamber pressure is about 1 or 2 cms Hg (gauge).

- (40) Remove the liquid nitrogen baths from around the traps (1) (Fig. 6) of the gas-sampling section and let the frozen aminomethane be evacuated into the trap of the vacuum pump. It can be discarded from there.
- (41) Shut down the coolant flow to the concentric pipe heat exchangers.
- (42) Transfer the cooling load to the feeding tanks if they are to serve as the receiving tanks for the next experiment and allow the receiving tanks to come to room temperature.
- (43) The experimental run is complete at this point and the gas-liquid exchange system may be cleaned and completely evacuated in preparation for the next experiment.

A2.2 PMA Solution Make-Up

The following sequential procedure may be used to make up a charge of PMA catalyst solution in aminomethane.

- (1) Estimate the quantity of aminomethane and potassium metal required for a desired charge of PMA solution by using stoichiometric relationships.
- (2) Assuming a 0.8% moisture content by weight in the aminomethane determine the amount of lithium metal required to dry the amine using equation (2-45).
- (3) Lithium is stored under toluene and is available in lump or stick form from Fischer Scientific Co.
- (4) Cut the required amount of lithium metal using a sharp knife and shave off the top skin thus exposing the shining surface of the metal. This operation should be performed under toluene. Cut

the cleaned lithium into small pieces.

- (5) Weigh the required amount of cleaned lithium pieces and immerse them in n-pentane to remove the film of toluene.
- (6) Introduce the lithium in a dry, clean steel vessel against a stream of argon. This is done to ensure minimal contact with air and moisture.
- (7) Seal the port through which the lithium was introduced and evacuate the vessel to pump out the remnants of argon, and n-pentane. The lines connecting the vessel to the aminomethane cylinder, should also be evacuated at this stage.
- (8) When a vacuum of 1μ has been achieved, immerse the vessel in a bath of liquid nitrogen and open the feed valve of the aminomethane cylinder. The aminomethane will distill into the steel vessel.
- (9) The level of liquid nitrogen should be maintained close to the top of the vessel making sure that the fittings through which the aminomethane is entering do not dip in the liquid nitrogen. This is done to prevent freezing up a line with aminomethane thus blocking entry into the tank.
- (10) The aminomethane cylinder should be placed on a balance so that the weight of aminomethane distilling can be monitored.
- (11) When the desired weight of aminomethane has been distilled into the vessel, close the amine feed valve and lift the vessel out of the liquid nitrogen bath.
- (12) In order to limit the pressure buildup in the vessel due to hydrogen evolution a relief valve set to about 80 psig should be provided.

- (13) Allow the vessel to come to room temperature; the aminomethane will begin to thaw out and this can be seen on a pressure gauge which will start showing an increase of pressure (when cold the pressure gauge will indicate a vacuum in the vessel).
- (14) When the pressure gauge indicates a positive pressure, connect the relief valve into the system.
- (15) The aminomethane will take about 12 hours to thaw out. The reaction of lithium with moisture in the amine begins as soon as first contact with liquid aminomethane is made. Since the reaction results in heat evolution, the thaw out process is accelerated and pressure buildup will occur fairly rapidly.
- (16) Bleed the hydrogen pressure into the vent system periodically to maintain a pressure of about 30 psig, till the pressure does not rise anymore after bleeding.
- (17) The aminomethane is now dry and ready for use. The process may take upto 2 days to reach this stage.
- (18) Cut the estimated amount of potassium metal under mineral oil in the same manner as indicated in step (4).
- (19) Follow steps (5) to (7) using the 316 SS storage vessel for the PMA solution.
- (20) When a vacuum of $1\ \mu$ has been reached immerse the vessel in a bath of liquid nitrogen and flash distill the aminomethane dried with lithium.
- (21) Follow steps (9) to (16) keeping the solution in the vessel circulating by the use of a polypropylene diaphragm pump.
- (22) When the colour of the solution changes from blue to straw yellow

the reaction may be considered to have gone to completion.

A sight glass should be provided with the vessel so that the colour may be conveniently seen.

APPENDIX B2Sample Calculation

The following procedure was followed to estimate the value of the reaction rate constant $k_1(\text{sec}^{-1})$ from the analysis of the gas samples taken during an experiment. The experiment conducted on 11th October 1972 is used to illustrate the calculation procedure.

The raw data sheet as obtained from the experiment is given below. During the experiment columns 1-5 and column 7 were recorded. The analysis of the gas samples was conducted subsequently and the results were transferred to column 6 of the data sheet. The numbers in column 6 represented as R^* are the ratios of the currents I_3/I_2 uncorrected for the H_3^+ contribution and obtained at a constant value of $I_2 = 24.0 \times 10^{-10}$ amperes.

For the closed system under consideration, the rate of depletion of D from the gas phase is essentially independent of system pressure and as such the readings in column 4 namely the oil manometer differential pressure, were not needed but were recorded in case some correction had to be applied.

The gas analysis was done on the mass spectrometer and the results were interpreted to give the absolute values of D/H. This was done with the aid of four known standards which were analyzed before and after the analysis of the gas samples obtained during the experiment. The values obtained from the mass spectrometer for the standards along with their absolute values are given in Table B2-2.

TABLE B2-1

Raw Data from a Typical Experiment

Time(sec)	Rotameter Reading Liq/Gas	Sample Bomb Number	Oil Manometer Diff. Press. (cms)	Thermocouple Measurements (mv) Liq/Gas	$R \times 10^6$	Comments
Initial	-	28	-	-0.473/-0.406	533.9	Level of top of saturator=75.020 cms
500	7.5/18	60	2.3+3.1	-0.459/-0.404	480.5	
1,000	7.5/18	14	4.5+5.2	-0.455/-0.401	431.2	
1,500	7.5/18	18	7.7+8.3	-0.453/-0.401	385.4	
2,000	7.5/18	25	11.5+12.0	-0.452/-0.400	339.8	Level of amine in saturator = 63.935 cms
2,500	7.5/18	16	15.5+16.0	-0.451/-0.400	305.2	
3,000	7.5/18	27	19.7+20.2	-0.451/-0.400	272.9	
3,500	7.5/18	12	23.9+24.4	-0.450/-0.401	240.1	
4,000	7.5/18	23	28.3+28.8	-0.450/-0.400	212.4	
4,500	7.5/18	30	32.9+33.4	-0.449/-0.400	187.0	Time to bring take-off Liquid Level to desired value = 183 sec.
5,000	7.5/18	32	37.5+38.0	-0.449/-0.399	170.0	
5,500	7.5/18	29	42.0+42.5	-0.447/-0.400	148.4	
6,000	7.5/18	19	6.0+6.7	-0.447/-0.399	128.9	← Reset Oil Manometer
6,500	7.5/18	24	10.5+11.0	-0.449/-0.399	115.6	New Systems Press. = (33.3+33.2) cms Hg
8,000	7.5/16	55	-	-0.445/-0.397	15.7	Concluded run at 6500 sec.
9,000	7.5/16	48	-	-0.445/-0.397	-7.4	Began spilling liquid out-
10,000	7.5/16	51	-	-0.444/-0.396	?	side the ball on purpose
11,000	7.5/16	46	-	-0.443/-0.396	-23.2	to create more area and
12,000	7.5/16	44	-	-0.443/-0.396	-22.3	reach equilibrium faster.

Ball size = 3.81 cms ϕ

Take-off Length = 1.25 cms

Jet size = 0.046 cms ϕ

Jet Length = 0.2650 cms

Catalyst Concentration = 4.95 gmsK/kg Amine. System Pressure = (36.2+36.3)cms Hg

Feed Tank Press/temp = 30 lbs/ \square "g/20°C

Barometric Press/temp.=1)712.6 mmHg/24.0°C

2)711.2 mmHg/24.0°C

Room Temperature = 17.2°C

TABLE B2-2Mass Spectrometer Analysis for the Gas Standards

	$R^* \times 10^6$	D/H Absolute(ppm)
Before	-51.6	1.5
	61.3	99
	346.3	365
	473.2	471
After	-54.1	1.5
	58.3	99
	349.0	365
	478.5	471

The analysis of the standards were converted in the following manner:

$$\delta_{DI} = \left(\frac{R^*}{R_{st}} - 1 \right) 1000 \quad (2-48)$$

$$\delta_{st} = \left(\frac{C_1^*}{C_{st}} - 1 \right) 1000 \quad (2-49)$$

where the terms of equations (2-48) and (2-49) have been defined in chapter 4. For the above experiment

$$R_{st} = 346.3, 349.0 \quad C_{st} = 365$$

From above equations one obtains

TABLE B2-3

Converted Form of Gas Standards Analysis

	δ_{DI}	δ_{st}
Before	-1149.0	-995.9
	- 823.0	-728.8
	0.0	0.0
	366.5	290.4
After	-1155.0	-995.9
	- 833.0	-728.8
	0.0	0.0
	371.1	290.4

The above data was fit to a linear and a quadratic equation using the linear least square criteria. The equations are of the form;

$$(1) \quad \delta_{DI} = B_1 + B_2 \delta_{st} \quad (B2-1)$$

$$(2) \quad \delta_{DI} = B_1 + B_2 \delta_{st} + B_3 \delta_{st}^2 \quad (B2-2)$$

The results indicate that the linear equation (1) is quite adequate for the analysis. The following parameters were obtained:

$$\text{For Model (1)} \quad B_1 = 17.136 \quad B_2 = 1.171$$

$$\text{For Model (2)} \quad B_1 = 12.148 \quad B_2 = 1.195 \quad B_3 = 0.337 \times 10^{-4}$$

The magnitude of B_3 indicates that the quadratic contribution is negligible; in addition, the variance-covariance matrix of the parameters indicated that the 95% confidence limit of B_3 was $\pm 0.7 \times 10^{-4}$ implying that it is not reliable. A linear model was thus considered adequate.

The gas analysis data was converted to the corresponding δ_{DI} values with equation (2-48) using an average value of R_{st} given by

$$R_{st(\text{mean})} = \frac{346.3 + 349.0}{2} = 347.7$$

The linear model was used to get the corresponding values of δ_{st} , and using equation (2-49) the absolute values of the gas samples in ppm were obtained. The final values obtained are given below:

TABLE B2-4

Data of Absolute D/H Concentrations vs. Time

Time (sec)	y = D/H (ppm)
0	527
500	479
1000	435
1500	394
2000	353
2500	322
3000	293
3500	263
4000	238
4500	216

TABLE B2-4 (Cont.)

189.

Time(sec)	Y=D/H(PPM)
5000	200
5500	181
6000	164
6500	152 End of Run; Created Spill
8000	62
9000	41
10,000	?
11,000	27
12,000	28

Since the earliest part of the run (the period between the initial sample and $t = 500$ sec) includes some stabilizing effects like setting the take-off level, adjusting the flow rates, setting the oil manometer etc., the first point was usually neglected. The time axis was thus moved to $T' = t - 500$ (sec). At $t = 6500$ sec the liquid was allowed to spill out of the take-off tube into the gas absorption chamber. This was done to increase the area of contact and thus reach equilibrium faster. The data points to be used for the estimation of the rate constant are

TABLE B2-5

Data of Absolute D/H Concentration vs. Time
Used for Rate Constant Estimation

T' (sec)	Y (ppm)
0	479
500	435
1000	394
1500	353
2000	322
2500	293
3000	263
3500	238
4000	216

T' (sec)	y (PPM)
4500	200
5000	181
5500	164
6000	152

Deliberate spilling of the PMA solution to obtain the equilibrium value was not done as a routine procedure for every experiment. This was done a few times during the entire course of this investigation so that the equilibrium value obtained in this manner could be compared with the value obtained by a mass balance of the deuterated specie in the liquid phase. The separation factor for hydrogen-aminomethane was assumed to be the same as that for the hydrogen-ammonia system. The initial value of $(D/H)_{\text{aminomethane}}$ was determined from an experiment where the gas phase was taken to equilibrium. The concentration of $(D/H)_{\text{aminomethane}}$ was then corrected after every experiment by estimating the liquid phase enrichment as calculated by the following material balance equation

$$x_f' = \frac{x_i n_l + (Y_i - Y_f) n_g}{n_l} \quad (\text{B2-3})$$

where x_f' = D/H ratio in liquid after the experiment (ppm)

x_i = D/H ratio in liquid before the experiment (ppm)

Y_i = D/H ratio in the gas phase at the beginning of the experiment (ppm)

Y_f = D/H ratio in the gas phase at the end of the experiment (ppm)

n_g = Total number of moles of gas in the system

n_l = Total number of moles of liquid that passed over the sphere absorber.

The value x_i for the next experiment was estimated by another material balance which involves x_f , n_1 , $x_i(\text{previous})$ and the liquid remaining back in the feeding tanks (not used for the present run).

Equation (B2-4) was used to calculate y_e as

$$y_e = \frac{x_f}{\alpha_{eq}} \quad (\text{B2-4})$$

where α_{eq} is the separation factor.

The value of y_e obtained from this particular experiment by direct gas analysis was equal to 25 ppm. The PMA solution which was allowed to spill into the gas chamber was a stagnant pool of liquid which aided in depleting the gas phase of its deuterium content. The stagnant liquid was enriched in the process and the transfer of deuterium was eventually expected to take place from the liquid to the gas phase. A plot of y vs T would thus go through a minimum. The value of y corresponding to the minimum was taken as the equilibrium value. Fig. B2-1 shows a typical plot of this nature. The value of y_e obtained with equation (B2-4) was 24.9 ppm. It may be mentioned here that an average value of x_i and x_f or, for runs where the initial gas concentration y_{in} was low, the use of x_i may be better justified to calculate y_e . However, the very small differences in x_i and x_f (~1 ppm) make it immaterial whether equation (B2-4) is used with x_i , x_f or an average of the two.

Using a value of $y_e = 24.9$ ppm, the ordinate $\ln \left(\frac{y - y_e}{y_{in} - y_e} \right)$ may be estimated. These values are given below. y_{in} is the D/H concentration in the gas at $T' = 0$.

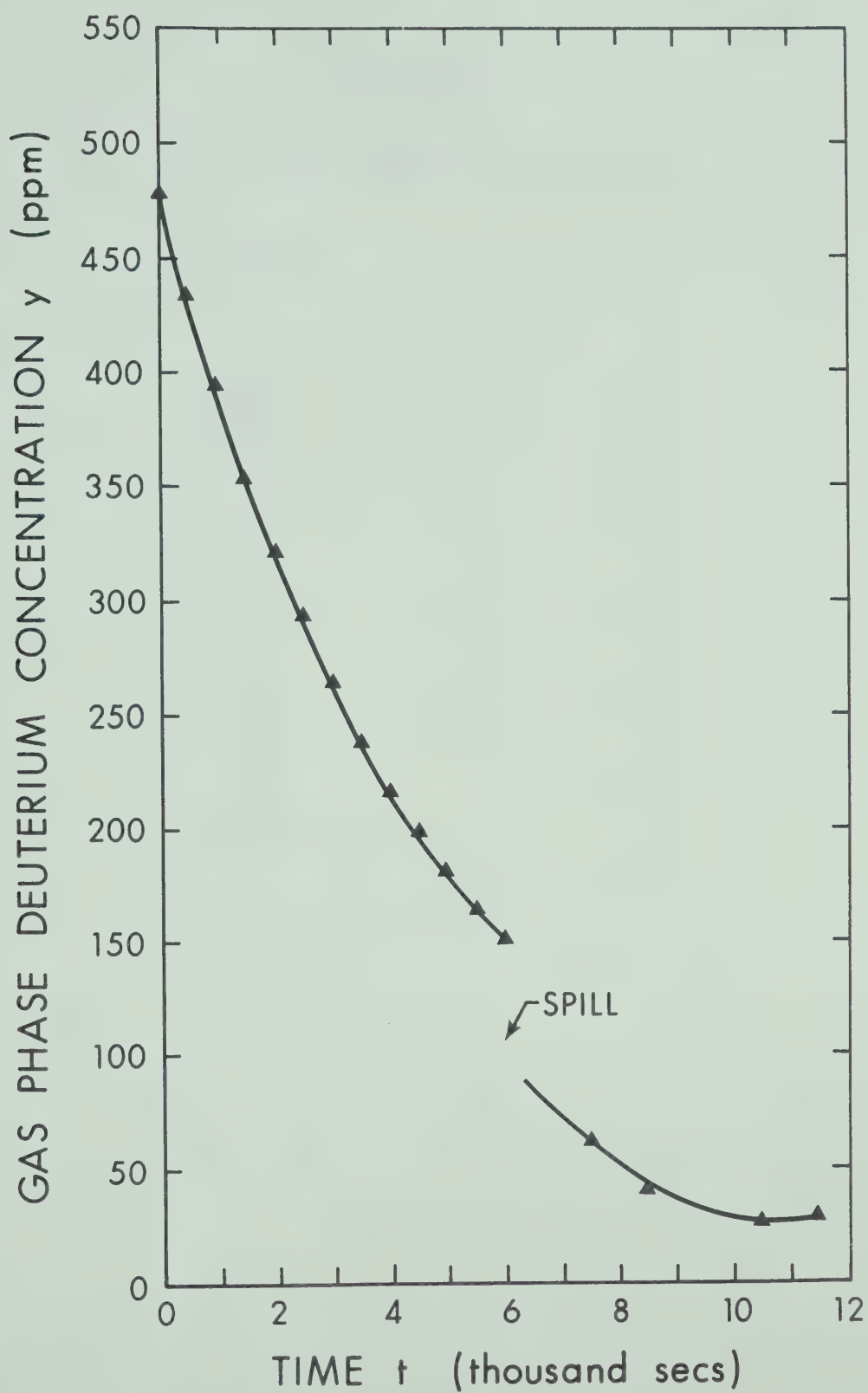


FIGURE B2-1

Plot of y vs. t to Determine the Gas Phase Equilibrium Value

TABLE B2-6

Data of Cumulative Depletion vs. Time

$\ln \left(\frac{y-y_e}{y_{in}-y_e} \right)$	T' (sec)
0.0	0
-0.1024	500
-0.2080	1000
-0.3256	1500
-0.4250	2000
-0.5277	2500
-0.6440	3000
-0.7540	3500
-0.8668	4000
-0.9500	4500
-1.0669	5000
-1.1856	5500
-1.2755	6000

The slope ($-k^*$) of the least square line through the above data of $\ln \left(\frac{y-y_e}{y_{in}-y_e} \right)$ vs. T' was found to be

$$\begin{aligned} -k^* &= -0.214 \times 10^{-3} \\ \text{or } k^* &= 0.214 \times 10^{-3} \text{ (sec}^{-1}\text{)} \end{aligned}$$

Referring to equations (2-57) and (2-58)

$$k^* = \frac{K_L A_T \rho_L R_g T}{V H_2} \quad (\text{B2-5})$$

$$\text{where } A_T = A_A + A_J \quad (\text{B2-6})$$

A_A = Area of the sphere absorber corrected for liquid film thickness (cm^2)

A_J = Area of the liquid jet (cm^2)

Interfacial Area of Contact

Sphere diameter = 3.81 cms

Jet diameter = 0.0460 cms

Length of Jet = 0.2650 cms

Liquid film thickness

at the sphere equator = 0.0066 cms

$$\therefore \text{Area of the dry sphere} = \pi d_s^2 = \pi \times 3.81^2 = 45.6 \text{ cm}^2$$

Correcting for liquid film thickness by using equation (2-58)

$$\begin{aligned} A_A &= A_s \left(1 + \frac{2.58 \times 0.0066}{1.905} \right) \\ &= 45.6 (1.00894) = 46.0 \text{ cm}^2 \end{aligned}$$

Area of Jet = $\pi d_j L$ where d_j = diameter of the jet (cm)

$$\therefore A_J = \pi \times 0.0460 \times 0.265 = 0.0383 \text{ cm}^2$$

$$A_T = 46.0 + 0.0383 = 46.04 \text{ cm}^2$$

The same calculation on the computer resulted in $A_T = 46.05 \text{ cm}^2$

System Temperature

The average temperature of the liquid was taken as being representative. From the data sheet, average thermocouple output from $t = 500 \text{ sec}$ to $t = 6500 \text{ sec} = -0.4509 \text{ mv}$.

Use linear interpolation of the standard E.M.F. data of copper-constantan thermocouples (Ref. 0°C)

$$T_1 = -11.0^\circ\text{C} \quad \text{mv}_1 = -0.417$$

$$T_2 = -12.0^\circ\text{C} \quad \text{mv}_2 = -0.455$$

The equation of the mean curve representing the calibration of the thermocouples with respect to temperature is given by

$$\epsilon_s = \frac{\epsilon_A + 0.0064}{0.9962} \quad (\text{B2-7})$$

where

ϵ_s = the standard E.M.F. generated by the thermocouple as listed in the "Leeds and Northrup" thermocouple tables (copper-constantan) (mv)

ϵ_A = The actual E.M.F. generated by the thermocouple (mv)

The actual calibration data for the above thermocouples is given in Moore's thesis [9].

$$\epsilon_A = -0.4509$$

$$\epsilon_s = \frac{-0.4509 + 0.0064}{0.9962}$$

$$= -0.4463 \text{ mv}$$

$$\begin{aligned}\text{Factor} &= \frac{-0.4170 - (-0.4463)}{-0.4170 - (-0.4550)} (-1^\circ\text{C}) \\ &= -\frac{0.0293}{0.0380} = -0.77^\circ\text{C}\end{aligned}$$

$$\text{Temp of System} = -11.0^\circ\text{C} - 0.77^\circ\text{C} = -11.77^\circ\text{C}$$

Density of Aminomethane

The following equation was used [9].

$$\rho = a_1 + a_2T + a_3T^2 \quad (\text{B2-8})$$

where $a_1 = 0.905798$

$$a_2 = -4.009472 \times 10^{-4}$$

$$a_3 = -1.457690 \times 10^{-6}$$

$$T = \text{Temperature } ^\circ\text{K}$$

$$\rho = \text{aminomethane density } \frac{\text{gms}}{\text{cc}}$$

$$T = 273.18 - 11.77 = 261.41 ^\circ\text{K}$$

Using equation (B2-8) the density ρ may be found to be

$$\rho = 0.7014 \frac{\text{gms}}{\text{cc}}$$

Henry's Law Coefficient

Using equations (2-13) and (2-14) one obtains

$$\ln H_2 = 4.1403 + 1.6612 \left(\frac{1000}{261.41} \right) - 0.1160 \left(\frac{1000}{261.41} \right)^2$$

$$\text{or } H_2 = 6625.7 \frac{\text{atm}}{\text{mole fraction}}$$

System Gas Volume

The total volume occupied by the gas in the gas-liquid exchange system was estimated by expanding a known test volume of a gas at a

known pressure and temperature into the system. The initial pressure of the system was also known. The final pressure of the test volume and the system was recorded after the expansion. The following equation may then be used to estimate the unknown volume.

$$V_s = \left(\frac{P_1 - P_f}{P_f - P_{11}} \right) V_1 \quad (B2-9)$$

Since no temperature change was observed during the test the above equation assumes a constant temperature.

V_s = The unknown system volume (cc)

V_1 = Volume of the test tank and its connecting lines (cc)

P_1 = Initial pressure of the test tank (cm, Hg) (absolute)

P_{11} = Initial pressure of the system (cms Hg) (absolute)

P_f = Final pressure of test tank and system after expansion (cm Hg) (absolute)

Equation (B2-9) was derived by a simple molar balance of the gas before and after expansion. The procedure involves the following:

$$\text{No. of moles of gas in test tank + lines} = \frac{P_1 V_1}{RT_1} = n_1$$

$$\text{No. of moles of gas in system before expansion} = \frac{P_{11} V_s}{RT_1} = n_s$$

$$\text{Total number of moles of gas} = (n_1 + n_s)$$

$$\text{Total volume after expansion} = V_1 + V_s$$

$$\frac{P_f (V_1 + V_s)}{RT_1} = n_1 + n_s \quad (\text{Assumes no temperature change on expansion})$$

$$\text{or} \quad P_f V_1 + P_f V_s = P_1 V_1 + P_{11} V_s$$

$$(P_f - P_{11}) V_s = V_1 (P_1 - P_f)$$

$$\text{or } V_s = \frac{(P_1 - P_f)}{(P_f - P_{11})} V_1 \quad (\text{B2-9})$$

The system volume was estimated two or three times during the course of the investigation. Whenever a change in the apparatus constituting the gas-liquid exchange system was incorporated, a new test for gas volume was conducted. The last volume test was conducted on 18th May 1972. The following results were obtained.

$$V_1 + \text{connecting lines} = 1796.3 \text{ cc}$$

$$\text{Barometric Pressure} = 703.8 \text{ mm Hg}$$

$$P_1 = 703.8 \text{ mm Hg (Barometric Pressure)}$$

$$P_{11} = 171.37 \text{ mm Hg}$$

$$P_f = 388.53 \text{ mm Hg}$$

$$V_s = \frac{315.27}{217.16} (1796.3) = 2607.8 \text{ cc}$$

A cathetometer was used to take the pressure readings from a mercury manometer. The above volume includes the volume of the liquid lines in the system that were not isolated and the volume of the liquid aminomethane that would be introduced into the saturator before each experiment. The volume of the liquid lines was estimated as 43.0 cc.

Volume of gas in the system + volume

$$\text{of liquid aminomethane in saturator} = 2607.8 - 43.0 = 2564.8 \text{ cc.}$$

The volume of liquid aminomethane in the saturator was estimated at the end of each experiment by measuring the height of the saturator not occupied by the liquid. A cathetometer was used for the purpose. For the experiment of the 11th October 1972 the aminomethane volume in the saturator was 49.2 cc.

Volume of gas in the system = $2564.8 - 49.2 = 2515.6$ cc.

Diffusivity of HD in Aminomethane

The following method was used to obtain the value of the diffusivity of hydrogen-deuteride in aminomethane.

Over a temperature range of -5°C to -35°C the diffusivity of $\text{HD-CH}_3\text{NH}_2$ and $\text{H}_2\text{-CH}_3\text{NH}_2$ was estimated at 5°C intervals using equation (1-49) given in the first part of this thesis. The mean ratio of $D_{\text{HD}}/D_{\text{H}}$ over the entire temperature range was then estimated as being 0.9102.

The experimental data of the diffusivity of $\text{H}_2\text{-CH}_3\text{NH}_2$ was taken from the mean line of Fig. 6 in part I of this thesis and a least square fit to the data of $\log_{10} D$ vs. $\frac{1000}{T^{\circ}\text{K}}$ was generated. The equation is given as

$$\log_{10} D_{\text{H}_2} = -2.25564 - 0.432524 \beta \quad (\text{B2-10})$$

$$\text{where } \beta = \frac{1000}{T^{\circ}\text{K}} \quad (\text{B2-11})$$

The 95% confidence interval of the parameters is better than 0.5%.

The value of D_{HD} was then taken to be given by

$$D_{\text{HD}} = 0.9102 D_{\text{H}_2} \quad (\text{B2-12})$$

For the specific experiment under investigation

$$\begin{aligned} \log_{10} D_{\text{H}_2} &= -2.25564 - 0.432524 \times \frac{1000}{261.41} \\ &= -3.9102 \end{aligned}$$

$$D_{\text{H}_2} = 10.0^{(-3.9102)} = 123.0 \times 10^{-6} \frac{\text{cm}^2}{\text{sec}}$$

$$\text{and } D_{HD} = 111.9 \times 10^{-6} \frac{\text{cm}^2}{\text{sec}}$$

The overall liquid phase mass transfer coefficient K_L may now be estimated from equation (B2-5)

$$k^* = \frac{K_L A_T \rho_L R_g T}{V H_2} \quad (\text{B2-5})$$

$$\rho_L = \frac{0.7014}{31.07} \frac{\text{gm moles}}{\text{cc}}$$

$$R_g = 82.06 \frac{\text{cc atm}}{\text{gm mole } ^\circ\text{K}}$$

$$T = 261.41 (^\circ\text{K})$$

$$V = 2515.6 (\text{cc})$$

$$H_2 = 6625.7 \frac{\text{atm}}{\text{mole fraction}} \quad \text{or} \quad \frac{\text{atm}}{\frac{\text{moles}}{\text{moles}}}$$

$$A_T = 46.05 (\text{cm}^2)$$

$$k^* = 0.214 \times 10^{-3} (\text{sec}^{-1})$$

$$K_L = \frac{k^* V H_2}{A_T \rho_L R_g T} \quad \text{sec}^{-1} \quad \text{cc} \quad \frac{\text{atm moles}}{\text{moles}} \quad \frac{1}{\text{cm}^2} \quad \frac{\text{cc}}{\text{moles}} \quad \frac{\text{moles } ^\circ\text{K}}{\text{cc atm}} \quad \frac{1}{^\circ\text{K}}$$

$$= \frac{0.214 \times 10^{-3} \times 2515.6 \times 6625.7 \times 31.07}{46.05 \times 0.7014 \times 82.06 \times 261.41} \quad \frac{\text{cms}}{\text{sec}}$$

$$= \frac{2.14 \times 2.5156 \times 6.6257 \times 3.107}{4.605 \times 7.014 \times 8.206 \times 2.6141} = 0.1601$$

Now for the fast reaction regime neglecting gas phase resistance

$$K_L = \sqrt{k_1 D_{HD}} \quad (\text{B2-13})$$

$$k_1 = \frac{K_L^2}{D_{HD}} = \frac{(0.1601)^2}{111.9 \times 10^{-6}} = 229.0 (\text{sec}^{-1})$$

Details of the calculation of y_e by estimation of Liquid Enrichment
Vapour Pressure of Aminomethane

The following equation was used to express the aminomethane vapour pressure as a function of system temperature.

$$\ln P = C_1 + \frac{C_2}{T} + C_3 T + C_4 \ln T \quad (B2-14)$$

where $C_1 = 100.90554$

$$C_2 = -5716.32506$$

$$C_3 = 0.022480$$

$$C_4 = -15.3000$$

P = vapour pressure of aminomethane (atm.)

T = temperature ($^{\circ}\text{K}$)

Using $T = 261.41$ $^{\circ}\text{K}$ one obtains

$$P = 0.7806 \text{ atm.}$$

The partial pressure P_H of hydrogen was assumed to be given by

$$P_H = P_T - P \quad (B2-15)$$

where P_T = total system pressure at the beginning of the experiment.

One could use an average total pressure of the system given by the mean of the initial and final pressures but since this is used only to estimate the total number of moles of hydrogen in the system (of the order of 0.15) use of the initial pressure only is sufficient for a reasonably close estimate of the liquid enrichment

$$P_T = \frac{72.5 + 71.19}{76.0} = \frac{143.69}{76.0} = 1.89 \text{ atm.}$$

$$P_H = 1.11 \text{ atm}$$

Number of moles of hydrogen in the system are

$$n_g = \frac{P_H V}{R_g T} = \frac{1.11 \times 2.5156}{0.08206 \times 261.41} = 0.1302 \text{ moles}$$

Consider the time of the run before the spill i.e. at 6500 sec.

Average Liquid flow rate = 0.292 cc/sec

The details of converting the liquid rotameter readings to the corresponding aminomethane flow rates are given in Moore's thesis [9].

Number of Moles of liquid passed over ball absorber is given

$$\begin{aligned} \text{by } n_l &= \frac{0.292 \times 6500 \times 0.7014}{31.07} \\ &= 42.9 \text{ moles} \end{aligned}$$

The final D/H concentration of the gas at time $t = 6500$ sec is 151.6 ppm.

Y initial at time $t = 0$ is = 526.9 ppm

$$(Y_i - Y_f) n_g = (526.9 - 151.6) 0.1302 = 48.9$$

Initial liquid concentration of D/H from analysis of previous experiment is = 114.3 ppm

Using equation (B2-3) one obtains

$$\begin{aligned} x_f' &= \frac{114.3 \times 42.9 + 48.9}{42.9} \\ &= 114.3 + \frac{48.9}{42.9} \\ &= 115.4 \text{ ppm.} \end{aligned}$$

The equation of the separation factor is represented as

$$\log_{10} \alpha_{eq} = -0.2422 + \frac{237.59}{T} \quad (2-21)$$

$$\begin{aligned} \log_{10} \alpha_{eq} &= -0.2422 + \frac{237.59}{261.41} \\ &= -0.2422 + 0.9089 = 0.6667 \end{aligned}$$

$$\alpha_{eq} = 10^{0.6667} = 4.6419$$

$$y_e = \frac{x_f^i}{\alpha_{eq}} = \frac{115.4}{4.6419} = 24.9 \text{ ppm.}$$

The overall liquid concentration x_i used for the next experiment was estimated by using a linear mixing rule essentially of the same form as equation (B2-3).

APPENDIX C2

Error Analysis

The standard error in a measured quantity may be defined by

$$\alpha = \frac{\sigma}{\sqrt{n}} \quad (C2-1)$$

where σ is the standard deviation of the measured quantity and n is the total number of observations.

For any function

$$G = f(A, B, C, D) \quad (C2-2)$$

The standard error in \bar{G} is given by

$$\alpha_{\bar{G}}^2 = \left(\frac{\partial f}{\partial A} \right)^2 \alpha_A^2 + \left(\frac{\partial f}{\partial B} \right)^2 \alpha_B^2 + \left(\frac{\partial f}{\partial C} \right)^2 \alpha_C^2 + \left(\frac{\partial f}{\partial D} \right)^2 \alpha_D^2 \quad (C2-3)$$

where \bar{G} is the mean of G and α_A , α_B , α_C and α_D are the standard errors of the means of A, B, C, D .

The equation used to express the depletion of the hydrogen-deuteride concentration with time is given as

$$\ln \left(\frac{y - y_e}{y_{in} - y_e} \right) = - \frac{K_L A_T \rho_L R_g T}{V H_2} t \quad (2-57)$$

where A_T includes the area of the liquid jet.

For a fast first order reaction, the relationship of K_L with the rate constant k_1 is given as

$$K_L = \sqrt{k_1 D} \quad (2-6)$$

Expressing K_L as a function of the other quantities

$$K_L = - \frac{V H_2}{A_T \rho_L R_g T t} \ln \left(\frac{y - y_e}{y_{in} - y_e} \right) \quad (C2-4)$$

$$\text{or } K_L = f(V, H, A_T, \rho_L, T, t, y, y_e, y_{in}) \quad (C2-5)$$

The universal gas constant R_g is not included in (C2-5) because it is assumed invariant and as such $\frac{\partial K_L}{\partial R_g} = 0$ (C2-6)

Expressing equation (C2-5) in terms of standard errors one obtains

$$\begin{aligned} \alpha_{K_L}^2 = & \left(\frac{\partial f}{\partial V} \right)^2 \alpha_V^2 + \left(\frac{\partial f}{\partial H} \right)^2 \alpha_H^2 + \left(\frac{\partial f}{\partial A_T} \right)^2 \alpha_{A_T}^2 + \left(\frac{\partial f}{\partial \rho_L} \right)^2 \alpha_{\rho_L}^2 + \dots \\ & + \left(\frac{\partial f}{\partial y_{in}} \right)^2 \alpha_{y_{in}}^2 \end{aligned} \quad (C2-7)$$

The derivatives may be expressed as

$$\frac{\partial K_L}{\partial V} = - \frac{H}{A_T \rho_L R_g T t} \ln \left(\frac{y - y_e}{y_{in} - y_e} \right) = \frac{K_L}{V} \quad (C2-8)$$

$$\frac{\partial K_L}{\partial H} = \frac{K_L}{H} \quad (C2-9)$$

$$\frac{\partial K_L}{\partial A_T} = \frac{V H}{A_T^2 \rho_L R_g T t} \ln \left(\frac{y - y_e}{y_{in} - y_e} \right) = - \frac{K_L}{A_T} \quad (C2-10)$$

$$\frac{\partial K_L}{\partial \rho_L} = - \frac{K_L}{\rho_L} \quad (C2-11)$$

$$\frac{\partial K_L}{\partial T} = - \frac{K_L}{T} \quad (C2-12)$$

$$\frac{\partial K_L}{\partial t} = - \frac{K_L}{t} \quad (C2-13)$$

$$\frac{\partial K_L}{\partial y} = - \frac{VH}{A_T \rho_L R_g T t} \left(\frac{1}{y-y_e} \right) = \frac{K_L}{(y-y_e) \ln \left(\frac{y-y_e}{y_{in}-y_e} \right)} \quad (C2-14)$$

$$\frac{\partial K_L}{\partial y_e} = \frac{K_L (y-y_{in})}{\ln \left(\frac{y-y_e}{y_{in}-y_e} \right) (y-y_e) (y_{in}-y_e)} \quad (C2-15)$$

$$\frac{\partial K_L}{\partial y_{in}} = \frac{K_L}{(y_{in}-y_e) \ln \left(\frac{y-y_e}{y_{in}-y_e} \right)} \quad (C2-16)$$

Substituting equations (C2-8) to (C2-16) in (C2-7)

$$\begin{aligned} \left(\frac{\alpha_{K_L}}{K_L} \right)^2 &= \left(\frac{\alpha_V}{V} \right)^2 + \left(\frac{\alpha_H}{H} \right)^2 + \left(\frac{\alpha_{A_T}}{A_T} \right)^2 + \left(\frac{\alpha_{\rho_L}}{\rho_L} \right)^2 + \left(\frac{\alpha_T}{T} \right)^2 + \left(\frac{\alpha_t}{t} \right)^2 \\ &+ \left(\frac{\alpha_y}{(y-y_e)^\beta} \right)^2 + \left(\frac{\alpha_{y_e} (y-y_{in})}{\beta (y-y_e) (y_{in}-y_e)} \right)^2 + \left(\frac{\alpha_{y_{in}}}{(y_{in}-y_e)^\beta} \right)^2 \end{aligned} \quad (C2-17)$$

$$\text{where } \beta = \ln \left(\frac{y-y_e}{y_{in}-y_e} \right) \quad (C2-18)$$

It may be noted that the terms involving $(y - y_e)$ are the ones which could contribute significantly to the total error if the data at $t \rightarrow \infty$ (i.e. $y \rightarrow y_e$) are used. It is advisable therefore, to shift the time scale so as to include data upto a time 't' where the 'y' value is still significantly different from y_e . In general

most of the data taken during this investigation was obtained from experiments which were conducted for about two hours.

Re-arranging equation (2-6) one obtains

$$k_1 = \frac{K_L^2}{D} \quad (C2-19)$$

$$\therefore \alpha_{k_1}^2 = \left(\frac{\partial k_1}{\partial K_L} \right)^2 \alpha_{K_L}^2 + \left(\frac{\partial k_1}{\partial D} \right)^2 \alpha_D^2 \quad (C2-20)$$

The derivatives are given as

$$\frac{\partial k_1}{\partial K_L} = \frac{2K_L}{D} = 2 \frac{k_1}{K_L} \quad (C2-21)$$

$$\frac{\partial k_1}{\partial D} = -\frac{K_L^2}{D^2} = -\frac{k_1}{D} \quad (C2-22)$$

$$\therefore \left(\frac{\alpha_{k_1}}{k_1} \right)^2 = 4 \left(\frac{\alpha_{K_L}}{K_L} \right)^2 + \left(\frac{\alpha_D}{D} \right)^2 \quad (C2-23)$$

Error in Gas Volume Estimation

Re-writing equation (B2-9)

$$V = \left(\frac{P_1 - P_f}{P_f - P_{11}} \right) V_1 \quad (B2-9)$$

$$\alpha_V^2 = \left(\frac{\partial V}{\partial P_1} \right)^2 \alpha_{P_1}^2 + \left(\frac{\partial V}{\partial P_f} \right)^2 \alpha_{P_f}^2 + \left(\frac{\partial V}{\partial P_{11}} \right)^2 \alpha_{P_{11}}^2 + \left(\frac{\partial V}{\partial V_1} \right)^2 \alpha_{V_1}^2 \quad (C2-24)$$

$$\text{where } \frac{\partial V}{\partial P_1} = \frac{V_1}{P_f - P_{11}} = \frac{V}{P_1 - P_f} \quad (C2-25)$$

$$\frac{\partial V}{\partial P_f} = \frac{V(P_{11} - P_1)}{(P_1 - P_f)(P_f - P_{11})} \quad (C2-26)$$

$$\frac{\partial V}{\partial P_{11}} = \frac{V}{P_f - P_{11}} \quad (C2-27)$$

$$\frac{\partial V}{\partial V_1} = \frac{V}{V_1} \quad (C2-28)$$

Substituting the derivatives in (C2-24)

$$\left(\frac{\alpha_V}{V}\right)^2 = \left(\frac{\alpha_{P_1}}{P_1 - P_f}\right)^2 + \left(\frac{\alpha_{P_f}(P_{11} - P_1)}{(P_1 - P_f)(P_f - P_{11})}\right)^2 + \left(\frac{\alpha_{P_{11}}}{P_f - P_{11}}\right)^2 + \left(\frac{\alpha_{V_1}}{V_1}\right)^2 \quad (C2-29)$$

Representative estimates of the standard and fractional errors of the pertinent variables are:

$$\alpha_{P_1} = \pm 0.2 \text{ mm}$$

$$\alpha_{P_f} = \pm 0.1 \text{ mm} = \alpha_{P_{11}}$$

$$\alpha_{V_1} = \pm 1.0 \text{ cc}$$

$$\alpha_Y = \alpha_{Y_e} = \alpha_{Y_{in}} = \pm 1 \text{ ppm}$$

A Fortin's barometer was used to measure P_1 and a cathetometer to measure the heights of the two limbs of a mercury manometer to obtain P_f and P_{11} . The fractional errors are of the following order of magnitude.

$$\left. \begin{aligned} \left(\frac{\alpha_V}{V}\right) &= 0(10^{-3}) & \left(\frac{\alpha_D}{D}\right) &= 0(5 \times 10^{-2}) \\ \left(\frac{\alpha_H}{H}\right) &= 0(10^{-2}) & \left(\frac{\alpha_T}{T}\right) &= 0(10^{-4}) & \left(\frac{\alpha_{A_T}}{A_T}\right) &= 0(10^{-4}) \\ \left(\frac{\alpha_{\rho_L}}{\rho_L}\right) &= 0(5 \times 10^{-3}) & \left(\frac{\alpha_t}{t}\right) &= 0(10^{-3}) \end{aligned} \right\} \quad (C2-30)$$

Using the general equations derived above along with typical values of y , y_{in} and y_e , the fractional error in the overall mass transfer coefficient may be represented by

$$\frac{\alpha_{K_L}}{K_L} = 0(10^{-2}) \quad (C2-31)$$

This leads to an estimated fractional error in the rate constant of

$$\frac{\alpha_{k_1}}{k_1} = 6 \times 10^{-2} \quad (C2-32)$$

It may be safely stated therefore that the rate constant values obtained are reliable to $\pm 10\%$.

APPENDIX D2Detailed Experimental Data

The detailed experimental data taken for the depletion of deuterium in the gas phase with time is given in Table D2-1. The gas phase compositions 'y' shown in the table represent the absolute ppm concentrations of D/H obtained after conversion from the raw data in the manner shown in Appendix B2. Table D2-1 may be used to obtain k_1 vs. T and k_1 vs C data reported in Chapter 5 of this thesis.

TABLE D2-1

Detailed Experimental Data

Run No./Date	1/(23/3/72)		2/(5/4/72)		3/(17/4/72)		4/(5/7/72)			
	T (sec)	Y = D/H (PPM)	T (sec)	Y = D/H (PPM)	T (sec)	Y = D/H (PPM)	T (sec)	Y = D/H (PPM)		
Time vs. Gas Phase Deuter- ium Concentra- tion Data	0	1586	0	533	0	542	a	b	a	b
	903	1473	650	517	600	499				
	1204	1444	967	504	1200	470	0	0	464	206
	1504	1427	1240	499	1800	438				
	2403	1346	1500	489	2400	410	600	600	399	180
	3002	1281	2057	470	3000	379				
	3609	1245	2550	456	4200	334	1200	1170	341	155
	7230	985	3150	442	5400	292				
	9633	843	3650	428	6600	256	1800	1700	295	138
	10835	793	4250	412	7800	214	Mean of k_1 values obtained from both sets was taken as representative.			
	12634	717	4857	401	9000	197				
	17650	538	5850	357	10200	174				
			6850	354	11300	156				
			7850	336						
			8850	316						
			9850	298						
Total Interfacial Area	20.67 (cm ²)		20.67		20.65		46.03			
Catalyst Concentration	15.80(gmsK/kg.Amine)		15.80		15.80		15.80			
Henry's Law Coeff.	8204.7(atm/mole frac.)		8210.2		6643.2		7006.0			
Gas Phase Equilibrium Value	21.1 (PPM)		21.1		24.8		24.4			
System Temperature	-30.11 (°C)		-30.16		-12.00		-16.66			
Total Initial Press.	1.476 (atm.Absolute)		1.378		1.866		1.681			
Gas Volume in System	3108 cc		3107		3091		2538			
HD-Amine Diffusivity	83.9x10 ⁻⁶ (cm ² /sec)		83.8x10 ⁻⁶		111.5x10 ⁻⁶		104.0x10 ⁻⁶			
Liquid Flow Rate	0.400 (cc/sec)		0.399		0.409		0.261			
Aminomethane Density	0.7222 (gms/cc)		0.7223		0.7017		0.7071			

Run No./Date	5/(7/7/72)		6/(11/7/72)		7/(26/7/72)		8/(31/7/72)	
	T (sec)	Y = D/H (PPM)	T (sec)	Y = D/H (PPM)	T (sec)	Y = D/H (PPM)	T (sec)	Y = D/H (PPM)
Time vs. Gas Phase Deuter- ium Concentration Data	0	442	0	304	0	351	0	483
	593	377					500	441
	993	338	500	275	500	317	850	414
	1593	287					1300	380
	2193	242	1000	251	1000	288	1800	340
	2793	210					2300	303
	3393	179	1500	227	1500	258	2700	285
	3993	154					3100	259
	4593	133	2000	207	2000	235	3500	235
	5193	114					3900	224
	5373	110	2500	186				
Total Interfacial Area	46.03 (cm ²)		46.06		46.06		46.06	
Catalyst Concentration	15.80(gmsK/kg.Amine)		15.80		15.80		15.80	
Henry's Law Coeff.	6917.5(atm/mole frac.)		7644.9		7581.9		7571.5	
Gas Phase Equilibrium Value	24.5 (PPM)		22.9		23.1		23.1	
System Temperature	-15.55(°C)		-24.15		-23.45		-23.33	
Total Initial Press.	1.507 (atm Abs.)		1.435		1.481		1.514	
Gas Volume in System	2540 (cc)		2526		2523		2519	
HD-Amine Diffusivity	105.8x10 ⁻⁶ (cm ² /sec)		92.6x10 ⁻⁶		93.6x10 ⁻⁶		93.8x10 ⁻⁶	
Liquid Flow Rate	0.263 (cc/sec)		0.280		0.281		0.282	
Aminomethane Density	0.7058 (gms/cc)		0.7156		0.7148		0.7147	

TABLE D2-1 Cont.

Run No./Date	9/(2/8/72)		10/(28/8/72)		11/(14/9/72)		12/(22/9/72)	
	T (sec)	Y = D/H (PPM)	T (sec)	Y = D/H (PPM)	T (sec)	Y = D/H (PPM)	T (sec)	Y = D/H (PPM)
Time vs. Gas	0	272	0	443	0	442	0	456
	400	245					400	408
	800	222	400	403	400	388	900	352
	1200	198					1400	307
	1600	175	775	359	1400	286	1900	269
Phase Deuter-	2000	158					2400	234
	2400	141	1150	322	1900	246	2900	207
ium Concentra-	2800	128					3400	181
	3200	116	1500	289	2400	210	3900	159
	3600	105					4400	139
	4000	96	1800	268	3400	157	4900	122
			2100	237	3900	136		
Total Interfacial Area	46.04 (cm ²)		46.04		46.05		46.05	
Catalyst Concentration	15.80 (gmsK/kg.Amine)		15.80		15.80		10.42	
Henry's Law Coeff	6704.6 (atm/mole frac.)		6677.6		6618.8		6604.9	
Gas Phase Equilibrium Value	25.3 (PPM)		25.6		24.8		24.9	
System Temperature	-12.81 (°C)		-12.46		-11.68		-11.49	
Total Initial Press.	1.815 (atm.Abs.)		1.442		1.890		1.900	
Gas Volume in System	2526 (cc)		2531		2521		2524	
HD-Amine Diffusivity	110.2x10 ⁻⁶ (cm ² /sec)		110.8x10 ⁻⁶		112.0x10 ⁻⁶		112.3x10 ⁻⁶	
Liquid Flow Rate	0.277 (cc/sec)		0.291		0.292		0.293	
Aminomethane Density	0.7026 (gms/cc)		0.7022		0.7013		0.7011	

Run No./Date	13/(30/9/72)		14/(9/10/72)		15/(11/10/72)		
	T (sec)	Y = D/H (PPM)	T (sec)	Y = D/H (PPM)	T (sec)	Y = D/H (PPM)	
Time vs. Gas	0	424	0	481	0	479	
	580	359	1000	397	500	435	
	1050	316	1500	357	1000	394	
	1400	291	2500	290	1500	353	
	1850	254	3000	264	2000	322	
Phase Deuter-	2360	224	3500	238	2500	293	
	2870	195	4000	216	3000	263	
ium Concentra-	3350	173	4500	198	3500	238	
	3850	152	5500	161	4000	216	
	4350	134	6000	147	4500	200	
	4850	118			5000	181	
	5350	104			5500	164	
	5850	93			6000	152	
Total Interfacial Area	46.05 (cm ²)		46.05		46.05		
Catalyst Concentration	10.42 (gmsK/kg.Amine)		4.95		4.95		
Henry's Law Coeff	6597.4 (atm/mole frac.)		6575.4		6625.7		
Gas Phase Equilibrium Value	25.0 (PPM)		25.0		24.9		
System Temperature	-11.39 (°C)		-11.09		-11.77		
Total Initial Press.	1.909 (atm.Abs.)		1.851		1.891		
Gas Volume in System	2534 (cc)		2525		2516		
HD-Amine Diffusivity	112.5x10 ⁻⁶ (cm ² /sec)		113.0x10 ⁻⁶		111.9x10 ⁻⁶		
Liquid Flow Rate	0.298 (cc/sec)		0.296		0.292		
Aminomethane Density	0.7010 (gms/cc)		0.7006		0.7014		

B30054